NOAA Technical Memorandum GLERL-126

GREAT LAKES CLIMATE CHANGE HYDROLOGIC IMPACT ASSESSMENT
I.J.C. LAKE ONTARIO-ST. LAWRENCE RIVER REGULATION STUDY

Thomas E. Croley II
NOAA, Great Lakes Environmental Research Laboratory, Ann Arbor, MI 48105

Great Lakes Environmental Research Laboratory
Ann Arbor, Michigan

September 2003

UNITED STATES
DEPARTMENT OF COMMERCE

Donald Evans
Secretary

NATIONAL OCEANIC AND
ATMOSPHERIC ADMINISTRATION

Conrad C. Lautenbacher, Jr.
Administrator

NOTICE

 This is GLERL Contribution No. 1286.

This work was supported in part by funds from the International Joint Commission for their study of Lake Ontario—St. Lawrence River Regulation, administered by the Hydrology and Hydraulics Technical Working Group.

This publication is available as a PDF file and can be downloaded from GLERL's web site: www.glerl.noaa.gov. Hard copies can be requested from GLERL, Information services, 2205 Commonwealth Blvd., Ann Arbor, MI 48105. pubs.glerl@noaa.gov.

TABLE OF CONTENTS

LIST OF FIGURES

LIST OF TABLES

ABSTRACT

Climatic change will impact on many aspects of the hydrological cycle with consequences for mankind that are interrelated and often difficult to discern. Climate warming will have impacts on Great Lakes water supply components and basin storages of water and heat that must be understood before lake level impacts can be assessed. Because the Laurentian Great Lakes possess tremendous water and heat storage capacities, they respond slowly to changed meteorological inputs. This memory damps short-term meteorological fluctuations, but allows response to longer-period fluctuations characteristic of climate change. Thus the large Great Lakes system is ideal for studying regional effects of climate changes.

This project estimates hydrological impacts of changed climates over the Great Lakes from the latest general circulation model (GCM) results for the International Joint Commission's five-year study of Lake Ontario—St. Lawrence regulation. This report concerns the US study of climate change performed by The Great Lakes Environmental Research Laboratory (GLERL). They extracted GCM output changes between a baseline period of 1961—1990 and a future 30-year period (2040—2069). GLERL adjusted historical meteorology data for the Great Lakes basin with the GCM climate changes. GLERL used a base climate (observed data) time series over 1950—1999 to define the reference of 1960—1990 suggested by the Intergovernmental Panel on Climate Change. GLERL simulated Great Lakes hydrology to estimate net water supply scenarios for each lake under each climate scenario.

This report provides background on earlier Great Lakes climate change impact studies, describes the Great Lakes and their climate, presents hydrological models used in assessing climate change, and summarizes results. Detailed time series of net basin supplies to all of the Great Lakes are available for an unchanged climate scenario and four GCM-generated changed-climate scenarios.

The higher air temperatures under the changed-climate scenarios lead to higher over-land evapotranspiration and lower runoff to the lakes with earlier runoff peaks since snow pack is reduced and the snow season is greatly reduced. This also results in a reduction in available soil moisture. Water temperatures increase and peak earlier; heat resident in the deep lakes increases throughout the year. Mixing of the water column diminishes, as most of the lakes become mostly monomictic, and lake evaporation increases. Ice formation is greatly reduced over winter on the deep Great Lakes, and lake evaporation increases; average net supplies drop most where precipitation increases are modest.

Great Lakes Climate Change Hydrologic Impact Assessment for IJC Lake Ontario—St. Lawrence River Study

(Hydrology and Hydraulics Technical Working Group)

US Analysis of Great Lakes Net Basin Supplies For Extreme Climate Scenarios

This project estimates hydrological impacts of changed climates over the Great Lakes from the latest general circulation model results for the International Joint Commission's five-year study of Lake Ontario—St. Lawrence regulation. This report concerns the US study of climate change performed by The Great Lakes Environmental Research Laboratory.

Project Rationale

Background

The International Joint Commission (IJC) is conducting a Study for Criteria Review in the Orders of Approval for Regulation of Lake Ontario—St. Lawrence River Levels and Flows. In recent IJC and US Global Change Research Program studies, The Great Lakes Environmental Research Laboratory (GLERL) completed modeling of hydrologic impacts of climate change for the Great Lakes region. This work used climate change scenarios from two general circulation models (GCMs) and transformed them into hydrological impacts with models of rainfall/runoff, lake evaporation, connecting channel flows, lake regulation, and lake water balances. However, climate change scenarios were not included in this work for the Ottawa River basin and lower St. Lawrence River. In 2001, GLERL made GCM scenarios available over these extended areas and hydrologic modelers at Hydro Quebec extended, in 2002, the estimation of climate change hydrological impacts over these areas. GLERL and Hydro Quebec, under the auspices of the Hydrology and Hydraulics Technical Working Group (H&H TWG), coordinated their climate change methodologies in preparation for a new joint assessment of climate change impacts on hydrology over the entire Great Lakes—St. Lawrence River basin attendant to the latest GCM simulations (the Canadian and U.K. Hadley GCMs). Their cooperative examples concerned the future 20-year periods for 2030 (2021-2040), 2050 (2041-2060), and 2090 (2081-2100), used by GLERL for the US National Assessment and IJC Reference on Consumption, Diversions and Removals of Great Lakes Water. They used the Canadian Centre for Climate Modelling and Analysis's Coupled General Circulation Model version 1 (CGCM1) and the United Kingdom's Hadley Centre Climate Model version 2 (HadCM2), both using IS92A emissions forcing scenarios.

GLERL has since worked with the Ottawa hydrologic modeling group, consisting of researchers at Hydro Quebec and the Ministère de l'Environnement (Province of Quebec), on the future 30-year period for 2050 (2040-2069), as determined of interest to the IJC study by the H&H TWG at their climate change workshop in 2002. In a contracted report prepared for the H&H TWG on the Canadian Climate Impacts Scenarios Project, prior to the 2002 workshop, Dr. Elaine Barrow selected GCM climate change scenarios for the Great Lakes-St. Lawrence region (*Barrow* 2002) according to the recommendations of the Intergovernmental Panel on Climate Change (IPCC) Task Group on Scenarios for Climate Impact Assessment (*IPCC* 2000). Output from nine GCMs and 34 climate change model run experiments was available for the construction of climate change scenarios. However, only five GCMS provided the climate variables required for hydrologic modeling (minimum and maximum air temperature, precipitation, wind speed, solar radiation, and humidity), but this still provided a set of 27 climate change scenarios over the study area. The candidate GCMs included version 1 and 2 models from the Canadian Centre for Climate Modeling and Analysis (respectively, CGCM1 and CGCM2), the German Max Planck Institute for Meteorology's model (ECHAM4), and version 2 and 3 models from the United Kingdom Hadley Centre for Climate Prediction and Research (respectively, HadCM2 and HadCM3). Scenarios were constructed from both recent (IS92A) and the newest (SRES) emission scenarios. The H&H TWG used scatter plots (of areally averaged annual changes in mean temperature and annual precipitation) to determine the choice of GCMs for scenario development in the hydrologic modeling. The goal was to "box the uncertainty" by selecting four scenarios of climate change that depict 1) most warming and wettest, 2) most warming and driest, 3) least warming and wettest, and 4) least warming and driest conditions over the IJC study region. While four GCM scenarios were chosen at the time of the workshop, newer GCM model runs using SRES forcing scenarios became available, subsequent to the workshop, and the H&H TWG wanted to use these latest experiments . Dr. Elaine Barrow again provided the H&H TWG with additional GCM climate change scenario output for six GCMs and 28 SRES model run experiments. H&H TWG personnel Joan Klaassen and Linda Mortsch and their subcontractor Marianne Alden repeated the determination of GCM scenarios. The GCM selection was again constrained to GCMs with climate variables required for hydrologic modeling. Four GCMs were selected, including the Canadian CGCM2, the German ECHAM4, the Japanese CCSR and the United Kingdom HadCM3. A new set of four GCM scenarios was selected from the resulting 24 climate change scenarios for use in the IJC study. They are: HadCM3 A1FI (warm and wet), HadCM3 B22 (not as warm but wet), CGCM2 A21 (warm and dry), and CGCM2 B23 (not as warm but dry). Scenarios were not created from the GCM ensemble mean of runs (because of issues of consistency between the averaged climate elements), but only individual model runs were used. GLERL acquired the identified GCM climate change scenarios and made them available over the extended Great Lakes—St. Lawrence area to hydrologic modelers at Hydro Quebec and the Ministère de l'Environnement.

As recommended by the H&H TWG climate change workshop and in consultation with Dr. Elaine Barrow, downscaling of the GCM scenarios is limited to interpolation of the GCM grids. Other, more labor intensive and detailed downscaling techniques such as statistical downscaling (i.e. SDSM) or weather generators (i.e. LARS-WG, as described in Dr. Barrow's report prepared prior to the workshop) are not used. Downscaling of more than 1600 stations within the Great Lakes-St. Lawrence basin does not produce spatially coherent results or cost-effective, value added results. A regional climate model (RCM) scenario would be beneficial but neither Canadian nor US RCM results will be available in time to use for this study.

Present Study

GLERL extracted, and supplied to Hydro Quebec, GCM output changes between a baseline period of 1961—1990 and a future 30-year period (2040—2069). GLERL adjusted historical meteorology data for the Great Lakes basin with the GCM climate changes while Hydro Quebec and the Ministère de l'Environnement did the same for the Ottawa River basin. GLERL used a base climate (observed data) time series over 1950—1999 to define the reference suggested by the IPCC of 1960—1990. GLERL simulated Great Lakes hydrology to estimate net water supply scenarios for each lake under each climate scenario. Hydro Quebec and the Ministère de l'Environnement did the same for the Ottawa River basin by using the appropriate hydrology and management models. Finally, GLERL, Hydro Quebec, and the Ministère de l'Environnement combined their estimates for the IJC study of Lake Ontario—St. Lawrence River regulation.

Introduction

Climatic change will impact on many aspects of the hydrological cycle with consequences for mankind that are interrelated and often difficult to discern. Climate warming will have impacts on Great Lakes water supply components, and basin storages of water and heat, that must be understood before lake level impacts can be assessed. Because the Laurentian Great Lakes possess tremendous water and heat storage capacities, they respond slowly to changed meteorological inputs. This memory damps short-term meteorological fluctuations, but allows response to longer-period fluctuations characteristic of climate change. Thus the large Great Lakes system is ideal for studying regional effects of climate changes.

Early Great Lakes Climate Change Impact Studies

Considerations of future climate situations that may occur (scenarios) help to identify possible effects and can bound future conditions, if widely different scenarios are tested. Preliminary impact estimates considered simple constant changes in air temperature or precipitation. *Quinn and Croley* (1983) estimated net basin supply to Lakes Superior and Erie. *Cohen* (1986) estimated net basin supply to all Great Lakes. *Quinn* (1988) estimated lower water levels due to decreases in net basin supplies on Lakes Michigan-Huron, St. Clair, and Erie.

Beginning with *Manabe and Wetherald* (1975), researchers have run general circulation models (GCMs) of the earth's atmosphere to simulate climates for current conditions and for a doubling of global carbon dioxide levels (2xCO_2). This 2xCO_2 benchmark remained a widely used measure of greenhouse warming sensitivity through the early 1990s, when scenarios of transient increases in greenhouse gases using coupled atmosphere-ocean GCMs supplanted it. Using a global domain and coarse spatial resolution (evolving over time from roughly 8 degrees to 3 degrees), these models produce many internally consistent dialy meteorological values. The U.S. Environmental Protection Agency (*USEPA* 1984) and *Rind* (personal communication, 1988) used the hydrological components of general circulation models. They assessed changes in water availability in several regions throughout North America, but the regions were very large. Rind used only four regions for the entire continent and indicated needs for smaller region assessments. Regional hydrological models can link to GCM outputs to assess changes associated with climate change scenarios. *Allsopp and Cohen* (1986) used Goddard Institute of Space Sciences (GISS) 2xCO_2 climate scenarios with net basin supply estimates.

Other efforts that linked hydrological models to GCM outputs originated in studies commissioned by the U. S. Environmental Protection Agency (EPA). EPA, at the direction of the U.S. Congress, coordinated several regional studies of the potential effects of a 2xCO_2 atmosphere. The studies addressed various aspects of society, including agriculture, forestry, and water resources (*USEPA* 1989). They directed others to consider alternate climate scenarios by changing historical meteorology similar to the changes observed in GCM simulations of 2xCO_2, observing changed process model outputs, and comparing to model results from unchanged data. *Cohen* (1990a, 1991) discusses other studies that use this type of linkage methodology and also presents his concerns for comparability between studies using different types.

Recent Great Lakes Climate Change Impact Studies

GLERL-EPA 2xCO_2 Impacts. As part of the 1989 EPA study, the Great Lakes Environmental Research Laboratory (GLERL) assessed steady-state and transient changes in Great Lakes hydrology consequent with simulated $2xCO_2$ atmospheric scenarios from three GCMs (*Croley* 1990; *Hartmann* 1990; *USEPA* 1989). EPA required that GLERL first simulate 30 years of "present" Great Lakes hydrology by using historical daily data with present diversions and channel conditions. GLERL arbitrarily set initial conditions but used an initialization period to allow their models to converge to conditions initial to the simulation. GLERL repeated their simulation, with initial conditions set equal to the end conditions over the simulation period, until these conditions were unchanging. This facilitated investigation of "steady-state" conditions. The next step was to conduct simulations with adjusted data sets.

EPA obtained output from atmospheric GCM simulations, representing both "present" and $2xCO_2$ steady-state conditions, from GISS, the Geophysical Fluid Dynamics Laboratory (GFDL), and the Oregon State University (OSU). They supplied monthly adjustments of "present" to $2xCO_2$ for each meteorological variable. GLERL applied them to daily historical data sets to estimate 33-year sequences of atmospheric conditions associated with the $2xCO_2$ scenarios. This method keeps spatial and temporal (inter-annual, seasonal, and daily) variability the same in the adjusted data sets as in the historical base period. GLERL then used the $2xCO_2$ scenarios in hydrology impact model simulations similar to those for the base case scenario. They interpreted differences between the $2xCO_2$ scenario and the base case scenario as resulting from the changed climate. They observed that the three scenarios changed precipitation little but snowmelt and runoff were greatly decreased, evapotranspiration and lake evaporation were greatly increased, and net basin supplies to the lakes and lake levels were decreased. The scenario derived from the GFDL GCM was the most extreme with evaporation 44% higher than the base case and net basin supply less than 50% of the base case.

Other EPA studies at that time include partial assessments of large-lake heat storage associated with climate change on Lakes Michigan (*McCormick* 1989) and Erie (*Blumberg and DiToro* 1989). The IJC study looked in less detail but more breadth at large-lake thermodynamics in that while only lake-wide effects were considered, all lakes were assessed.

GLERL-IJC $2xCO_2$ Impacts. The 1989 EPA studies, in part, and the high water levels of the mid 1980s prompted the International Joint Commission (IJC) to reassess climate change impacts on Great Lakes hydrology and lake thermal structure. GLERL adapted the 1989 EPA study methodology for the IJC studies (*Croley* 1992b) to consider $2xCO_2$ GCM scenarios supplied by the Canadian Climate Centre (CCC) for the period 1948-88. GLERL's procedure to estimate "steady-state" suggested, for a few subbasins, very different initial groundwater storages than were used in model calibrations. Since there is little confidence in estimates of very large groundwater half-lives on these subbasins with only 10 to 20 years in calibrations, those initial values used in calibrations were also used in the simulations for those subbasins.

Average monthly meteorological outputs were supplied for each month of the year over a 1º latitude by 1º longitude grid (*Louie* 1991) by the CCC as resulting from their second-generation GCM; see *McFarlane* (1991). GLERL computed $2xCO_2$ monthly adjustments at each location, used them with historical data to estimate the $2xCO_2$ 41-year sequences (1948-88) for each Great Lake basin, and then used the $2xCO_2$ scenario in simulations similar to the base case as before. This scenario proved similar to the earlier GFDL-based scenario in that net basin supplies were reduced to almost 50% of the base case. However, the CCC-based scenario reduced runoff more and evaporation less than the GFDL-based scenario.

GCM Linkage Problems

The hydrological study results from the 1989 EPA and IJC studies should be used with caution. They are, of course, dependent on GCM outputs with inherent large uncertainties in the GCM components, assumptions, and data. Transfer of information between the GCMs and GLERL's hydrological models in the manners described above involves several assumptions. Solar insolation at the top of and through the atmosphere on a clear day is assumed to be unchanged under the changed climate, modified only by changes in cloud cover, humidity, or (lately) aerosols. Over-water corrections are made in the same way, albeit with changed meteorology, which presumes that over-water/over-land atmospheric relationships are unchanged.

Heat budget data from GCM simulations for Great Lakes grid points may not adequately describe conditions over the lakes due to the coarse resolution of the grids. GLERL's procedure for transferring information from the GCM grid is an objective approach but simple in concept. It ignores interdependencies in the various meteorological variables as all are averaged independently in the same manner. Of secondary importance, the spatial averaging of meteorological values over a box centered on the GCM grid point (implicit in the use of the nearest grid point to each square kilometer of interest) filters all variability that exist in the GCM output over that box. If GCM output were interpolated between these point values, then at least some of the spatial variability might be preserved. The interpolation performed by *Louie* (1991) from the original GCM grid to a finer grid reduced this problem, but it still exists in the use of the finer grid with the hydrology models. Of course, little is known about the validity of various spatial interpolation schemes and, for highly variable spatial data, they may be inappropriate. Furthermore, much of the variability at the smallest resolvable scale of GCMs is, unfortunately, spurious.

Spatial and temporal variabilities in meteorology of the $2xCO_2$ data sets are the same as the base case, in both the 1989 EPA and IJC studies. The methodology does not address changes in variabilities that would take place under a changed climate. The method of coupling does not reproduce seasonal timing differences under a changed climate from the GCMs but preserves seasonal meteorological patterns as they exist in the historical (base case) data. This is a result of applying simple ratios or differences to calculate $2xCO_2$ scenarios from base case scenarios. This implicitly ignores spatial and temporal phase and frequency changes consequent in the $2xCO_2$ GCM simulations. For example, a changed climate alters the movement (direction, speed, frequencies) of air masses over the lakes. This implies an alteration of the seasonal temporal structure for storms and cyclonic events as well as the intensities of storms. The above method only allows modification of the latter. Seasonal changes induced by the changed meteorology because of a time-lag storage effect are observable, however. Shifts in snow pack or in the growth and decay of water surface temperatures are examples. Changes in annual variability are less clear, again as a result of using the same historical time structure for both the base case and the changed climate scenarios.

Finally, the use of GCM outputs in the 1989 EPA and IJC studies, to drive GLERL's hydrological process models, forced the use of inappropriately large spatial and temporal scales for studying the Great Lakes impacts of climate change. While the hydrological process models were defined over daily intervals and subbasin areas averaging 4,300 km^2, the GCM adjustments were made over monthly time intervals and grids of 7.83° latitude by 10° longitude (GISS), 4.44° by 7.5° (GFDL), and 4° by 5° (OSU), and 3.75° by 3.75° interpolated to 1° by 1°(CCC GCM).

Climate Transposition

While the 1989 EPA and IJC studies looked at changes in the mean values of hydrological variables, changes in ***variability*** were unaddressed. This variability is the singular key problem for shipping, power production, and resource managers. GLERL and the Midwest Climate Center (MCC) recognized the importance of investigating the effects of shifts in the daily, seasonal, inter annual, and multi-year climate variability on lake net supply behavior, as well as related changes in mean supplies. They considered studies that used climate change scenarios that were not drawn so directly from historical data that they preserved historical spatial and temporal patterns. Such "instrumental analogues" are one empirical approach identified by *Robinson and Finkelstein* (1989) to develop realistic scenarios since the actual values of the past were used to form the wet and dry extremes. However, the climate changes represented by these 12-year time series were not as large as many GCMs predict could happen in the future over the basin, and the effect of weather fluctuations over time due to large climatic changes could not be assessed by that approach. Atmospheric modelers are developing nested mesoscale numerical models of the Great Lakes basin (*Bates et al.* 1995) but these are not yet capable of generating multi-decadal series of conditions essential for the sensitivity study. In summary, these approaches simply could not provide the spatial and long temporal climatic data needed for the hydrological model and can not accomplish the desired sensitivity study of fluctuations in the hydrological system of the Great Lakes.

GLERL and MCC investigated these changes in variability by utilizing data for climates which actually exist to the south and west of the Great Lakes and that resemble some of the 2xCO_2 GCM scenarios. Lengthy (at least 40 years) and detailed records of daily weather conditions at about 2000 sites were available to represent physically plausible and coherent scenarios of alternate climates. Such data sets incorporated reasonable values and frequencies of extreme events, ensuring that the desired temporal and spatial variabilities were represented, and were being transposed over the Great Lakes.

MCC supplied the data and GLERL transposed them to the Great Lakes by relocating all meteorological station data and Thiessen-weighting to obtain areal averages over the 121 watersheds and 7 lake surfaces for all days of record (1948-1992). GLERL also reduced all historical data (base case) within the Great Lakes (1900-1990). This involved extensive error checking and data correction for thousands of stations, and regeneration of areal averages. Since the Great Lakes affect the climate near the shoreline and these effects are not present in the transposed data sets, MCC prepared maps of generalized seasonal lake effects on the area's meteorology, to be applied to the transposed climates.

The Great Lakes hydrology of each transposed climate was estimated, as before, by applying the system of hydrological models to these data sets (but this time, directly) and comparing outputs for each transposed climate to a base case derived with the model outputs from historical meteorological data. This approach allowed preservation of reasonable spatial and temporal variations in meteorology and preserves the interdependencies that exist between the various meteorological variables. It also allowed the use of appropriate spatial and temporal scales, better matching the models than do the GCM output corrections. Similar studies were made to transpose the climate occurring during the 1993 Mississippi flood to assess climate change impacts on hydrology in the Great Lakes (*Quinn et al.* 1997).

The transposed climates lead to higher and more variable over-land evapotranspiration and lower soil moisture and runoff with earlier runoff peaks since the snow pack is reduced up to 100%. Water temperatures increase and peak earlier. Heat resident in the deep lakes increases throughout the year. Buoyancy-driven water column turnover frequency drops and lake evaporation increases and spreads more throughout the annual cycle. The response of runoff to temperature and precipitation changes is coherent among the lakes and varies quasi-linearly over a wide range of temperature changes, some well beyond the range of current GCM predictions for doubled CO_2 conditions.

US National Assessment of Climate Change in the Great Lakes

A more recent quantification of the effects of climate change on Great Lakes levels is documented in *Lofgren et al.* (2002). This study, funded by EPA, was a part of the US National Assessment of the Potential Consequences of Climate Variability and Change (NACC), which was part of the US Global Change Research Program. The study used as input the results of the version 1 Canadian model, CGCM1, and the version 2 United Kingdom model, HadCM2. Each of these is an earlier version of the two GCMs used in the present study, current in 1999, when the NACC study was initiated. The major improvement in these GCM runs over those used in prior studies is that the scenarios created a time series of simulated climate with a prescribed gradual increase in greenhouse gas concentrations. This enabled the investigation of climate change effects within any chosen range of years within the scenario, not just at a static level of greenhouse gases. The use of transient greenhouse gas concentrations was made more realistic through the use of full coupling between the atmospheric and oceanic components of these GCMs. Also new was the use of parameterizations of the direct radiative effect of sulfate aerosols, a mechanism that gained recognition during the 1990s as an effect with a significant trend, beginning with *Charlson et al.* (1992). Finally, these models were run in an ensemble of realizations, each with slightly different initial conditions, but quickly evolving into independent time sequences of climate variables, but each remaining consistent with the same time series of forcing factors (i.e. greenhouse gas and aerosol concentrations).

Lofgren et al. (2002) found that CGCM1 predicted increased temperature and precipitation into the future. However, the increased evaporation associated with increased temperature overbalanced the increased precipitation, and resulted in lake levels lowered by up to 0.72 m in a time period centered about 2030 relative to a base time period centered at 1989, and a drop of as much as 1.38 m for a time period centered at 2090. The HadCM2 model also had increases in both temperature and precipitation. However, the increase in temperature was much less than in CGCM1 and the increase in precipitation was much greater and tended to take the more dominant role. For the 2030 time period, the changes in lake levels ranged among the Great Lakes from a drop of 0.01 m to a rise of 0.05 m. For the 2090 time period, rises in lake levels ranged from 0.01 m to 0.35 m.

Lofgren et al. (2002) also showed decreases in lake ice cover, with larger decreases in the CGCM1 runs than in the HadCM2 runs. They simulated effects of greenhouse warming on the supply of groundwater for municipal use in the vicinity of Lansing, Michigan, illustrating the possibility of complete drawdown of the aquifer in some spots [see also *Croley and Luukkonen* (2003)]. They also used an interest satisfaction model, which attempted to quantify the degree to which shipping and hydropower interests in the upper St. Lawrence River and the outlet of Lake Ontario might be satisfied, given the projected changes in lake levels and water supplies. This model showed considerably reduced interest satisfaction for most of the interests when using the output from the CGCM1, but little change when using the HadCM2.

Present Study

GLERL extracted GCM output changes between a baseline period of 1961—1990 and the future 30-year period 2040—2069 for models: HadCM3 A1FI (warm/wet), HadCM3 B22 (not as warm/wet), CGCM2 A21 (warm/dry), and CGCM2 B23 (not as warm/dry). They provided these changes for: daily precipitation increase (ratio), minimum daily air temperature increase at 2 m (°C), average daily air temperature increase at 2 m (°C), maximum daily air temperature increase at 2 m (°C), wind speed increase at 2 m (ratio), specific humidity increase (ratio), and cloud cover increase (ratio). GLERL adjusted historical daily meteorology data for the Great Lakes basin over 1950—1999 with the GCM climate changes and simulated Great Lakes hydrology under the various scenarios. GLERL used their conceptual models for simulating moisture storages in, and runoff from, the 121 watersheds draining into the Laurentian Great Lakes, over-lake precipitation into each lake, and the heat storages in, and evaporation from, each lake. GLERL combined these components as net water supplies for each lake to consider the climate scenarios.

This 2003 GLERL study of climate scenarios in the Great Lakes basin for the IJC Lake Ontario—St. Lawrence River study is presented here. The next section (Great Lakes Dynamics and Climate) describes the present Great Lakes climate, the physical characteristics of the Great Lakes and the dynamics of these large water bodies. The following section (Methodology) outlines the methodology of climate scenario consideration from GCM experiments. The hydrological models for basin runoff, over-lake precipitation, and lake thermodynamics are described in the next section (Great Lakes Physical Process Models) and results from these models are presented in the succeeding section (Great Lakes Climate Change Hydrologic Response). The final section (Hydrological Sensitivities) recapitulates the major points of this research.

Great Lakes Dynamics and Climate

There is a major tendency to think of Great Lakes water levels in terms of extremes rather than of normal conditions. Within recent memory we had the record low lake levels of 1964. This resulted in docks sitting out of the water, insufficient depths for navigation in many harbors and channels, and greatly reduced recreational opportunities. Record high lake levels with resultant flooding and shore damage and erosion followed these low levels in 1973. The lake levels remained high until 1986 and new record highs were once again set on Lakes Superior, Michigan-Huron, St. Clair, and Erie, after which they returned to near-average conditions,. More recently (2000-2003) we again experienced low level conditions on all lakes.

This section presents an overview of the physical characteristics of the Great Lakes from a water quantity perspective, outlines the basin and lake physical processes, summarizes the climatology of the Great Lakes, examines the types of natural lake level fluctuations and their causes, compares the natural fluctuations with existing diversions and regulation effects, describes current conditions, and concludes with a long-term perspective on lake levels.

Great Lakes Overview

The Great Lakes basin, in Figure 1, has an area of approximately 770,000 km^2 (300,000 mi^2), about one-third of which is water surface. Others give cursory descriptions; see *Freeman and Haras* (1978), the *U. S. Army Corps of Engineers* (1985), and the *Coordinating Committee on Great Lakes Basic Hydraulic and Hydrologic Data* (1977). The basin extends some 3,200 km (2,000 mi) from the western edge of Lake Superior to the Moses-Saunders Power Dam on the St. Lawrence River. The water surface drops in a cascade over this distance some 180 m (600 ft). The most upstream, largest, and deepest lake is Lake Superior. The lake has two interbasin diversions of water into the system from the Hudson Bay Basin: the Long Lac and Ogoki Diversions. Lake Superior waters flow through the lock and compensating works at Sault St. Marie and down the St. Mary's River into Lake Huron where it is joined by water flowing from Lake Michigan. Lake Superior is completely regulated, to balance Lakes Superior, Michigan, and

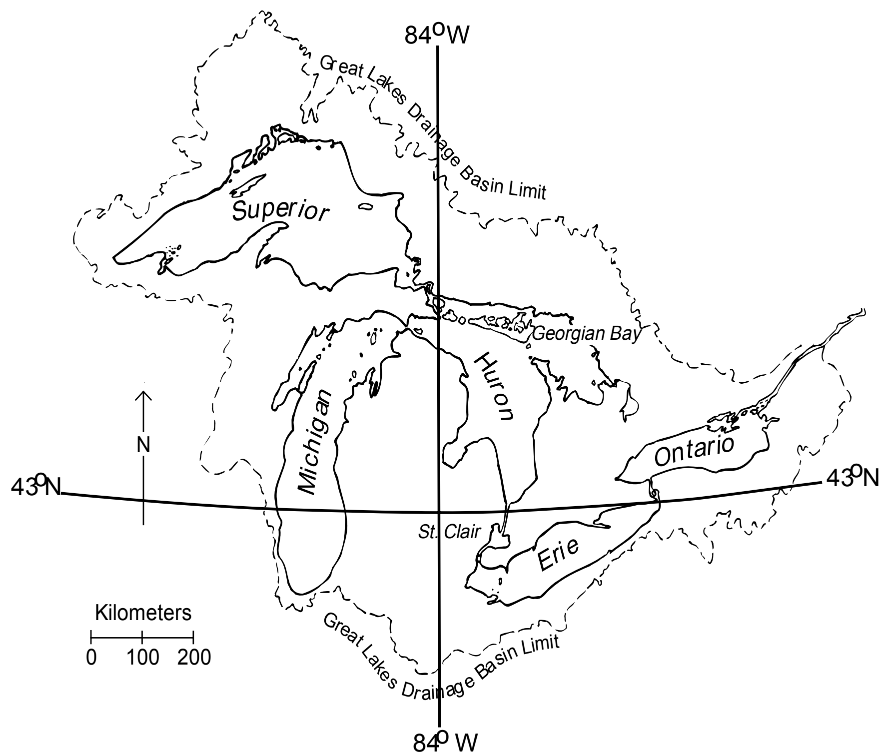

Figure 1. The Laurentian Great Lakes Basin.

Huron water levels, according to Regulation Plan 1977, under the auspices of the International Joint Commission (*International Lake Superior Board of Control* 1981, 1982).

Lakes Michigan and Huron are considered to be one lake hydraulically because of their connection through the deep Straits of Mackinac. Another interbasin diversion takes place from Lake Michigan at Chicago. Here water is diverted from the Great Lakes to the Mississippi River Basin. The water flows from Lake Huron through the St. Clair River, Lake St. Clair, and Detroit River system into Lake Erie. The drop in water surface between Lakes Michigan-Huron and Lake Erie is only about 2 m (8 ft). This results in a large backwater effect between Lakes Erie, St. Clair, and Michigan-Huron; changes in Lakes St. Clair and Erie levels are transmitted upstream to Lakes Michigan and Huron. From Lake Erie, the flow is through the Niagara River and Welland Diversion into Lake Ontario. The major drop over Niagara Falls precludes changes on Lake Ontario from being transmitted to the upstream lakes. The Welland Diversion is an intrabasin diversion bypassing Niagara Falls and is used for navigation and hydropower. There is also a small diversion into the New York State Barge Canal System, which is ultimately discharged into Lake Ontario. Lake Ontario is completely regulated in accordance with Regulation Plan 1958D to balance interests upstream on Lake Ontario with those downstream on the St. Lawrence Seaway [estimated to have lowered Lake Ontario 0.75 m (2.5 ft) during the record high water levels of 1986]. The Moses-Saunders Power Dam between Massena, New York and Cornwall, Ontario controls the outflows. From Lake Ontario, the water flows through the St. Lawrence River to the Gulf of St. Lawrence and to the ocean.

Lakes Superior, Michigan, Huron, and Ontario are very deep, while Lakes Erie and St. Clair are very shallow. Table 1 contains pertinent gross statistics on the sizes of the Great Lakes, Lake St. Clair, and their basins.

Physical Processes

The behavior of the Laurentian Great Lakes system is governed by its huge storages of water and energy. There are three main conservation laws to consider relative to these huge storages: 1) mass balances in the basins, 2) mass balances in the lakes, and 3) energy balances in the lakes. There are also mass and energy balances to consider for the lakes' ice cover. The first conserva-

Table 1. Laurentian Great Lake Size Statistics[a].

Characteristic		Superior	Michigan	Huron	St. Clair	Erie	Ontario
Basin Area[b],	km^2	128,000	118,000	131,000	12,400	58,800	60,600
	mi^2	49,300	45,600	50,700	4,800	22,700	23,400
Surface Area,	km^2	82,100	57,800	59,600	1,114	25,700	18,960
	mi^2	31,700	22,316	23,000	430	9,920	7,320
Volume,	km^3	12,100	4,920	3,540	3	484	1,640
	mi^3	2,900	1,180	850	1	116	393
Average Depth,	m	147	85	59	3	19	86
	ft	482	280	190	10	62	280
Maximum	m	405	281	229	6	64	244
	ft	1,330	923	750	21	210	802

[a]*Coordinating Committee on Great Lakes Basic Hydraulic and Hydrologic Data* (1977).
[b]This does not include the surface area of the lake.

tion law (mass balance on the basins) comprises the primary process determining lake levels: the hydrological cycle of the Great Lakes Basin (*Croley* 1983a). As shown in Figure 2, precipitation enters the snow pack, if present, and is then available as snow melt depending mainly on air temperature and solar radiation. Snowmelt and rainfall partly infiltrate into the soil and partly run off directly to rivers, depending upon the moisture content of the soil. Infiltration is high if the soil is dry, and surface runoff is high if the soil is saturated. Soil moisture evaporates or is transpired by vegetation depending upon the types of vegetation, the season, solar radiation, air temperature, humidity, and wind speed. The remainder percolates into deeper basin storages, which feed the rivers and lakes through interflows and groundwater flows. Generally, these river supplies are high if the soil and groundwater storages are large. Because of this buffering effect of the large snow pack and the large soil, groundwater, and surface storages, runoff from rivers into a lake can remain high for many months or years after high precipitation has stopped.

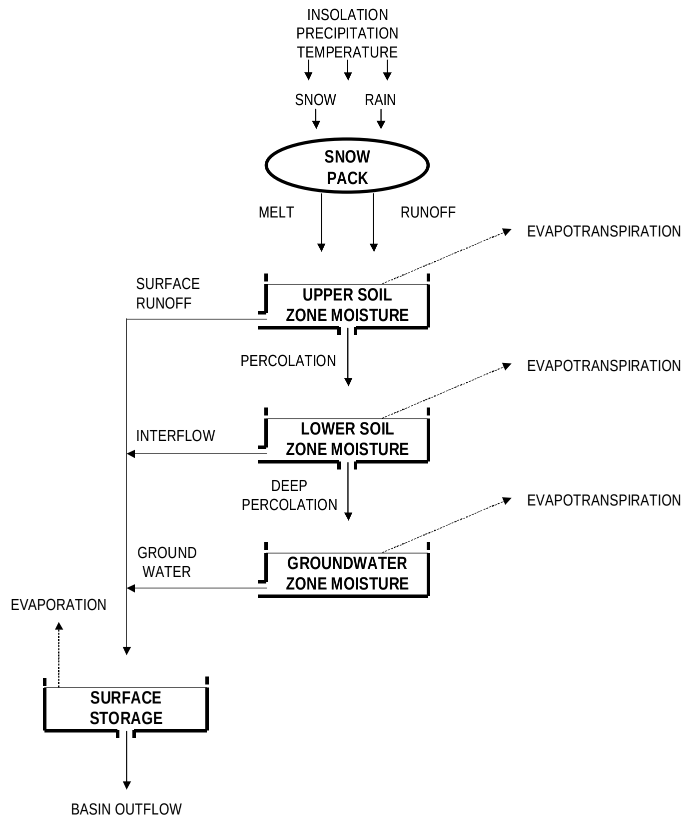

Figure 2. Great Lakes Subbasin Mass Balance

Mass conservation in the lake is the next major determinant of lake levels. Major sources of water into a lake include precipitation on the land basin, which results in runoff into the lake, precipitation over the lake surface, inflow from upstream lakes, and diversions into the lake. Net groundwater flows directly to each of the Great Lakes are generally neglected (*DeCooke and Witherspoon* 1981). The outflows consist of evaporation from the lake surface, flow to downstream lakes, and diversions. The imbalance between the inflow and outflow results in the lake levels either rising if there is more inflow than outflow, represented by a positive change in storage, or falling if there is more outflow than inflow, represented by a negative change in storage. The large lake water storages provide a buffering of the input fluctuations with regard to output variations. The large surface areas of the lakes enable large storage changes with very small water level changes; hence, outputs (which are a function of water levels) change slowly.

Energy conservation in a lake actually must be considered together with a lake's mass balance. Lake heat storage is a function of the lake's size and shape and of its surface inputs of solar insolation and reflection (short wave exchanges), thermal emission and atmospheric emission (net long wave exchange), conduction to the atmosphere (sensible heat transfer), heat loss through evaporation (latent and some advection), other advection terms (precipitation, inflows, and outflows), and ice growth and melt. Evaporation is a function of surface temperature (heat storage), air temperature (atmospheric stability), humidity, and wind speed. Water surface temperatures generally peak in August (September for Superior) at 15-25°C resulting in stable summertime temperature stratification in the water column (high-density cool water at depth and low-density warm water at the surface). Surface temperatures drop during the fall and winter, and the water column in each lake "turns over" as temperatures drop through 4°C where water density is maximum (now-heavier surface layers sink and mix with deep now-lighter waters). Turn over occurs again in the spring as surface temperatures rise to that of maximum density.

There is also extensive ice cover on most of the lakes during most winters. Lake Superior averages about 75% ice-covered, Michigan is 45%, Huron is 68%, Erie is 90%, and Ontario is 24%. Ice formation and breakup is governed by additional mass and energy balances that take place simultaneously with those of the lakes' water bodies. The Great Lakes do not ordinarily freeze-over completely (*Assel et al.* 1983) because of the combination of their large heat storage capacity, large surface area, and their location in the mid-latitude winter storm track. Alternating periods of mild and cold air temperatures combine with episodic high and low wind stresses at the water surface to produce transitory ice conditions during the winter. Ice cover in mid-lake regions is often in motion. Lake Erie ice speeds have been observed to average 8 cm/s with a maximum speed of 46 cm/s (*Campbell et al.* 1987). Ice can form, melt, or be advected toward or from most mid-lake areas throughout the winter (*Rondy* 1976). When ice is advected into areas with existing ice cover, it can under- or over-ride the ice cover, forming rafted rubble 5-10 m thick. The normal seasonal progression of ice formation begins in the shallow shore areas of the Great Lakes in December and January. The deeper mid-lake areas normally do not form extensive ice cover until February and March. Ice is lost over all lake areas during the last half of March and during April.

Ice formation alters the surface thermodynamics of the lakes, changing subsequent ice formation, surface heating or cooling, lake evaporation, and lake responses to atmospheric changes. The large heat storages of the lakes provide a buffering; they forestall and reduce ice formation and shift the large evaporation response. Water temperatures lag air temperatures and evaporation lags surface heating (insolation). Evaporation peaks in October-November on Lake Erie and in November-December on Lake Superior.

The large basin and lake storages of water and ice and the large lake and ice storages of energy represent an "intrinsic memory" that allow scientists to forecast basin moisture storage and runoff (basin storage buffering) in the face of uncertain meteorology. It also allows prediction of evaporation (heat storage buffering) and lake levels (lake storage buffering) of up to about six months of low-frequency changes. It further enables estimation of ice formation amounts and timing as well as all secondary hydrological variables.

Climatology

Precipitation causes the major long-term variations in lake levels (*Quinn and Croley* 1981; *Quinn* 1985). Table 2 shows that annual precipitation ranges from about 82 cm (32 in) for Superior to 93 cm (37 in) for Ontario. Figure 3 depicts total annual precipitation over Lakes Michigan-Huron, St. Clair, and Erie for the 1900-1979 period (*Quinn* 1981; *Quinn and Norton* 1982). From 1900 through 1939, a low precipitation regime predominated with the majority of the years falling below the mean. From about 1940 until recently, a high precipitation regime has existed.

Table 2. Partial Great Lakes Annual Water Balance (1951-1988).

Component	Superior		Michigan		Huron		Erie		Ontario	
	(cm)	(in)	(cm)	(in)	(cm)	(in)	(cm)	(in)	(cm)	(in)
Lake Precipitation[a]	82	32	83	32	87	34	81	36	93	37
Lake Runoff[a]	62	24	64	25	84	33	80	32	169	67
Lake Evaporation[a]	56	22	65	25	63	25	90	35	67	26

[a]Equivalent depth over the lake area.

Of particular interest is the high precipitation in the early 1950s, the low precipitation in the early 1960s that led to the record lows, and a consistently very high precipitation regime from the late 1960s through the late 1980s. Table 3 summarizes Great Lakes annual precipitation totals by basin for several periods. Of particular interest are the progressions of increasing precipitation for each basin. While the 1940-90 period is generally above normal (2-8% higher than the 1900-69 average and -2-6% higher than the 1900-90 average), the last 20 of those years are higher still (8-13% than the 1900-69 average and 2-11% higher than the 1900-90 average); 1985 set many new records with the highest precipitation to that date (8-40% higher than the 1900-69 average and 7-33% higher than the 1900-90 average).

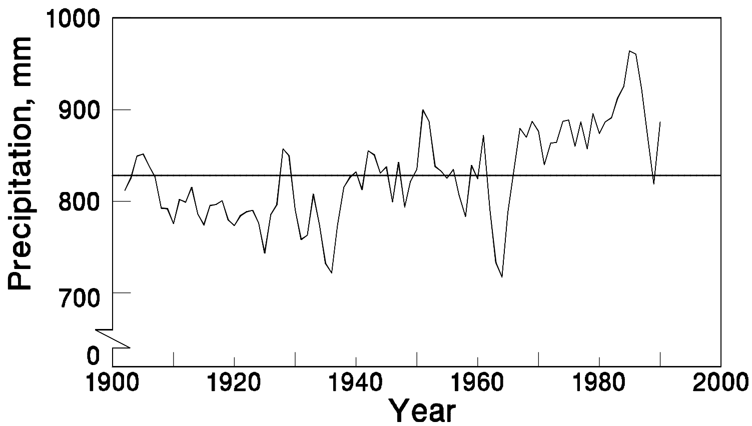

Figure 3. Lakes Michigan, Huron, St. Clair, and Erie 3-year-Mean Precipitation (1900-90)

Variations in air temperature also influence lake level fluctuations. At higher air temperatures, plants tend to use more water, resulting in more transpiration, and there are higher rates of evaporation from both the ground surface and the lake. This yields less runoff for the same amount of precipitation than would exist during a low temperature period when there is less evaporation and transpiration. Coupled with the higher lake evaporation, lake levels drop with increasing air temperature, all other things being equal. The annual mean air temperature around the perimeter of the Great Lakes since 1900, summarized in Figure 4, indicate three distinct temperature regimes: a low temperature regime from 1900-1929, a higher temperature regime from about 1930-1959,

Table 3. Great Lakes Annual Precipitation Summary.

Period	Superior		Michigan		Huron		Erie		Ontario	
	(cm)	(in)	(cm)	(in)	(cm)	(in)	(cm)	(in)	(cm)	(in)
1900-39	72	29	78	31	77	31	85	34	86	34
1940-90	81	32	82	33	86	34	89	35	93	37
1970-90	84	33	86	34	89	35	94	37	98	39
1985	98[a]	39[a]	102[a]	40[a]	105[a]	41[a]	106	42	100	40
1900-69[b]	75	30	79	31	80	32	87	34	87	34
1900-90[b]	79	31	84	33	84	33	89	35	88	35

[a]Record high for 1900-90.
[b]Long-term period averages are supplied for comparison.

and an additional low regime from 1960-present period. The difference between the previous and current regime is a drop of about 1°F.

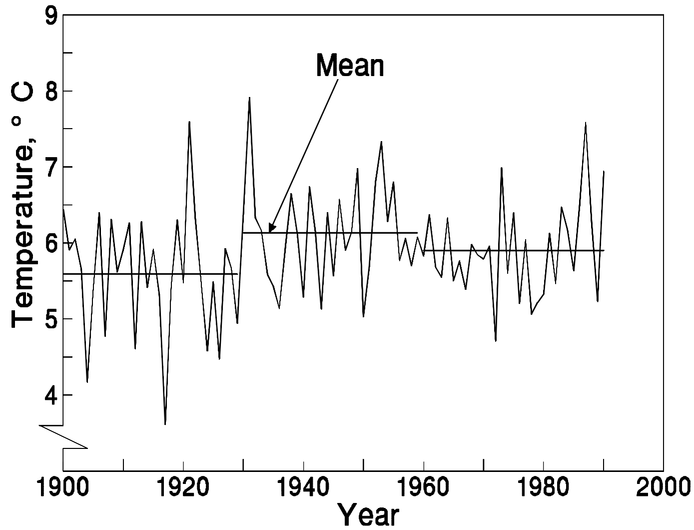

Figure 4. Great Lakes Annual Air Temperature (1900-29, 1930-59, 1960-90)

The magnitude of the hydrological variables varies with season, as shown in Figure 5 for Lake Erie (*Quinn* 1982; *Quinn and Kelley* 1983). The monthly precipitation is fairly uniformly distributed throughout the year, while the runoff has a peak during the spring which results primarily from the spring snow melt. The runoff is at a minimum in the late summer and early fall due to large evapotranspiration from the land basin. The lake evaporation reaches a minimum during the spring and gradually increases until it reaches a maximum in the late fall or early winter. The high evaporation period is due to very cold dry air passing over warm lake surfaces. The integration of these components is depicted in the net basin supply, which consists of the precipitation plus the runoff minus the evaporation. As seen from Table 2, these three components of net basin supply are all of the same order of magnitude for each lake. Annual runoff to the lake ranges from about 62 cm (24 in) for Superior to 169 cm (67 in) for Ontario, and annual lake evaporation ranges from about 56 cm (22 in) for Superior to 90 cm (35 in) for Erie. The net basin supply is seen in Figure 5 to reach a maximum in April and a minimum in the late fall. The negative values indicate that more water is leaving the lake through evaporation than is being provided by precipitation and runoff.

Lake Level Fluctuation and Trends

There are three primary types of lake level fluctuations: long-term lake levels (represented on an annual basis), seasonal lake levels, and short-period lake level changes due to wind setup and storm surge. Annual fluctuations result in most of the variability leading to the record high and low lake levels. The annual lake levels are shown in Figure 6 from 1860 through the present to illustrate the long-term variability of the system. The record highs in 1952, 1973, and 1986 and record lows in 1935 and 1964 are readily apparent. There is an overall range of about 2 m (6 ft) in the annual levels. Of particular interest is the fall in the levels of Lakes Michigan and Huron occurring in the mid-1880's from which the lakes never recovered. This probably results from dredging for deeper draft navigation in the St. Clair River. Other changes in the St. Clair River include

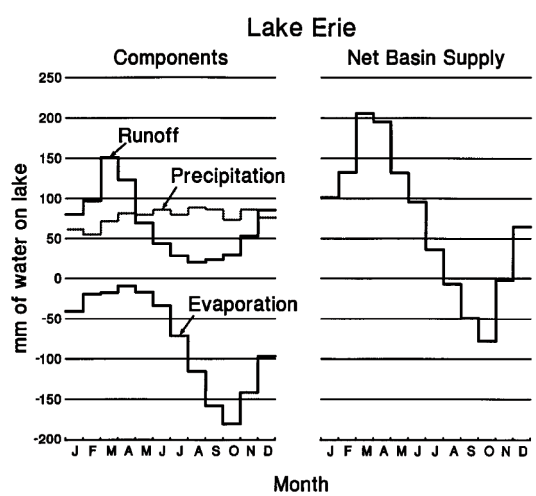

Figure 5. Lake Erie Seasonal Net Basin Supplies

sand and gravel dredging between about 1908 and 1924, a 7.6 m (25 ft) navigational project in the mid-1930's, and an 8.2 m (27 ft) navigation project in the late 1950's and early 1960's. Without these changes, Lake Michigan-Huron would be approximately 0.5 m (1.5 ft) higher than it is today.

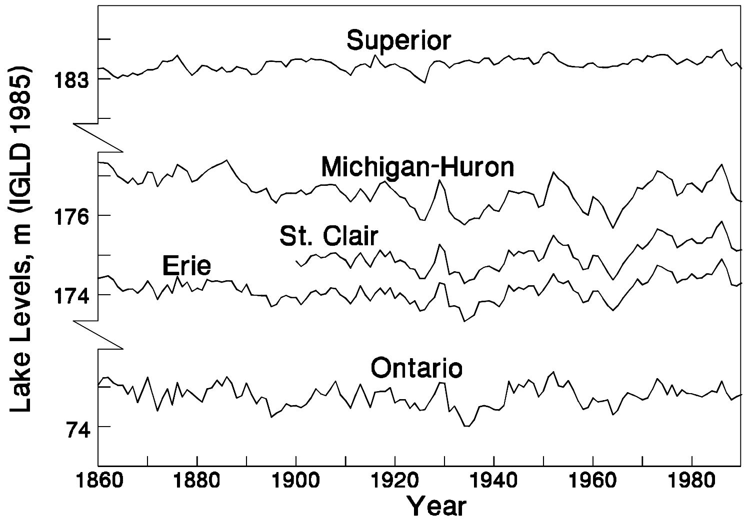

Figure 6. Great Lakes Annual Water Levels (1900-90).

The three-year precipitation mean in Figure 3 correlates very well with annual lake levels as observed by superimposing the annual precipitation on the annual Lake Erie water levels in Figure 7. The precipitation tends to lead the water levels by approximately one year, as shown here by the 1929 highs, the 1935 lows, the 1952 highs, and the 1963 lows. In particular, the last 15 years of high precipitation resulted in very high water levels. Thus, the continuing high levels are the result of the increased precipitation regime since 1940 coupled with the lower temperature regime since 1960.

Superimposed on the annual levels are the seasonal cycles shown in Figure 8; each lake undergoes a seasonal cycle every year. The magnitude depends upon the individual water supplies. The range varies from about 30 cm (1 ft) on the upper lakes to about 38 cm (1.3 ft) on the lower lakes. In general, the seasonal cycles have a minimum in the winter, usually January or February. The levels then rise due to increasing water supplies from snow melt and spring precipitation until they reach a maximum in June for the smaller lakes, Erie and Ontario, and September in the case of Lake Superior. When the net water supplies diminish in the summer and fall, the lakes begin their seasonal decline.

The final type of fluctuation, common along the shallower areas of the Great Lakes, particularly Lake Erie, Saginaw Bay, and in some cases on Green Bay, are storm surges and wind set-up. When the wind is blowing along the long axis of a shallow lake or bay, a rapid difference in levels can build over the water. This difference can be as large as 5 m (16 ft) for Lake Erie (storm of 2 December 1985). These storm conditions, when superimposed on high lake levels, cause most of the Great Lakes shoreline damage.

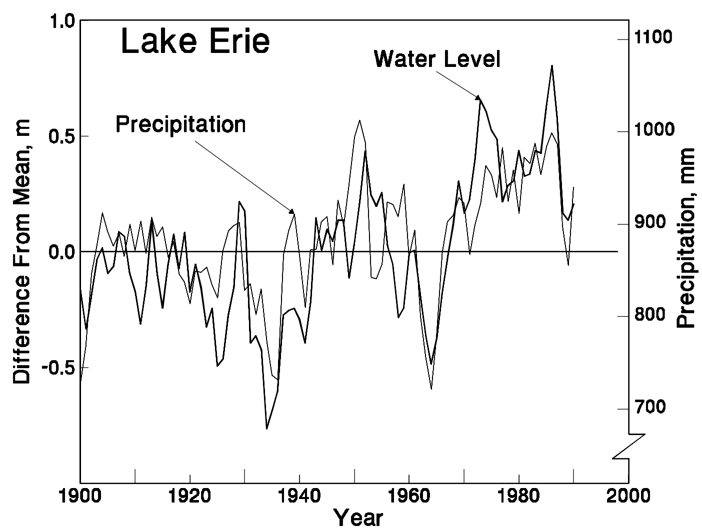

Figure 7. Lake Erie Annual Water Levels and Precipitation

Looking in more detail at past trends in lake levels, along with more recent conditions for Lake Erie, we see a steady progression of changes in lake levels with time in Figure 9. These changes reflect the changes in precipitation, illustrated in Figure 3 and summarized in Table 3. At the bottom of Figure 9 are the record low lake levels for each month, which were set primarily in 1964. Proceeding upwards we have the 40-year average from 1900-1939. From 1940-1979, the lake is at a still higher average level. Taking the 21-year period from 1970-1990, we see that the lake level average is higher yet, followed by the record highs set in 1985. Record levels for the month were set in April and May 1985 on Lakes Michigan-Huron, St. Clair, and Erie; they were set for November 1985 through April 1986 on Lakes Erie and St. Clair. Since that time, a record drought brought water levels back to their long-term normal values in the late 1980s and early 1990s.

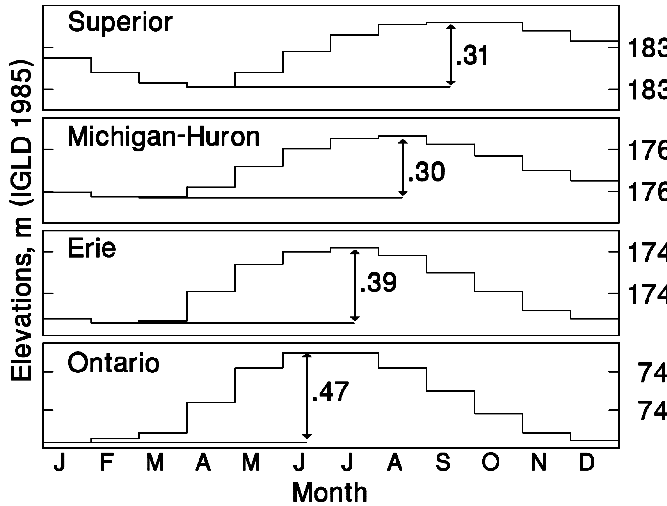

Figure 8. Average Seasonal Great Lakes Levels (1900-90)

Diversions

It is interesting to compare each impact of an existing diversion on all lakes levels in Table 4 with natural lake-level fluctuations (*International Great Lakes Diversions and Consumptive Uses Study Board* 1985). This enables a comparison of man's impacts with natural fluctuations. The Long Lac and Ogoki Diversions average about 160 m^3s^{-1} (5,600 ft^3s^{-1}) and raise lake levels between 6 cm (0.21 ft) and 11 cm (0.37 ft). The Chicago Diversion averages about 90 m^3s^{-1} (3,200 ft^3s^{-1}) and lowers lake levels between 2 cm (0.07 ft) and 6 cm (0.21 ft). The Welland Canal, which bypasses Niagara Falls, averages about 270 m^3s^{-1} (9,400 ft^3s^{-1}) and lowers lake levels between 2 cm (0.06 ft) and 13 cm (0.44 ft) with no effect on Lake Ontario. The combined effect on the lakes ranges from a 2 cm (0.07 ft) rise for Lake Superior to a 10 cm (0.33 ft) drop for Lake Erie. The diversion effects are therefore small in comparison with the one or more meter (several foot) variation associated with short-term storm movements, the 30-38 cm (1-1.3 ft) seasonal cycle, and the 2 m (6 ft) range of annual variations.

The small effects of the diversions along with the long response time of the system illustrate why diversions are not suitable for lake regulation. Due to the large size of the

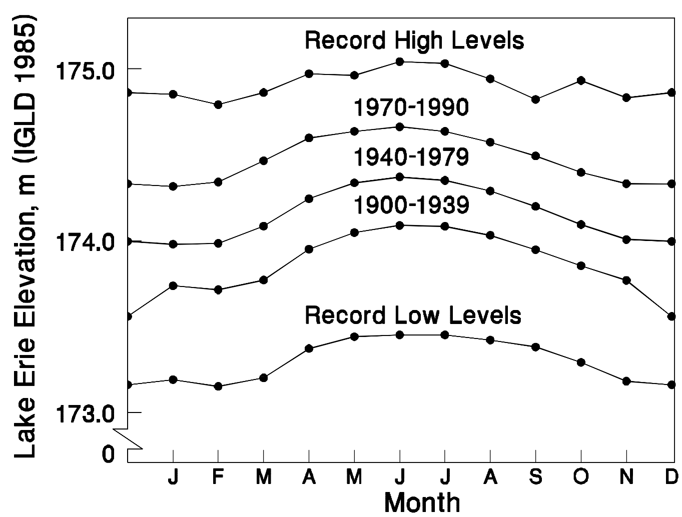

Figure 9. Lake Erie Seasonal Water Level Comparisons

Table 4. Impact of Existing Diversions on Lake Levels.

Diversion	Amount		Superior		Mich-Hur		Erie		Ontario	
	(m^3s^{-1})	(ft^3s^{-1})	(cm)	(ft)	(cm)	(ft)	(cm)	(ft)	(cm)	(ft)
Ogoki-Long Lac	160	5600	+6	+0.21	+11	+0.37	+8	+0.25	+7	+0.22
Chicago	90	3200	-2	-0.07	-6	-0.21	-4	-0.14	-3	-0.10
Welland	270	9400	-2	-0.06	-5	-0.18	-13	-0.44	0	0
COMBINED			+2	+0.07	-1	-0.02	-10	-0.33	+2	+2

Great Lakes system, it responds very slowly to man-induced changes. This is illustrated in Figure 10 by the length of time it takes from the start of a hypothetical diversion on Lakes Michigan and Huron (of the magnitude of the Chicago diversion) until the ultimate effect of that diversion is reached on Lakes Michigan-Huron, and Erie. It takes approximately 3-3.5 years to achieve 50% of the ultimate effect and 12-15 years to get 99% of the effect. (These results depend somewhat on the lake levels at the beginning of the diversion.) Thus, regulation by diversion would not produce changes responsive to natural fluctuations. Recent studies at GLERL indicate that an increase of 10% in the Niagara River discharge from Lake Erie (and consequent increases in Lake Erie inflow) would lower it 27 cm (0.89 ft) in about 11-12 years and lower Lakes Michigan and Huron 14 cm (0.46 ft) in this same period. If Lake Erie inflows were held constant (not possible at the present time), then it would take 6 months to 1 year to achieve this lowering.

Additional interbasin diversions are a highly controversial issue at the present time around the Great Lakes. Possible uses of Great Lakes water outside the basin are flow augmentation for navigation, energy uses such as synthetic fuels or pipelines, agriculture and aquifer recharge, and municipal water supplies. A small pipeline project such as the Powder River coal slurry pipeline would require 0.2 m^3s^{-1} (7 ft^3s^{-1}) of water and would have no measurable impact on lake levels. A synthetic fuels project, highly unlikely at this time, could require approximately 23 m^3s^{-1} (800 ft^3s^{-1}) and result in a lake level lowering of 1-2 cm (0.04-0.06 ft). A major agricultural or aquifer recharge project could require 300 m^3s^{-1} (10,000 ft^3s^{-1}) and would result in lake level decreases ranging from 12 cm (0.4 ft) on Lake Erie to 21 cm (0.7 ft) on Lake Michigan-Huron. It should be emphasized that these are hypothetical projections for illustration only.

Future

Water levels ordinarily do not change quickly, as shown by the above consideration of diversions. Other studies at GLERL indicate that if normal meteorological conditions were realized ("normal" being the average conditions over 1900-69) instead of the record drought of the late 1980s, it would have taken about 6 years for Lake Michigan-Huron to return from its January

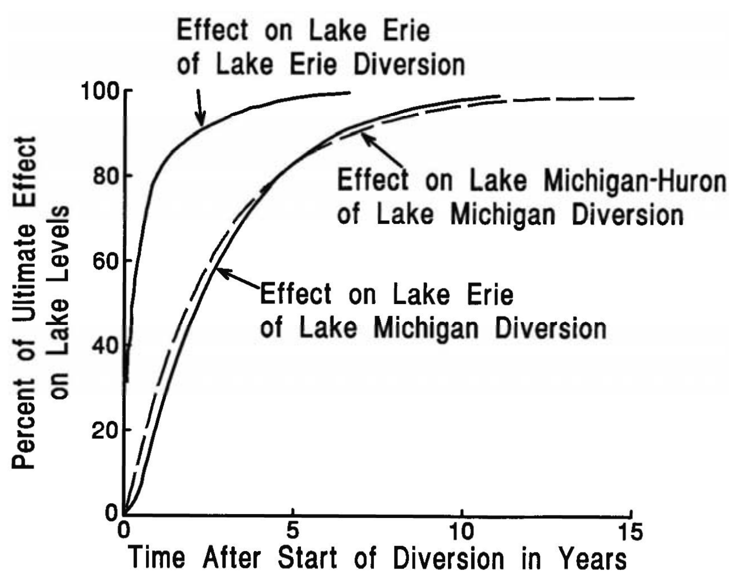

Figure 10. Selected Great Lake Responses to Diversions

1986 level to its normal (1900-69) level. About 7 years would have been required for Lakes St. Clair and Erie to return to within 10 cm (4 in) of normal, and about 9 years would have been required for them to return to within 5 cm (2 in) of normal. Even supposing that we encountered a drought similar to the 1960-64 conditions, about 3.5 years would have been required for Lake Michigan-Huron and about 4 years would have been required for Lakes St. Clair and Erie.

A long-term perspective on Lake Michigan levels for 7,000 years was reconstructed through geologic and archaeological evidence (*Larsen* 1985) under work sponsored by the Illinois State Geological Survey. Conditions several thousand years ago were not necessarily the same as today due to isostatic rebound and uplift during the intervening time. But, in general, this provides additional perspective on possible conditions we may experience in the future. Looking at just the last 2,500 years, during which time the Great Lakes were in their current state, there were major lake level fluctuations. During most of this time the levels were much higher and more variable than they have been during the last 120 years of record. If the past is any indication, lake levels in the future could go through a considerably larger range than we have experienced lately. Indeed, the period of record, which makes up what many consider to be normal, the early 1900's through the 1960's, may represent abnormal conditions.

Summary Comments on Great Lakes Dynamics

Huge storages of water in the basins and the lakes and of energy in the lakes give the Laurentian Great Lakes their characteristic behavior. They filter the variability of the meteorological inputs and enable hydrological predictions in the face of uncertain meteorology, if the storage amounts are known. Historically, lake levels are most affected by temporal patterns of precipitation; air temperature patterns play a lesser but important role also. It is important to keep in perspective that while we have ranges in annual lake levels of 1-2 m (4-6 ft), and additional short-term effects on the order of 2-3 m (7-8 ft), the effects of man on the system are relatively small, on the order of about 5 cm (0.2 ft). While the lakes are slow changing over the long term in the face of normal meteorology, past fluctuations have been very large. Future changes will depend mostly on future climate.

Methodology

Climate Data

The Great Lakes hydrological models used in this study (described subsequently) require daily values of precipitation, air temperature, wind speed, humidity, and cloud cover or insolation at many surface locations. In past determinations of water supply effects from climate change scenarios (*Croley* 1990, 1992b, 1993a; *Croley and Hartmann* 1989; *Hartmann* 1990; *Lofgren et al.* 2002), GLERL used about 1,800 meteorological stations for overland precipitation and air temperature and about 40 meteorological stations for over-lake air temperature, humidity, wind speed, and cloud cover (for determining insolation). Recent experience (*Croley and Hartmann* 1986, 1987) suggests that 200-300 stations per lake basin for overland meteorology and about 5-8 stations per lake for over-lake meteorology would be sufficient for operation of the large-area runoff and evaporation models at daily time intervals for studies of the type considered here.

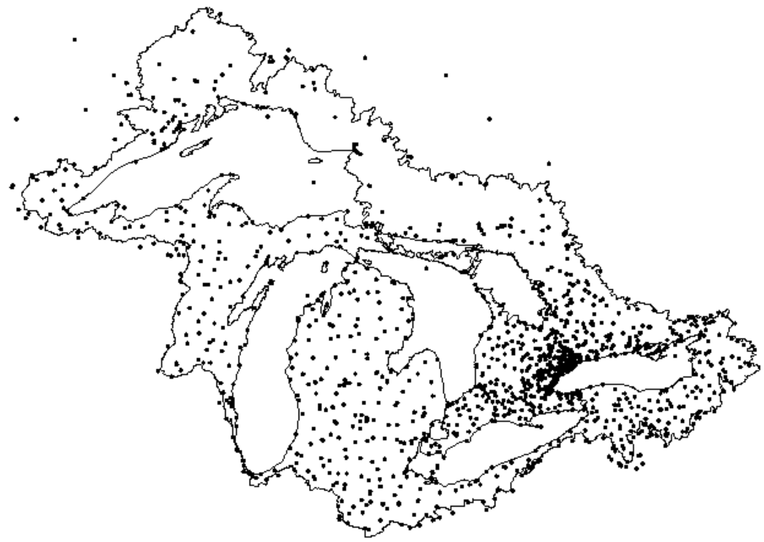

Figure 11. Base Case Temperature and Precipitation Stations

Daily maximum and minimum air temperatures, precipitation, and snowfall were obtained for the 52-year period of 1948-1999 from the dense array of stations in the National Weather Service's cooperative observer network and from Environment Canada; see Figure 11. Out of this dense array of stations, a subset have daily records of wind speed, humidity, and cloud cover, and are generally located at the weather service offices and airport observing stations; see Figure 12. These stations were used in earlier studies (*Croley* 1990, 1992b, 1993a; *Croley and Hartmann* 1986, 1987, 1989; *Hartmann* 1990; *Lofgren et al.* 2002); they were augmented here to extend their data period through 1999. The data reductions of these earlier studies, to determine areal Thiessen-averaged meteorologi-

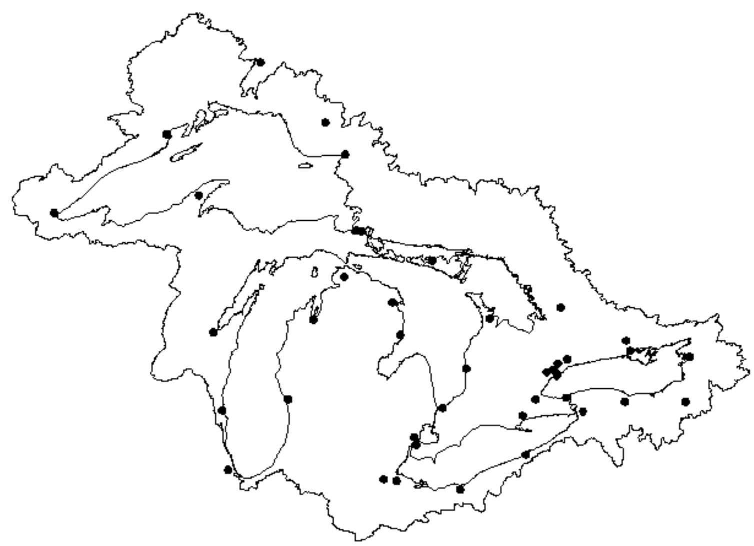

Figure 12. Base Case Temperature, Humidity, Wind Speed, and Cloud Cover Stations

cal time series over each of the 121 sub-basins and the 7 lake surfaces, were enormous (*Croley and Hartmann* 1985), but the software for this was developed at that time. Now, improved computers allow re-reduction of all data in a timely fashion with this software.

Changed Climate

GLERL constructed a master computer procedure to integrate their Large Basin Runoff Model, over-lake precipitation estimates, and their lake evaporation models for all Great Lakes to provide a net water supply model for the entire Great Lakes system. They developed it specifically to look at the impact of changed climate by doing simulations with changed meteorology that represent scenarios of changed climate and comparing with simulations based on historical meteorology (representing an unchanged climate). Inputs are areal-average daily precipitation and maximum and minimum air temperatures for each of the 121 watersheds about the Great Lakes and areal-average daily air temperature, cloud cover, humidity, and wind speed for each of the five Great Lakes and Lake St. Clair.

GLERL's general procedure for the investigation of steady-state behavior under a changed climate is similar to that used for the 1989 EPA study, as detailed elsewhere (*Croley* 1990; *Louie* 1991); it required that GLERL first simulate 50 years of "present" hydrology by using historical daily maximum and minimum air temperatures, precipitation, wind speed, humidity, and cloud cover data for the 1950-1999 period; this is called the "base case" scenario. The initial conditions were arbitrarily set but an initialization simulation period of 1 January 1948 through 31 December 1949 was used to allow the models to converge to conditions (basin moisture storages, water surface temperatures, and lake heat storages) initial to the 1 January 1950 through 31 December 1999 period. GLERL then attempted to estimate "steady-state" conditions, but there were problems.

The procedure to estimate "steady-state" conditions is to repeat the 52-yr simulation with initial conditions (basin moisture storages, lake heat storages, and surface temperatures) set equal to their values at the end of the simulation period, until they are unchanging. This procedure requires much iteration for a few subbasins with very slow groundwater storages and suggests very different initial groundwater storages than were used in calibrations. Actually, the original calibrations of the models used arbitrary (but fixed) initial conditions. GLERL should have determined initial conditions also in the calibrations, but that was unfeasible; there is little confidence in calibrated parameter sets that suggest very slow groundwater storages (half-lives on the order of several hundred years in some cases) since only 10 to 20 years were used in the calibrations. Therefore, the best estimate of "present" hydrology is to use calibrated parameters with initial conditions on "the same order" as those assumed for the calibrations. GLERL did the latter and then conducted simulations with adjusted data sets.

GLERL acquired average monthly differences (between base case and each climate change scenario) for air temperature (daily minimum, maximum, and average), relative humidities or vapor pressure, and solar radiation (from which they back-calculated cloud cover), and average monthly ratios for precipitation and wind speed for each month of the year. They did this for each of the GCM-generated climate change scenarios: HadCM3 A1FI (warm and wet, referred to henceforth as HADCM3A), HadCM3 B22 (not as warm but wet, referred to herein as HADCM3B), CGCM2 A21 (warm and dry, referred to as CGCM2A), and CGCM2 B23 (not as warm but dry, referred to as CGCM2B). GLERL inspected each of the 770,000 square kilometers within the

Great Lakes Basin to see which grid point it is closest to and applied the monthly adjustment at that grid point to data representing that square kilometer. By combining all square kilometers representing a watershed or a lake surface, GLERL derived an areally averaged adjustment to apply to their areally averaged historical data sets for the watershed or lake surface, respectively. They then used this climate change scenario in simulations similar to the base case scenario. They repeated the 52-yr simulation with initial conditions set equal to their values at the end of the simulation period, until they were unchanging to estimate "steady-state" future conditions. They then interpreted differences between the GCM-generated climate change scenario and the base case scenario, for the 1950-1999 period, as resulting from the changed climate. Problems of linkage, with this methodology, between hydrology models and the GCMs are outlined in the subsection, **GCM Linkage Problems**, on page 5.

This page intentionally left blank.

Great Lakes Physical Process Models

The Great Lakes Environmental Research Laboratory developed, calibrated, and verified conceptual model-based techniques for simulating hydrological processes in the Laurentian Great Lakes (including Georgian Bay and Lake St. Clair, both as separate entities). GLERL integrated the models into a system to estimate lake levels, whole-lake heat storage, and water and energy balances for forecasts and for assessment of impacts associated with climate change (*Croley* 1990, 1993a,b; *Croley and Hartmann* 1987, 1989; *Croley and Lee* 1993; *Hartmann* 1990; *Lofgren et al.* 2002). These include models for rainfall-runoff [121 daily watershed models (*Croley* 1982, 1983a,b; *Croley and Hartmann* 1984)], over-lake precipitation (a daily estimation model), one-dimensional (depth) lake thermodynamics [7 daily models for lake surface flux, thermal structure, and heat storage (*Croley* 1989a,b, 1992a; *Croley and Assel* 1994)], channel routing [4 daily models for connecting channel flow and level, outlet works, and lake levels (*Hartmann* 1987, 1988; *Quinn* 1978)], lake regulation [a monthly plan balancing Lakes Superior, Michigan, and Huron (*International Lake Superior Board of Control* 1981, 1982) and a quarter-monthly plan balancing Lake Ontario and the St. Lawrence Seaway (*International St. Lawrence River Board of Control* 1963)], and diversions and consumptions (*International Great Lakes Diversions and Consumptive Uses Study Board* 1981). Basin runoff, over-lake precipitation, and lake thermodynamics models are described in this chapter; results are presented in the next chapter.

Runoff Modeling

The GLERL Large Basin Runoff Model (LBRM) is an interdependent tank-cascade model, which employs analytic solutions of climatologic considerations relevant for large watersheds (*Croley* 1983a,b). It consists of moisture storages arranged as a serial and parallel cascade of "tanks" to coincide with the perceived basin storage structure of Figure 2. Water enters the upper soil zone tank and flows from the upper to the lower soil zone and surface storage tanks, from the lower to the groundwater and surface tanks, from the groundwater to the surface tank, and from the surface tank out of the watershed.

Snowmelt and Infiltration. Water enters the snowpack, if present, and some then infiltrates into the upper soil zone based on degree-day determinations of snowmelt and net supply:

$$\begin{aligned} m_p &= 0, && T_a \le 0, \\ &= a_s\, DD, && T_a > 0 \end{aligned} \tag{1}$$

where m_p = daily potential snowmelt rate (m^3 d^{-1}); a_s = proportionality constant for snowmelt per degree-day (m^3 °C^{-1} d^{-1}]); T_a = air temperature, estimated as the average of the daily maximum and minimum air temperatures (°C); and DD = degree-days per day (°C d d^{-1}), the integral of air temperature with time over those portions of the day when it is positive. Since the diurnal fluctuation of air temperature is unknown, a triangular distribution is used (to approximate an expected sinusoidal variation) for computation ease. The resulting expression for degree-days is:

$$\begin{aligned} DD &= 0, && T_{\max} \le 0, \\ &= \frac{T_{\max}^2}{2\left(T_{\max} - T_{\min}\right)}, && T_{\min} < 0 < T_{\max}, \\ &= T_a, && 0 \le T_{\min} \end{aligned} \tag{2}$$

where T_{max} = maximum daily air temperature (°C) and T_{min} = minimum daily air temperature (°C). Actual snowmelt depends upon the snowpack:

$$\begin{aligned} m &= m_p, & m_p d &\le SNW_0, \\ &= SNW_0/d, & m_p d &> SNW_0 \end{aligned} \tag{3}$$

where m = daily snowmelt rate (m^3 d^{-1}) and SNW_0 = water content of the snowpack at the beginning of the day (m^3). Snowpack mass balance and water supply to the watershed surface can now be determined:

$$\begin{aligned} \frac{\partial}{\partial t} SNW &= p, & T_a &\le 0, \\ &= -m, & T_a &> 0 \end{aligned} \tag{4}$$

$$\begin{aligned} ns &= 0, & T_a &\le 0, \\ &= p + m, & T_a &> 0 \end{aligned} \tag{5}$$

where t = time, p and ns = precipitation and net supply rates to watershed surface (m^3 d^{-1}).

Heat Available for Evapotranspiration. The heat available for evapotranspiration is estimated empirically from the average air temperature as follows:

$$\Psi = K \exp(T_a/T_b) \tag{6}$$

where Ψ = total heat available for evapotranspiration during the day (cal), K = units and proportionality constant (cal), and T_b = a base scaling temperature (°C). The constant, K, is determinable, given T_b, from the long-term heat balance (taken over the entire simulation):

$$\sum_{i=1}^{M} \Psi_i = \sum_{i=1}^{M} \left(rr_i - m_i \, \rho_w \, \gamma_f \right) d \tag{7}$$

where rr = daily solar insolation at the watershed surface (cal d^{-1}), ρ_w = density of water (= 10^6 gm m^{-3}), γ_f = latent heat of fusion (= 79.7 cal gm^{-1}), M = number of days in long-term heat balance, and the subscript, i, refers to daily values. Equation 7 conserves energy in that all absorbed insolation not used for snowmelt appears sooner or later as other components of the heat balance that determine Ψ. Daily insolation is taken as:

$$rr = 10000 \, A_b \, \tau (b_1 + b_2 \, X) \tag{8}$$

where A_b = area of the watershed (m^2), τ = daily extra-terrestrial solar radiation (langleys d^{-1}), b_1 and b_2 = constants, and X = daily ratio of hours of bright sunshine to maximum possible hours of bright sunshine, estimated from daily air temperatures:

$$X = \mathrm{MIN}\left[(T_{\max} - T_{\min}) / 15, 1.0 \right] \tag{9}$$

While calculations for *ns* and Ψ are performed on a daily basis, the mass balance computations (following) are performed on an *n*-day basis (*n* = 1, 7, and 28-31 are typical). The net supply and energy available for evapotranspiration are summed over the *n*-day periods prior to the mass balance:

$$ns_a = \frac{1}{n}\sum_{i=1}^{n} ns_i \tag{10}$$

$$\Psi_a = \sum_{i=1}^{n} \Psi_i \tag{11}$$

where ns_a = average net supply rate for *n* days ($m^3\ d^{-1}$), Ψ_a = accumulated energy available for evapotranspiration over *n* days (cal), and *n* = number of days in the mass balance computation periods (*n* = 1 in this study). The subscripts refer to daily values within the computation period.

Infiltration. Infiltration is taken as instantaneously proportional to the supply rate and to the areal extent of the unsaturated portion of the upper soil zone (partial-area infiltration concept).

$$f = ns_a\left(USZC - USZM\right)/USZC \tag{12}$$

where f = infiltration rate ($m^3\ d^{-1}$), $USZC$ = capacity of the upper soil zone (m^3), and $USZM$ = content of upper soil zone (m^3). The difference between the net supply rate and infiltration is surface runoff in Figure 2.

Evapotranspiration. Consider all incoming heat to be released by the watershed surface by ignoring heat storage and the energy advected by evaporation or transpiration. The release consists of short-wave reflection, atmospheric heating (the resultant of net long wave exchange, sensible heat exchange, net atmospheric advection, and net hydrospheric advection), and evaporation-transpiration (referred to herein jointly as evapotranspiration). The total heat available for evapotranspiration over a day is composed of the heat actually used for evapotranspiration and that used for atmospheric heating. At any instant, the rate of evapotranspiration, *e*, is proportional to the amount of water available, *Z* (reflecting both areal coverage and extent of supply), and to the rate of nonlatent heat released to the atmosphere, $\partial H_s/\partial t$ (atmospheric heating):

$$e = \beta Z e_p, \qquad e_p = \frac{\partial H_s}{\partial t}\Big/\left(\rho_w \gamma_v\right) \tag{13}$$

where e = evapotranspiration rate ($m^3\ d^{-1}$), β = partial linear reservoir coefficient (m^{-3}), Z = volume of water in storage (m^3), e_p = rate of evapotranspiration, respectively ($m^3\ d^{-1}$), still possible and γ_v = latent heat of vaporization (596 - 0.52 T_a cal gm^{-1}). This agrees with existing climatologic and hydrological concepts for evapotranspiration opportunity.

Over large areas, climatic observations suggest that actual evapotranspiration affects temperatures, wind speeds, humidities, and so forth, and hence it affects the potential evapotranspiration (evapotranspiration opportunity or capacity); the heat used for evapotranspiration reduces the opportunity for additional evapotranspiration (complementary evapotranspiration and evapotranspiration opportunity concept). This concept is modified here by considering that, for short time periods, the total amount of energy available for evapotranspiration, Ψ, during the time period is split into that used for evapotranspiration and that used for atmospheric heating. From (13), for the daily time period,

$$\Psi = H_s + \rho_w \gamma_v \left(E_u + E_l + E_g + E_s \right) \tag{14}$$

where H_s = nonlatent heat released to the atmosphere during the day (cal) and E_u, E_l, E_g, and E_s = evapotranspiration from the upper soil zone, lower soil zone, groundwater, and surface storages (m^3), respectively. The evaporation from stream channels and other water surfaces (surface zone) in a large basin is very small compared to the basin evapotranspiration; groundwater evapotranspiration is also taken here as being relatively small.

Mass Conservation. Percolation from the upper zone enters the lower soil zone, and deep percolation from the lower zone enters the groundwater zone; see Figure 2. Lateral flows from these zones of surface runoff, interflow, and groundwater flow, respectively, enter the surface storage zone which represents surface waters that ultimately flow from the basin. These flow rates are taken as instantaneously proportional to their respective storages (linear-reservoir flow concept). The mass balances for snowpack, upper and lower soil zones, groundwater, and surface water use these physically-based concepts, in the cascade of Figure 2, to form a set of simultaneous ordinary linear differential equations whose joint solution depends upon the relative magnitude of all parameters, inputs, and system states (storages) pictured in Figure 2.

$$\frac{\partial}{\partial t} USZM = ns_a \left(1 - \frac{USZM}{USZC} \right) - \alpha_{per} USZM - \beta_{eu} e_p USZM \tag{15}$$

$$\frac{\partial}{\partial t} LSZM = \alpha_{per} USZM - \alpha_{\text{int}} LSZM - \alpha_{dp} LSZM - \beta_{el} e_p LSZM \tag{16}$$

$$\frac{\partial}{\partial t} GZM = \alpha_{dp} LSZM - \alpha_{gw} GZM - \beta_{eg} GZM \tag{17}$$

$$\frac{\partial}{\partial t} SS = ns_a \frac{USZM}{USZC} + \alpha_{\text{int}} LSZM + \alpha_{gw} GZM - \alpha_{sf} SS - \beta_{es} e_p SS \tag{18}$$

$$Q = \alpha_{sf} \int_0^{\Delta} SS \, \partial t \tag{19}$$

where α_{per} = percolation coefficient (d^{-1}), β_{eu} = upper zone evapotranspiration coefficient (m^{-3}), α_{int} = interflow coefficient (d^{-1}), $LSZM$ = content of lower soil zone (m^3), α_{dp} = deep percolation coefficient (d^{-1}), β_{el} = lower zone evapotranspiration coefficient (m^{-3}), α_{gw} = groundwater coefficient (d^{-1}), GZM = content of groundwater zone (m^3), β_{eg} = groundwater zone evapotranspiration coefficient (m^{-3}), α_{sf} = surface outflow coefficient (d^{-1}), SS = content of surface storage zone (m^3), β_{es} = surface zone evapotranspiration coefficient (m^{-3}), Q = basin outflow volume for n days (m^3), and $\Delta = n$ times d. The value of e_p is determined by simultaneous solution of (15)-(19) and the following complementary relationship between actual evapotranspiration and that still possible from atmospheric heat, derived from (13) and (14):

$$\int_0^{\Delta} \left[e_p + \left(\beta_{eu} USZM + \beta_{el} LSZM + \beta_{eg} GZM + \beta_{es} SS \right) e_p \right] \partial t = \Psi_a / \left(\rho_w \gamma_v \right) \tag{20}$$

Analytical Solution. In the analytical solution, results from one storage zone are used in other zones where their outputs appear as inputs. There are 30 different analytic results, depending upon the relative magnitudes of the inputs (ns), the initial conditions ($USZM_0$, $LSZM_0$, GZM_0, SS_0, SNW_0), and the model parameters (T_b, a_s, α_{per}, β_{eu}, α_{int}, α_{dp}, β_{el}, α_{gw}, and α_{sf}) in (15)-(19) (note that β_{eg} and β_{es} are taken as zeroes). Complete analytic solutions for all possible ranges of values are available (*Croley* 1982). Since the inputs and initial storages each day change from day to day, the appropriate analytic result, as well as its solution, varies with time; mathematical continuity between solutions is preserved however. Small parameter values for a tank outflow imply small releases and large storage volumes; large values imply small storages and outflows nearly equal to inflows. The differential equations for the mass balances can be applied over any time increment by assuming that the input (precipitation and snowmelt) and heat available for evapotranspiration are uniform over the time increment. Thus, the resolution of the equations is limited only by the intervals over which precipitation and temperature data are available; numerical solutions are unnecessary so that approximation errors are avoided. Furthermore, solutions may proceed for either flow rates or storage volumes directly. The mass-balance computation interval must be greater than or equal to the interval for which meteorological data are available.

Application. The model is applied to daily data with either a fixed 1-d or a fixed 7-d mass-balance computation interval. Input and heat available for evapotranspiration are combined on a daily basis and summed over the interval as input to the mass-balance computations. The model is applied to monthly data with a variable mass-balance computation interval. The interval may represent 28 to 31 d, depending on the month and year. Input and heat available for evapotranspiration are computed over the same monthly interval. Again, the 1-d mass-balance computation interval was used herein. Data requirements include initial storage values, daily maximum and minimum air temperatures, daily precipitation, and for comparison purposes, daily basin outflow. Other data requirements are easily met. The mid-monthly extra-terrestrial solar radiation (from which daily values are interpolated) and the empirical constants, b_1 and b_2, are available in standard climatologic summaries. Watershed area is also required.

For application of the LBRM to a Great Lakes drainage basin, the basin is first divided into subbasins draining directly to the lake (there are 121 subbasins in the entire Great Lakes basin). The meteorological data from typically 150-300 stations about and in the subbasins are combined through Thiessen weighting to produce areally-averaged daily time series of precipitation and minimum and maximum air temperatures for each subbasin. Weights are determined for each day of record, if necessary, since the data collection network changes frequently as stations are added, dropped, and moved or fail to report from time to time. This is feasible through the use of an algorithm for determining a Thiessen area-of-influence about a station by its edge [*Croley and Hartmann*, 1985]. Records for all "most-downstream" flow stations are combined by aggregating and extrapolating for ungaged areas to estimate the daily runoff to the lake from each subbasin.

Thus, the LBRM is applied in a "distributed-parameter" application by combining model outflows from each of the subbasins to produce the entire basin runoff.

By combining the meteorological and hydrological data for all subbasins to represent the entire basin, the LBRM may be calibrated in a lumped-parameter application to the entire basin at one time. Although the application of lumped-parameter models to very large areas necessarily fails to represent areal distributions of watershed and meteorological characteristics, spatial filtering effects tend to cancel data errors for small areas as the areas are added together. Distributed-parameter applications, in which the LBRM is calibrated for each subbasin and model outflows are combined to represent the entire basin, make use of information that is lost in the lumped-parameter approach; the integration then filters individual subbasin model errors.

There are five variables to be initialized prior to modeling: *SNW*, *USZM*, *LSZM*, *GZM*, and *SS*. While the initial snow pack, SNW_0, is easy to determine as zero during major portions of the year, these variables are generally difficult to estimate. If the model is to be used in forecasting or for short simulations, then it is important to determine these variables accurately prior to use of the model. If the model is to be used for calibration or for long simulations, then the initial values are generally unimportant. The effect of the initial values of all storages except *GZM* diminishes with the length of the simulation and after 1 year of simulation, the effects are nil from a practical point of view. Some applications have groundwater parameters that allow initial *GZM* values to persist. Calibrations are repeated with initial conditions equal to calculated long-term averages until the averages do not change, to avoid arbitrary initial conditions when their effects persist.

Calibration. GLERL calibrates the LBRM for each subbasin with 30 years of daily weighted climatologic data. The nine parameters are determined (*Croley and Hartmann* 1984) by searching the parameter space systematically, minimizing the root mean square error between model and actual outflows for each parameter, selected in rotation, until all parameters converge within two significant digits. Comparisons to other models (*Croley* 1983a) and climatology (*Croley and Hartmann* 1984) show the LBRM is superior for estimates of runoff volumes from large basins.

The LBRM captures a "realism" in its structure that has several advantages over other models. Basin storages, modeled as "tanks", are automatically removed as respective parameters approach their limits. Thus, the structure of the model changes within a calibration. This is achieved without the use of "threshold" parameters in the model since physical concepts are used which avoid discontinuities in the goodness-of-fit as a function of the parameters; these concepts appear especially relevant for large-basin modeling. Because the "tanks" relate directly to actual basin storages, initialization of the model corresponds to identifying storages from field conditions which may be measured; interpretations of a basin's hydrology then can aid in setting both initial and boundary conditions. The tanks in Figure 2 may be initialized to correspond to measurements of snow and soil moisture water equivalents available from aerial or satellite monitoring. Snow water equivalents are used in Lake Superior applications (*Gauthier et al*. 1984).

The LBRM calibration periods generally cover 1965-1982 depending upon flow data availability. Tables 5-11 present the LBRM calibrated parameters. Table 12 presents overall calibration results for the distributed-parameter applications. The LBRM was also used in forecasts of Lake Superior water levels (*Croley and Hartmann* 1987), and comparisons with climatic outlooks

Table 5. Large Basin Runoff Model Parameters for the Lake Superior Subbasins.

No.	T_b ºC	a_s $m^3\ ºC^{-1}\ d^{-1}$	α_{per} d^{-1}	β_{eu} m^{-3}	α_{int} d^{-1}	α_{dp} d^{-1}	β_{el} m^{-3}	α_{gw} d^{-1}	α_{sf} d^{-1}	K cal
1	3.0	$.22\times10^{+8}$	$.30\times10^{+0}$	$.59\times10^{+2}$	$.21\times10^{-9}$	$.60\times10^{-2}$	$.10\times10^{-9}$	$.35\times10^{-1}$	$.86\times10^{-1}$	$2.28\times10^{+15}$
2	7.2	$.94\times10^{+7}$	$.12\times10^{+3}$	$.10\times10^{-5}$	$.10\times10^{+0}$	$.76\times10^{-1}$	$.79\times10^{-8}$	$.33\times10^{-1}$	$.23\times10^{+2}$	$4.06\times10^{+16}$
3	4.7	$.11\times10^{+8}$	$.23\times10^{+1}$	$.19\times10^{-7}$	$.39\times10^{-1}$	$.30\times10^{-1}$	$.32\times10^{+4}$	$.30\times10^{-1}$	$.22\times10^{+0}$	$6.88\times10^{+15}$
4	6.0	$.70\times10^{+7}$	$.71\times10^{+0}$	$.85\times10^{-7}$	$.11\times10^{-9}$	$.18\times10^{-1}$	$.30\times10^{-8}$	$.67\times10^{+0}$	$.22\times10^{+0}$	$1.38\times10^{+16}$
5	6.3	$.92\times10^{+7}$	$.23\times10^{+2}$	$.12\times10^{-9}$	$.40\times10^{+1}$	$.63\times10^{+1}$	$.26\times10^{+1}$	$.14\times10^{-1}$	$.26\times10^{+0}$	$2.24\times10^{+16}$
6	4.5	$.85\times10^{+7}$	$.54\times10^{+0}$	$.48\times10^{-7}$	$.21\times10^{-9}$	$.27\times10^{+0}$	$.95\times10^{-7}$	$.58\times10^{-1}$	$.43\times10^{+0}$	$5.49\times10^{+15}$
7	5.2	$.38\times10^{+7}$	$.10\times10^{+1}$	$.70\times10^{-7}$	$.11\times10^{-1}$	$.24\times10^{-2}$	$.35\times10^{-8}$	$.85\times10^{-2}$	$.17\times10^{+0}$	$5.95\times10^{+15}$
8	$9.2\times10^{+9}$	$.10\times10^{+10}$	$.14\times10^{+2}$	$.45\times10^{-7}$	$.10\times10^{-9}$	$.99\times10^{-2}$	$.78\times10^{-9}$	$.14\times10^{-1}$	$.13\times10^{-1}$	$1.05\times10^{+17}$
9	2.3	$.70\times10^{+7}$	$.46\times10^{+0}$	$.35\times10^{+4}$	$.14\times10^{-2}$	$.82\times10^{-2}$	$.40\times10^{-5}$	$.89\times10^{-3}$	$.75\times10^{-1}$	$8.39\times10^{+13}$
10	2.3	$.48\times10^{+7}$	$.46\times10^{+0}$	$.35\times10^{+4}$	$.14\times10^{-2}$	$.82\times10^{-2}$	$.40\times10^{-5}$	$.89\times10^{-3}$	$.75\times10^{-1}$	$6.70\times10^{+13}$
11	2.3	$.19\times10^{+7}$	$.46\times10^{+0}$	$.35\times10^{+4}$	$.14\times10^{-2}$	$.82\times10^{-2}$	$.40\times10^{-5}$	$.89\times10^{-3}$	$.75\times10^{-1}$	$2.90\times10^{+13}$
12	5.1	$.13\times10^{+8}$	$.68\times10^{+0}$	$.22\times10^{+4}$	$.11\times10^{+4}$	$.79\times10^{+4}$	$.90\times10^{+0}$	$.14\times10^{-1}$	$.19\times10^{+0}$	$2.01\times10^{+16}$
13	1.1	$.82\times10^{+7}$	$.93\times10^{+1}$	$.91\times10^{+4}$	$.11\times10^{-2}$	$.92\times10^{-2}$	$.69\times10^{-4}$	$.10\times10^{-2}$	$.95\times10^{-1}$	$2.00\times10^{+10}$
14	3.9	$.24\times10^{+8}$	$.47\times10^{+1}$	$.91\times10^{-8}$	$.27\times10^{-2}$	$.43\times10^{-2}$	$.20\times10^{-9}$	$.17\times10^{-2}$	$.84\times10^{-1}$	$1.87\times10^{+16}$
15	9.7	$.20\times10^{+8}$	$.47\times10^{+2}$	$.53\times10^{-6}$	$.20\times10^{-1}$	$.79\times10^{-2}$	$.39\times10^{-9}$	$.53\times10^{+0}$	$.11\times10^{+0}$	$1.59\times10^{+17}$
16	5.8	$.16\times10^{+8}$	$.54\times10^{+0}$	$.87\times10^{-8}$	$.10\times10^{-9}$	$.27\times10^{-1}$	$.33\times10^{-8}$	$.60\times10^{-1}$	$.10\times10^{+0}$	$4.91\times10^{+16}$
17	1.8	$.11\times10^{+8}$	$.55\times10^{+0}$	$.44\times10^{-1}$	$.32\times10^{-2}$	$.20\times10^{-2}$	$.98\times10^{-2}$	$.59\times10^{-2}$	$.71\times10^{-1}$	$1.02\times10^{+14}$
18	1.4	$.37\times10^{+7}$	$.34\times10^{+0}$	$.64\times10^{-3}$	$.99\times10^{-3}$	$.10\times10^{-2}$	$.96\times10^{-1}$	$.93\times10^{+1}$	$.81\times10^{-1}$	$7.02\times10^{+11}$
19	2.0	$.18\times10^{+8}$	$.91\times10^{+9}$	$.20\times10^{-9}$	$.79\times10^{-2}$	$.81\times10^{-1}$	$.27\times10^{-8}$	$.53\times10^{-2}$	$.52\times10^{-2}$	$4.23\times10^{+14}$
20	2.1	$.11\times10^{+8}$	$.61\times10^{+0}$	$.13\times10^{-6}$	$.22\times10^{-2}$	$.83\times10^{-3}$	$.57\times10^{-7}$	$.99\times10^{+9}$	$.42\times10^{-1}$	$1.74\times10^{+14}$
21	2.0	$.27\times10^{+8}$	$.57\times10^{+1}$	$.76\times10^{+1}$	$.42\times10^{-2}$	$.68\times10^{-2}$	$.46\times10^{-1}$	$.67\times10^{-2}$	$.11\times10^{+0}$	$1.18\times10^{+14}$
22	3.1	$.13\times10^{+8}$	$.54\times10^{+0}$	$.69\times10^{-1}$	$.11\times10^{-9}$	$.18\times10^{+0}$	$.63\times10^{+0}$	$.26\times10^{-1}$	$.18\times10^{+0}$	$4.17\times10^{+15}$

showed the runoff model was very close to actual runoff (monthly correlations of water supply were on the order of 0.99) for the period August 1982 - December 1984 which is outside of and wetter than the calibration period (*Croley and Hartmann* 1986). The model also was used to simulate flows for the time period 1956-63, outside of the period of calibration. The correlation of monthly flow volumes between the model and observed during this verification period are also contained in Table 12. They are a little lower than the calibration correlations but quite good except for Lakes Superior and Huron (there were less than two thirds as many flow gages available for 1956-63 as for the calibration period for these basins).

Studies on the Lake Ontario basin (*Croley* 1982, 1983b) show that the simple search algorithm described herein does not give unique optimums for calibrated parameter sets because of synergistic relationships between parameters. However, the calibration procedure does show a high degree of repeatability for recalibrations with different starting values, and consistent parameter values are obtained for subbasins with similar hydrological characteristics. On the other hand, the non-uniqueness of calibrated parameters was demonstrated by recalibrating for a synthetic data set. The model was calibrated for the entire Lake Superior basin and then used to simulate outflows to create a new data set for calibration. Subsequent calibration started with a very different initial parameter set and yielded an "optimum" parameter set different from the original with a relatively poor goodness-of-fit. If the original parameter set had been unique, the parameter values produced from the recalibration to the synthetic data set should have been the same as the parameters used to create that data set. This illustrates the non-uniqueness of the parameters, the importance of the starting values used in the search, and the problems inherent in searching the parameter space. Additionally, some components of the LBRM (such as linear reservoirs) are more likely to adequately represent their processes in the real world than others (such as degree-

Table 6. Large Basin Runoff Model Parameters for the Lake Michigan Subbasins.

No.	T_b °C	a_s $m^3\,°C^{-1}\,d^{-1}$	α_{per} d^{-1}	β_{eu} m^{-3}	α_{int} d^{-1}	α_{dp} d^{-1}	β_{el} m^{-3}	α_{gw} d^{-1}	α_{sf} d^{-1}	K cal
1	4.5	$.36\times10^{+7}$	$.25\times10^{+0}$	$.16\times10^{-6}$	$.11\times10^{+0}$	$.25\times10^{+0}$	$.10\times10^{-9}$	$.50\times10^{-2}$	$.58\times10^{-1}$	$2.83\times10^{+15}$
2	4.5	$.94\times10^{+7}$	$.25\times10^{+0}$	$.16\times10^{-6}$	$.11\times10^{+0}$	$.25\times10^{+0}$	$.10\times10^{-9}$	$.50\times10^{-2}$	$.58\times10^{-1}$	$6.97\times10^{+15}$
3	7.1	$.30\times10^{+7}$	$.10\times10^{+2}$	$.99\times10^{-6}$	$.47\times10^{-1}$	$.25\times10^{-1}$	$.86\times10^{-8}$	$.12\times10^{-1}$	$.69\times10^{+0}$	$1.08\times10^{+16}$
4	7.1	$.33\times10^{+7}$	$.10\times10^{+2}$	$.99\times10^{-6}$	$.47\times10^{-1}$	$.25\times10^{-1}$	$.86\times10^{-8}$	$.12\times10^{-1}$	$.69\times10^{+0}$	$1.20\times10^{+16}$
5	5.2	$.50\times10^{+7}$	$.72\times10^{+0}$	$.12\times10^{-6}$	$.92\times10^{-2}$	$.90\times10^{-7}$	$.26\times10^{-8}$	$.33\times10^{-1}$	$.11\times10^{+0}$	$7.48\times10^{+15}$
6	5.1	$.52\times10^{+7}$	$.29\times10^{+0}$	$.11\times10^{-6}$	$.10\times10^{-4}$	$.68\times10^{-1}$	$.83\times10^{-1}$	$.53\times10^{-1}$	$.96\times10^{-1}$	$7.66\times10^{+15}$
7	3.9	$.24\times10^{+8}$	$.32\times10^{+1}$	$.11\times10^{-7}$	$.74\times10^{-2}$	$.46\times10^{-2}$	$.15\times10^{-8}$	$.98\times10^{-3}$	$.96\times10^{-1}$	$9.74\times10^{+15}$
8	4.7	$.77\times10^{+7}$	$.17\times10^{+1}$	$.12\times10^{-6}$	$.80\times10^{-2}$	$.62\times10^{-2}$	$.63\times10^{-8}$	$.52\times10^{-2}$	$.12\times10^{+0}$	$5.53\times10^{+15}$
9	5.7	$.71\times10^{+7}$	$.35\times10^{+1}$	$.29\times10^{-6}$	$.89\times10^{-2}$	$.10\times10^{-1}$	$.51\times10^{-8}$	$.34\times10^{-2}$	$.12\times10^{+0}$	$9.42\times10^{+15}$
10	6.0	$.33\times10^{+7}$	$.11\times10^{+0}$	$.18\times10^{+2}$	$.38\times10^{-5}$	$.40\times10^{-5}$	$.10\times10^{+2}$	$.64\times10^{-1}$	$.22\times10^{+0}$	$4.43\times10^{+15}$
11	9.4	$.12\times10^{+10}$	$.27\times10^{+3}$	$.43\times10^{-6}$	$.10\times10^{-1}$	$.91\times10^{-7}$	$.25\times10^{-9}$	$.40\times10^{+0}$	$.21\times10^{+0}$	$1.78\times10^{+17}$
12	5.6	$.78\times10^{+7}$	$.13\times10^{+1}$	$.20\times10^{+2}$	$.18\times10^{-1}$	$.95\times10^{-6}$	$.75\times10^{+0}$	$.25\times10^{-5}$	$.45\times10^{+0}$	$6.40\times10^{+15}$
13	5.9	$.17\times10^{+8}$	$.16\times10^{+1}$	$.19\times10^{+0}$	$.19\times10^{-1}$	$.82\times10^{-5}$	$.99\times10^{-2}$	$.98\times10^{-5}$	$.15\times10^{+0}$	$1.36\times10^{+16}$
14	5.7	$.70\times10^{+7}$	$.40\times10^{+1}$	$.32\times10^{-5}$	$.28\times10^{-1}$	$.34\times10^{-1}$	$.21\times10^{-6}$	$.10\times10^{-1}$	$.38\times10^{+0}$	$5.78\times10^{+15}$
15	8.1	$.92\times10^{+7}$	$.48\times10^{+0}$	$.39\times10^{-6}$	$.80\times10^{-5}$	$.68\times10^{+6}$	$.38\times10^{+0}$	$.22\times10^{-1}$	$.30\times10^{+0}$	$1.72\times10^{+16}$
16	8.3	$.53\times10^{+8}$	$.17\times10^{+2}$	$.47\times10^{-7}$	$.86\times10^{-1}$	$.24\times10^{+0}$	$.39\times10^{-7}$	$.14\times10^{-1}$	$.13\times10^{+0}$	$8.19\times10^{+16}$
17	5.6	$.10\times10^{+9}$	$.84\times10^{+6}$	$.17\times10^{-6}$	$.42\times10^{-1}$	$.50\times10^{-1}$	$.13\times10^{-6}$	$.17\times10^{-1}$	$.26\times10^{+2}$	$2.03\times10^{+15}$
18	8.5	$.26\times10^{+8}$	$.89\times10^{+1}$	$.34\times10^{-6}$	$.11\times10^{-1}$	$.11\times10^{-1}$	$.13\times10^{-8}$	$.43\times10^{-2}$	$.18\times10^{+0}$	$3.88\times10^{+16}$
19	5.9	$.23\times10^{+7}$	$.11\times10^{-4}$	$.57\times10^{-2}$	$.93\times10^{+1}$	$.66\times10^{+0}$	$.11\times10^{-3}$	$.12\times10^{-4}$	$.58\times10^{+0}$	$1.68\times10^{+15}$
20	5.9	$.43\times10^{+8}$	$.20\times10^{+0}$	$.25\times10^{-6}$	$.10\times10^{-2}$	$.19\times10^{-1}$	$.90\times10^{-8}$	$.21\times10^{-1}$	$.57\times10^{-1}$	$4.01\times10^{+16}$
21	4.8	$.76\times10^{+6}$	$.50\times10^{+1}$	$.49\times10^{-6}$	$.44\times10^{-2}$	$.64\times10^{-2}$	$.51\times10^{-9}$	$.17\times10^{-3}$	$.15\times10^{+0}$	$3.36\times10^{+14}$
22	6.0	$.23\times10^{+8}$	$.38\times10^{+1}$	$.16\times10^{-6}$	$.57\times10^{-2}$	$.41\times10^{-2}$	$.39\times10^{-9}$	$.12\times10^{-2}$	$.13\times10^{+0}$	$2.76\times10^{+16}$
23	4.8	$.15\times10^{+8}$	$.50\times10^{+1}$	$.49\times10^{-6}$	$.44\times10^{-2}$	$.64\times10^{-2}$	$.51\times10^{-9}$	$.17\times10^{-3}$	$.15\times10^{+0}$	$8.22\times10^{+15}$
24	7.5	$.20\times10^{+10}$	$.18\times10^{+4}$	$.62\times10^{-4}$	$.60\times10^{-2}$	$.75\times10^{-2}$	$.24\times10^{-9}$	$.26\times10^{-3}$	$.76\times10^{+1}$	$3.82\times10^{+16}$
25	4.8	$.63\times10^{+7}$	$.50\times10^{+1}$	$.49\times10^{-6}$	$.44\times10^{-2}$	$.64\times10^{-2}$	$.51\times10^{-9}$	$.17\times10^{-3}$	$.15\times10^{+0}$	$3.45\times10^{+15}$
26	6.4	$.56\times10^{+7}$	$.60\times10^{+2}$	$.26\times10^{-5}$	$.22\times10^{-1}$	$.12\times10^{+0}$	$.32\times10^{-8}$	$.23\times10^{-3}$	$.51\times10^{+2}$	$1.82\times10^{+16}$
27	6.4	$.11\times10^{+7}$	$.60\times10^{+2}$	$.26\times10^{-5}$	$.22\times10^{-1}$	$.12\times10^{+0}$	$.32\times10^{-8}$	$.23\times10^{-3}$	$.51\times10^{+2}$	$4.01\times10^{+15}$

day melting or complementary evapotranspiration). Parameter estimation techniques that properly weight a model's more accurate parts could improve parameter estimates.

Over-Lake Precipitation

The lack of over-lake precipitation measurements means that estimates typically depend on land-

Table 7. Large Basin Runoff Model Parameters for the Lake Huron Subbasins.

No.	T_b °C	a_s $m^3\,°C^{-1}\,d^{-1}$	α_{per} d^{-1}	β_{eu} m^{-3}	α_{int} d^{-1}	α_{dp} d^{-1}	β_{el} m^{-3}	α_{gw} d^{-1}	α_{sf} d^{-1}	K cal
1	4.9	$.41\times10^{+7}$	$.16\times10^{+0}$	$.29\times10^{-6}$	$.31\times10^{-1}$	$.88\times10^{-5}$	$.55\times10^{-9}$	$.75\times10^{-1}$	$.23\times10^{+0}$	$4.76\times10^{+15}$
2	6.6	$.93\times10^{+6}$	$.14\times10^{+2}$	$.23\times10^{-6}$	$.65\times10^{-2}$	$.82\times10^{-2}$	$.10\times10^{-8}$	$.74\times10^{-3}$	$.14\times10^{+0}$	$1.59\times10^{+15}$
3	6.6	$.13\times10^{+8}$	$.14\times10^{+2}$	$.23\times10^{-6}$	$.65\times10^{-2}$	$.82\times10^{-2}$	$.10\times10^{-8}$	$.74\times10^{-3}$	$.14\times10^{+0}$	$2.44\times10^{+16}$
4	6.6	$.47\times10^{+7}$	$.14\times10^{+2}$	$.23\times10^{-6}$	$.65\times10^{-2}$	$.82\times10^{-2}$	$.10\times10^{-8}$	$.74\times10^{-3}$	$.14\times10^{+0}$	$8.08\times10^{+15}$
5	5.3	$.98\times10^{+7}$	$.47\times10^{+1}$	$.32\times10^{-6}$	$.89\times10^{-2}$	$.82\times10^{-2}$	$.91\times10^{-8}$	$.42\times10^{-2}$	$.23\times10^{+0}$	$1.01\times10^{+16}$
6	5.3	$.14\times10^{+7}$	$.47\times10^{+1}$	$.32\times10^{-6}$	$.89\times10^{-2}$	$.82\times10^{-2}$	$.91\times10^{-8}$	$.42\times10^{-2}$	$.23\times10^{+0}$	$1.32\times10^{+15}$
7	6.2	$.11\times10^{+8}$	$.10\times10^{+2}$	$.20\times10^{-6}$	$.46\times10^{-2}$	$.10\times10^{-1}$	$.49\times10^{-9}$	$.96\times10^{-3}$	$.27\times10^{+0}$	$2.60\times10^{+16}$
8	5.6	$.79\times10^{+7}$	$.30\times10^{+1}$	$.41\times10^{-6}$	$.10\times10^{-1}$	$.55\times10^{-6}$	$.83\times10^{-9}$	$.52\times10^{-3}$	$.36\times10^{+0}$	$9.46\times10^{+15}$
9	5.7	$.34\times10^{+7}$	$.91\times10^{-6}$	$.66\times10^{-3}$	$.71\times10^{+0}$	$.62\times10^{-2}$	$.70\times10^{-9}$	$.30\times10^{-1}$	$.97\times10^{-1}$	$3.68\times10^{+15}$
10	5.4	$.45\times10^{+8}$	$.20\times10^{+0}$	$.32\times10^{-6}$	$.97\times10^{-3}$	$.20\times10^{-1}$	$.55\times10^{-7}$	$.26\times10^{-1}$	$.11\times10^{+0}$	$3.63\times10^{+16}$
11	5.7	$.65\times10^{+7}$	$.80\times10^{-6}$	$.27\times10^{-4}$	$.30\times10^{+0}$	$.60\times10^{-2}$	$.70\times10^{-9}$	$.41\times10^{-1}$	$.21\times10^{+0}$	$6.25\times10^{+15}$
12	6.3	$.81\times10^{+7}$	$.10\times10^{+0}$	$.47\times10^{-2}$	$.17\times10^{-1}$	$.99\times10^{-6}$	$.26\times10^{-8}$	$.25\times10^{-2}$	$.30\times10^{+0}$	$5.69\times10^{+15}$
13	6.3	$.17\times10^{+8}$	$.10\times10^{+0}$	$.47\times10^{-2}$	$.17\times10^{-1}$	$.99\times10^{-6}$	$.26\times10^{-8}$	$.25\times10^{-2}$	$.30\times10^{+0}$	$1.24\times10^{+16}$
14	4.8	$.19\times10^{+8}$	$.42\times10^{+0}$	$.93\times10^{-5}$	$.15\times10^{-1}$	$.86\times10^{-6}$	$.15\times10^{-5}$	$.35\times10^{-3}$	$.23\times10^{+0}$	$4.97\times10^{+15}$
15	6.6	$.12\times10^{+8}$	$.16\times10^{+1}$	$.13\times10^{-1}$	$.19\times10^{-1}$	$.95\times10^{-6}$	$.76\times10^{-2}$	$.80\times10^{-1}$	$.73\times10^{+0}$	$6.83\times10^{+15}$
16	5.3	$.30\times10^{+8}$	$.16\times10^{+1}$	$.22\times10^{-6}$	$.12\times10^{-1}$	$.53\times10^{-2}$	$.50\times10^{-8}$	$.11\times10^{-1}$	$.17\times10^{+0}$	$1.21\times10^{+16}$

Table 8. Large Basin Runoff Model Parameters for the Georgian Bay Subbasins.

No.	T_b ºC	a_s $m^3\ ºC^{-1}\ d^{-1}$	α_{per} d^{-1}	β_{eu} m^{-3}	α_{int} d^{-1}	α_{dp} d^{-1}	β_{el} m^{-3}	α_{gw} d^{-1}	α_{sf} d^{-1}	K cal
1	4.3	$.16\times10^{+8}$	$.11\times10^{+0}$	$.18\times10^{-3}$	$.21\times10^{-1}$	$.83\times10^{-6}$	$.11\times10^{-4}$	$.87\times10^{-3}$	$.81\times10^{-1}$	$2.97\times10^{+15}$
2	6.1	$.14\times10^{+8}$	$.37\times10^{+1}$	$.20\times10^{-6}$	$.15\times10^{-1}$	$.89\times10^{-6}$	$.43\times10^{-8}$	$.20\times10^{-2}$	$.24\times10^{+0}$	$7.98\times10^{+15}$
3	6.0	$.21\times10^{+8}$	$.33\times10^{+1}$	$.41\times10^{-6}$	$.10\times10^{-1}$	$.77\times10^{-2}$	$.94\times10^{-8}$	$.70\times10^{-2}$	$.35\times10^{+0}$	$1.85\times10^{+16}$
4	4.7	$.23\times10^{+8}$	$.84\times10^{+1}$	$.46\times10^{-6}$	$.71\times10^{-2}$	$.57\times10^{-2}$	$.14\times10^{-7}$	$.13\times10^{-3}$	$.13\times10^{+0}$	$1.15\times10^{+16}$
5	4.8	$.41\times10^{+8}$	$.43\times10^{+4}$	$.80\times10^{-5}$	$.16\times10^{-1}$	$.74\times10^{-2}$	$.27\times10^{-8}$	$.31\times10^{-3}$	$.34\times10^{+0}$	$1.43\times10^{+16}$
6	3.9	$.25\times10^{+8}$	$.52\times10^{+2}$	$.59\times10^{-4}$	$.12\times10^{+0}$	$.53\times10^{-1}$	$.59\times10^{-6}$	$.38\times10^{-5}$	$.79\times10^{-1}$	$6.14\times10^{+15}$
7	2.6	$.16\times10^{+9}$	$.57\times10^{+6}$	$.82\times10^{-9}$	$.75\times10^{-2}$	$.58\times10^{-2}$	$.59\times10^{-9}$	$.50\times10^{-5}$	$.79\times10^{-1}$	$1.30\times10^{+15}$
8	3.7	$.45\times10^{+8}$	$.21\times10^{+2}$	$.22\times10^{-7}$	$.46\times10^{-2}$	$.18\times10^{-2}$	$.81\times10^{-9}$	$.85\times10^{-3}$	$.17\times10^{+0}$	$2.99\times10^{+15}$
9	4.4	$.46\times10^{+8}$	$.12\times10^{+1}$	$.75\times10^{-8}$	$.62\times10^{-2}$	$.35\times10^{-3}$	$.24\times10^{-9}$	$.19\times10^{-1}$	$.75\times10^{-1}$	$3.98\times10^{+16}$
10	4.4	$.99\times10^{+7}$	$.74\times10^{+0}$	$.34\times10^{-6}$	$.26\times10^{-1}$	$.27\times10^{-5}$	$.22\times10^{-8}$	$.46\times10^{-1}$	$.54\times10^{-1}$	$5.01\times10^{+15}$
11	2.2	$.22\times10^{+8}$	$.30\times10^{+1}$	$.70\times10^{-7}$	$.48\times10^{-2}$	$.22\times10^{-2}$	$.50\times10^{-9}$	$.26\times10^{-3}$	$.99\times10^{-1}$	$2.34\times10^{+14}$
12	4.9	$.99\times10^{+7}$	$.16\times10^{+0}$	$.29\times10^{-6}$	$.31\times10^{-1}$	$.88\times10^{-5}$	$.55\times10^{-9}$	$.75\times10^{-1}$	$.23\times10^{+0}$	$1.19\times10^{+16}$
13	4.9	$.29\times10^{+7}$	$.16\times10^{+0}$	$.29\times10^{-6}$	$.31\times10^{-1}$	$.88\times10^{-5}$	$.55\times10^{-9}$	$.75\times10^{-1}$	$.23\times10^{+0}$	$3.41\times10^{+15}$

Table 9. Large Basin Runoff Model Parameters for the Lake St. Clair Subbasins.

No.	T_b ºC	a_s $m^3\ ºC^{-1}\ d^{-1}$	α_{per} d^{-1}	β_{eu} m^{-3}	α_{int} d^{-1}	α_{dp} d^{-1}	β_{el} m^{-3}	α_{gw} d^{-1}	α_{sf} d^{-1}	K cal
1	6.4	$.11\times10^{+8}$	$.97\times10^{-1}$	$.11\times10^{+1}$	$.90\times10^{-6}$	$.10\times10^{-1}$	$.98\times10^{+0}$	$.42\times10^{-1}$	$.25\times10^{+0}$	$1.17\times10^{+16}$
2	8.2	$.72\times10^{+6}$	$.16\times10^{+2}$	$.42\times10^{-5}$	$.10\times10^{+0}$	$.16\times10^{+0}$	$.11\times10^{-6}$	$.15\times10^{-1}$	$.31\times10^{+1}$	$2.85\times10^{+15}$
3	8.2	$.53\times10^{+7}$	$.16\times10^{+2}$	$.42\times10^{-5}$	$.10\times10^{+0}$	$.16\times10^{+0}$	$.11\times10^{-6}$	$.15\times10^{-1}$	$.31\times10^{+1}$	$1.30\times10^{+16}$
4	8.2	$.37\times10^{+6}$	$.16\times10^{+2}$	$.42\times10^{-5}$	$.10\times10^{+0}$	$.16\times10^{+0}$	$.11\times10^{-6}$	$.15\times10^{-1}$	$.31\times10^{+1}$	$1.31\times10^{+15}$
5	8.5	$.53\times10^{+7}$	$.11\times10^{+0}$	$.53\times10^{-5}$	$.51\times10^{-1}$	$.60\times10^{-5}$	$.86\times10^{-7}$	$.51\times10^{-1}$	$.65\times10^{+0}$	$5.02\times10^{+15}$
6	7.8	$.24\times10^{+8}$	$.41\times10^{+5}$	$.72\times10^{+2}$	$.31\times10^{+0}$	$.11\times10^{+0}$	$.34\times10^{-7}$	$.21\times10^{-1}$	$.28\times10^{+0}$	$3.96\times10^{+16}$
7	6.4	$.18\times10^{+8}$	$.45\times10^{-1}$	$.34\times10^{-4}$	$.97\times10^{-2}$	$.11\times10^{-5}$	$.51\times10^{-8}$	$.59\times10^{-1}$	$.18\times10^{+0}$	$1.33\times10^{+16}$

based measurements and there may be differences between land and lake meteorology. Although gage exposures may significantly influence the results of lake-land precipitation studies (*Bolsenga* 1977, 1979), *Wilson* (1977) found that Lake Ontario precipitation estimates based on only near-shore stations averaged 5.6% more during the warm season and 2.1% less during the cold season than estimates based on stations situated in the lake. By using a network that also included stations somewhat removed from the Lake Ontario shoreline, *Bolsenga and Hagman* (1975) found that eliminating several gages not immediately in the vicinity of the shoreline increased over-lake precipitation estimates during the warm season and decreased them during the cold season. Thus, for the Great Lakes, where lake effects on near-shore meteorology are significant and the drainage basins have relatively low relief, the use here of all available meteorological stations throughout the basin is probably less biased than the use of only near-shore stations. Overlake precipitation is estimated via Thiessen weighting of all stations, which admittedly will more heavily weight near-shore stations.

Over-Lake Evaporation

Great Lakes hydrological research mandates the use of continuous-simulation models of daily lake evaporation over long time periods. Such models must be usable in the absence of water surface temperature and ice cover observations. They also must be physically based to have application under environmental conditions different than those under which they were derived. GLERL developed a lumped-parameter model of evaporation and thermodynamic fluxes for the Great Lakes based on an energy balance at the lake's surface (*Croley* 1989a,b) and on one-dimensional (verti-

Table 10. Large Basin Runoff Model Parameters for the Lake Erie Subbasins.

No.	T_b	a_s	α_{per}	β_{eu}	α_{int}	α_{dp}	β_{el}	α_{gw}	α_{sf}	K
	ºC	m^3 ºC^{-1} d^{-1}	d^{-1}	m^{-3}	d^{-1}	d^{-1}	m^{-3}	d^{-1}	d^{-1}	cal
1	8.0	$.47\times10^{+7}$	$.13\times10^{+1}$	$.67\times10^{-6}$	$.24\times10^{-1}$	$.53\times10^{-1}$	$.14\times10^{-6}$	$.14\times10^{-1}$	$.11\times10^{+1}$	$1.02\times10^{+16}$
2	10.	$.85\times10^{+7}$	$.30\times10^{+2}$	$.57\times10^{-5}$	$.45\times10^{-1}$	$.12\times10^{+0}$	$.59\times10^{-7}$	$.17\times10^{-1}$	$.40\times10^{+0}$	$2.30\times10^{+16}$
3	6.2	$.23\times10^{+7}$	$.73\times10^{+0}$	$.37\times10^{-2}$	$.10\times10^{-4}$	$.17\times10^{-1}$	$.65\times10^{-3}$	$.27\times10^{-1}$	$.36\times10^{+0}$	$2.29\times10^{+15}$
4	7.9	$.11\times10^{+8}$	$.88\times10^{-5}$	$.95\times10^{-2}$	$.90\times10^{-1}$	$.79\times10^{-1}$	$.88\times10^{-4}$	$.10\times10^{+0}$	$.10\times10^{+0}$	$1.79\times10^{+16}$
5	8.1	$.42\times10^{+7}$	$.58\times10^{-4}$	$.11\times10^{-5}$	$.60\times10^{+5}$	$.99\times10^{-1}$	$.10\times10^{-3}$	$.20\times10^{+0}$	$.33\times10^{+0}$	$5.92\times10^{+15}$
6	6.6	$.74\times10^{+8}$	$.39\times10^{-1}$	$.45\times10^{-7}$	$.97\times10^{-5}$	$.32\times10^{-5}$	$.64\times10^{-7}$	$.49\times10^{-1}$	$.19\times10^{+0}$	$6.07\times10^{+16}$
7	6.4	$.90\times10^{+7}$	$.43\times10^{-1}$	$.47\times10^{-6}$	$.86\times10^{-5}$	$.61\times10^{-5}$	$.12\times10^{-5}$	$.64\times10^{-1}$	$.41\times10^{+0}$	$7.50\times10^{+15}$
8	5.9	$.41\times10^{+8}$	$.49\times10^{-1}$	$.12\times10^{-5}$	$.60\times10^{-2}$	$.25\times10^{-5}$	$.16\times10^{-5}$	$.60\times10^{-1}$	$.28\times10^{+0}$	$1.10\times10^{+16}$
9	7.1	$.12\times10^{+8}$	$.92\times10^{-6}$	$.49\times10^{-5}$	$.10\times10^{-4}$	$.30\times10^{-5}$	$.59\times10^{-7}$	$.50\times10^{-1}$	$.12\times10^{+1}$	$9.28\times10^{+15}$
10	5.2	$.73\times10^{+7}$	$.11\times10^{+0}$	$.29\times10^{-6}$	$.12\times10^{-1}$	$.63\times10^{-5}$	$.23\times10^{-6}$	$.59\times10^{-1}$	$.66\times10^{+0}$	$3.77\times10^{+15}$
11	7.6	$.57\times10^{+7}$	$.70\times10^{+1}$	$.84\times10^{-6}$	$.11\times10^{+0}$	$.57\times10^{-1}$	$.16\times10^{-7}$	$.22\times10^{-1}$	$.32\times10^{+1}$	$1.12\times10^{+16}$
12	5.8	$.38\times10^{+7}$	$.11\times10^{+1}$	$.12\times10^{-5}$	$.65\times10^{-1}$	$.58\times10^{-5}$	$.19\times10^{-7}$	$.29\times10^{-1}$	$.34\times10^{+1}$	$2.44\times10^{+15}$
13	5.1	$.60\times10^{+7}$	$.64\times10^{-6}$	$.13\times10^{-5}$	$.10\times10^{-4}$	$.30\times10^{-5}$	$.59\times10^{-7}$	$.50\times10^{-1}$	$.33\times10^{+0}$	$3.16\times10^{+15}$
14	4.5	$.50\times10^{+8}$	$.64\times10^{-1}$	$.23\times10^{-5}$	$.85\times10^{-1}$	$.44\times10^{-5}$	$.19\times10^{-3}$	$.61\times10^{-1}$	$.68\times10^{+0}$	$6.33\times10^{+14}$
15	4.4	$.79\times10^{+7}$	$.32\times10^{-1}$	$.49\times10^{-6}$	$.39\times10^{-1}$	$.54\times10^{-5}$	$.10\times10^{-9}$	$.58\times10^{-1}$	$.66\times10^{+0}$	$1.99\times10^{+15}$
16	4.3	$.35\times10^{+7}$	$.17\times10^{+1}$	$.11\times10^{-5}$	$.15\times10^{+0}$	$.14\times10^{+0}$	$.53\times10^{-7}$	$.24\times10^{-1}$	$.68\times10^{+1}$	$1.57\times10^{+15}$
17	4.6	$.80\times10^{+7}$	$.16\times10^{+1}$	$.14\times10^{-4}$	$.17\times10^{+0}$	$.20\times10^{+0}$	$.15\times10^{-5}$	$.27\times10^{-1}$	$.66\times10^{+1}$	$2.55\times10^{+15}$
18	4.6	$.51\times10^{+6}$	$.16\times10^{+1}$	$.14\times10^{-4}$	$.17\times10^{+0}$	$.20\times10^{+0}$	$.15\times10^{-5}$	$.27\times10^{-1}$	$.66\times10^{+1}$	$1.33\times10^{+14}$
19	9.4	$.31\times10^{+8}$	$.27\times10^{+2}$	$.80\times10^{-2}$	$.33\times10^{+0}$	$.40\times10^{+0}$	$.38\times10^{-7}$	$.18\times10^{-1}$	$.35\times10^{+0}$	$7.44\times10^{+16}$
20	6.9	$.24\times10^{+8}$	$.26\times10^{+1}$	$.28\times10^{-5}$	$.57\times10^{-1}$	$.72\times10^{-1}$	$.16\times10^{-6}$	$.13\times10^{-1}$	$.51\times10^{+0}$	$2.08\times10^{+16}$
21	14.	$.14\times10^{+8}$	$.91\times10^{+2}$	$.11\times10^{-3}$	$.35\times10^{+0}$	$.44\times10^{-5}$	$.54\times10^{-7}$	$.75\times10^{-1}$	$.10\times10^{+1}$	$3.09\times10^{+16}$

Table 11. Large Basin Runoff Model Parameters for the Lake Ontario Subbasins.

No.	T_b	a_s	α_{per}	β_{eu}	α_{int}	α_{dp}	β_{el}	α_{gw}	α_{sf}	K
	ºC	m^3 ºC^{-1} d^{-1}	d^{-1}	m^{-3}	d^{-1}	d^{-1}	m^{-3}	d^{-1}	d^{-1}	cal
1	6.0	$.17\times10^{+8}$	$.51\times10^{-1}$	$.44\times10^{-4}$	$.61\times10^{-2}$	$.33\times10^{-5}$	$.15\times10^{-3}$	$.24\times10^{+0}$	$.33\times10^{+0}$	$1.39\times10^{+16}$
2	6.0	$.97\times10^{+7}$	$.51\times10^{-1}$	$.44\times10^{-4}$	$.61\times10^{-2}$	$.33\times10^{-5}$	$.15\times10^{-3}$	$.24\times10^{+0}$	$.33\times10^{+0}$	$7.70\times10^{+15}$
3	4.2	$.16\times10^{+8}$	$.90\times10^{-4}$	$.56\times10^{-7}$	$.20\times10^{-1}$	$.73\times10^{-5}$	$.14\times10^{-9}$	$.67\times10^{-1}$	$.63\times10^{-1}$	$5.70\times10^{+15}$
4	5.5	$.43\times10^{+7}$	$.49\times10^{+0}$	$.33\times10^{-5}$	$.17\times10^{-5}$	$.19\times10^{+0}$	$.36\times10^{-6}$	$.22\times10^{-1}$	$.40\times10^{+0}$	$3.66\times10^{+15}$
5	4.3	$.49\times10^{+8}$	$.12\times10^{+0}$	$.19\times10^{-7}$	$.41\times10^{-1}$	$.74\times10^{-5}$	$.96\times10^{-7}$	$.29\times10^{+0}$	$.45\times10^{-1}$	$1.12\times10^{+16}$
6	4.3	$.70\times10^{+7}$	$.18\times10^{+1}$	$.33\times10^{-5}$	$.12\times10^{+0}$	$.87\times10^{-1}$	$.39\times10^{-7}$	$.42\times10^{-1}$	$.36\times10^{+1}$	$2.28\times10^{+15}$
7	4.4	$.22\times10^{+8}$	$.10\times10^{-5}$	$.11\times10^{-7}$	$.20\times10^{-4}$	$.30\times10^{-5}$	$.81\times10^{-7}$	$.50\times10^{-1}$	$.59\times10^{-1}$	$8.62\times10^{+15}$
8	3.1	$.18\times10^{+8}$	$.11\times10^{+0}$	$.10\times10^{-6}$	$.21\times10^{-1}$	$.14\times10^{-5}$	$.10\times10^{-9}$	$.36\times10^{-1}$	$.94\times10^{-1}$	$9.13\times10^{+14}$
9	4.4	$.12\times10^{+8}$	$.83\times10^{+0}$	$.55\times10^{-1}$	$.89\times10^{-6}$	$.15\times10^{-1}$	$.20\times10^{-2}$	$.79\times10^{+2}$	$.10\times10^{+0}$	$2.11\times10^{+15}$
10	4.4	$.17\times10^{+8}$	$.83\times10^{+0}$	$.55\times10^{-1}$	$.89\times10^{-6}$	$.15\times10^{-1}$	$.20\times10^{-2}$	$.79\times10^{+2}$	$.10\times10^{+0}$	$3.39\times10^{+15}$
11	6.9	$.14\times10^{+8}$	$.49\times10^{+1}$	$.59\times10^{-1}$	$.15\times10^{+0}$	$.12\times10^{+0}$	$.27\times10^{-6}$	$.22\times10^{-1}$	$.10\times10^{+0}$	$1.68\times10^{+16}$
12	5.6	$.77\times10^{+8}$	$.57\times10^{+6}$	$.11\times10^{-9}$	$.17\times10^{-1}$	$.49\times10^{-2}$	$.19\times10^{-8}$	$.95\times10^{-2}$	$.53\times10^{+0}$	$4.46\times10^{+16}$
13	5.5	$.95\times10^{+7}$	$.19\times10^{+1}$	$.23\times10^{-4}$	$.95\times10^{-2}$	$.24\times10^{-1}$	$.25\times10^{-7}$	$.71\times10^{-2}$	$.15\times10^{+1}$	$7.43\times10^{+15}$
14	5.5	$.84\times10^{+7}$	$.19\times10^{+1}$	$.31\times10^{-5}$	$.20\times10^{-1}$	$.28\times10^{-1}$	$.23\times10^{-6}$	$.12\times10^{-1}$	$.48\times10^{+0}$	$7.22\times10^{+15}$
15	5.5	$.72\times10^{+7}$	$.19\times10^{+1}$	$.31\times10^{-5}$	$.20\times10^{-1}$	$.28\times10^{-1}$	$.23\times10^{-6}$	$.12\times10^{-1}$	$.48\times10^{+0}$	$6.14\times10^{+15}$

cal) lake heat storage (*Croley* 1992a). Ice formation and loss is coupled also to lake thermodynamics and heat storage (*Croley and Assel* 1994).

Thermodynamic Fluxes. The thermodynamic fluxes to and from a lake include incident short-wave radiation, q_i, reflected short-wave radiation, q_r and q_r' (over water and over ice, respectively), evaporative (latent and advected) heat transfer, q_e and q_e', sensible heat transfer, q_h and q_h', precipitation heat advection, q_p and q_p', net long-wave radiation exchange, Q_l, and surface flow advection, Q_I; see *Croley* (1989a,b) for details:

$$q_i = \left[0.355 + 0.68(1 - N)\right] q_0 \tag{21}$$

Table 12. Large Basin Runoff Model Calibration Statistics[a].

Lake	Number of Sub-basins	Mean 1-day Flow (mm)[b]	Flow Standard Deviation (mm)[b]	Root Mean Square Error (mm)[b]	Correlation Calibration	Independent Verification
Superior	22	1.12	0.67	0.25	0.93	0.77
Michigan	29	0.89	0.47	0.18	0.93	0.86
Huron	27	1.06	0.69	0.26	0.92	0.69
St. Clair	7	0.90	1.36	0.62	0.89	0.87
Erie	21	1.01	1.28	0.54	0.91	0.90
Ontario	15	1.41	1.13	0.43	0.93	0.89

[a]Statistics and calibrations generally are 1966-83; verification generally is 1956-63.
[b]Equivalent depth over the land portion of the basin.

where q_i = daily average unit (per unit area) rate of short-wave radiation incident to the earth's surface, N = fraction of the sky covered by clouds, and q_0 = daily average unit rate of short-wave radiation received on a horizontal unit area of the Earth's surface under cloudless skies;

$$q_r = 0.1\, q_i \tag{22}$$

where q_r = average unit reflected short-wave radiation rate from the water surface;

$$e_w = \rho_a\, C_E \left(q_w - q\right) U / \rho_w \tag{23}$$

where e_w = over-water evaporation rate, ρ_a = density of air, C_E = bulk evaporation coefficient over water, q_w = specific humidity of saturated air at the temperature of the water surface, q = specific humidity of the atmosphere over water, and U = wind speed over water;

$$q_e = \left(\gamma_v + C_w\, T\right) e_w\, \rho_w \tag{24}$$

where q_e = average unit evaporative (latent and advected) heat transfer rate from the water surface, C_w = specific heat of water, and T = water surface temperature;

$$q_h = \rho_a\, C_p C_H \left(T_a - T\right) U \tag{25}$$

where q_h = average unit sensible heat transfer rate to the water surface, C_p = specific heat of air at constant temperature, and C_H = sensible heat coefficient over water;

$$\begin{aligned} q_p &= \left(C_w\, T_a - \gamma_f\right) \rho_w\, p, & T_a &< 0^\circ\,\mathrm{C} \\ &= C_w\, T_a\, \rho_w\, p, & T_a &\geq 0^\circ\,\mathrm{C} \end{aligned} \tag{26}$$

where q_p = average unit precipitation heat advection rate to the water surface;

$$q_\uparrow = \varepsilon_w\, \sigma \left(T + 273.16^\circ\,\mathrm{C}\right)^4 \tag{27}$$

where $q_{\uparrow}$ = average unit long-wave radiation emitted by the water body, σ = Stephan-Bolzmann constant (5.67×10^{-8} W m^{-2} K^{-4}), and e_w = emissivity of the water surface;

$$q_{\downarrow} = (1 - r_a)\varepsilon_a\, \sigma(T + 273.16°\mathrm{C})^4 \tag{28}$$

where $q_{\downarrow}$ = average unit long-wave radiation from the atmosphere absorbed by the water surface, r_a = reflectivity of the water surface, and e_a = emissivity of the atmosphere;

$$Q_l = \left\{q_{\downarrow}\left[\eta \;+\; (1-\eta)(1-N)\right] - q_{\uparrow}\right\}(A_w + A) \tag{29}$$

where Q_l = average net long-wave radiation exchange rate between the entire water body and the atmosphere (effects of ice cover on the net long-wave exchange are ignored here), η = empirical coefficient relating cloudiness to atmospheric long-wave radiation, A_w = area of the open-water (ice-free) surface, and A = area of the ice surface;

$$Q_I = \rho_w\, C_w\, T(\Theta_i - \Theta_o) \tag{30}$$

where Q_I = daily net flow heat advection to the lake assuming inflows at surface temperatures, Θ_i = sum of all surface inflows to the lake, and Θ_o = sum of all outflows from a lake;

$$q_r' = (0.85\, f_n + 0.70\, f_o + 0.50\, f_m + 0.45\, f_b)\, q_i \tag{31}$$

where q_r' = average unit reflected short-wave radiation rate from the ice pack, f_n = fraction of ice covered with new snow, f_o = fraction of ice covered with old snow, f_m = fraction of ice covered with melting snow, and f_b = fraction of ice that is bare of snow;

$$e_w' = \rho_a\, C_E'(q_w' \;-\; q')U'/\rho_w \tag{32}$$

where e_w' = over-ice evaporation rate, C_E' = bulk evaporation coefficient over ice, q_w' = specific humidity of saturated air at temperature of ice, q' = specific humidity of the atmosphere over ice, and U' = wind speed over ice;

$$q_e' = (\gamma_v \;+ \gamma_f \;+ C_w\, T')\, e_w'\, \rho_w \tag{33}$$

where q_e' = average unit evaporative (latent and advected) heat transfer rate from the ice pack and T' = ice surface temperature;

$$q_h' = \rho_a\, C_p\, C_H'(T_a' \;-\; T')U' \tag{34}$$

where q_h' = average unit sensible heat transfer rate to the ice pack, C_H' = sensible heat coefficient over ice, and T_a' = temperature of the air over ice; and

$$q_p' = C_w\, T_a'\, \rho_w\, p \tag{35}$$

where q_p' = average unit precipitation heat advection rate to the ice pack.

Gray et al. (1973) provided (21), generalized maps of mid-monthly values from which q_0 may be interpolated by date, and the short-wave reflection of (22) and (31). Because data are unavailable and because subsequent heat budgets are insensitive to their values, f_n, f_o, and f_m are set to zero here and f_b is set to unity. Values of over-water and over-ice meteorology (q, U, T_a, N, q', U', and T_a') are determined from overland values by adjusting for over-water conditions. *Phillips and Irbe's* (1978) regressions for over-water corrections are used directly by replacing the fetch (and derived quantities) with averages. The bulk evaporation coefficients over water and over ice (C_E and C_E') are determined similar to *Quinn* (1979) from over-water or over-ice (respectively) wind speed, air temperature, and surface temperature. The over-water and over-ice sensible heat coefficients (C_H and C_H') are taken equal to the bulk evaporation coefficients, respectively (*Quinn* 1979). The emissivities of water and air in (27) and (28) [note the reflectivity of the water surface in (28) is $r_a = 1 - e_w$] are taken, respectively, as 0.97, and $0.53 + 0.065\, e_a^{1/2}$ where e_a is the vapor pressure of the air (mb) after *Keijman* (1974).

Heat Storage. The heat added to a lake and the heat added to the ice pack, from the surface fluxes, are governed by simple energy and mass balances, energy-storage relationships, and boundary conditions on ice growth, water temperature, and ice temperature; see Figure 13. The rate of change of heat storage in a lake with time is:

$$\frac{\partial H}{\partial t} = A_w\left(q_i - q_r - q_e + q_h + q_p\right) + Q_l + Q_I - Q_w \qquad (36)$$

where $\partial H/\partial t$ = time rate of change of heat storage H in the lake and Q_w = total heat flux between the water body and the ice pack. The rate of change of heat storage in the ice pack with time is:

$$\frac{\partial H'}{\partial t} = A\left(q_i - q_r' - q_e' + q_h' + q_p'\right) + Q_w \qquad (37)$$

where $\partial H'/\partial t$ = time rate of change of heat storage H' in the ice pack.

Kraus' and Turner's (1967) mixed-layer thermal structure concept is extended to allow the determination of simple heat storage. Effects of past additions or losses are superimposed to determine surface temperature on any day as a function of heat in storage; each past addition or loss is parameterized by age. Turnovers (convective mixing of deep lower-density waters with surface waters as surface temperature passes through that at maximum density) can occur as a fundamental behavior of this superposi-

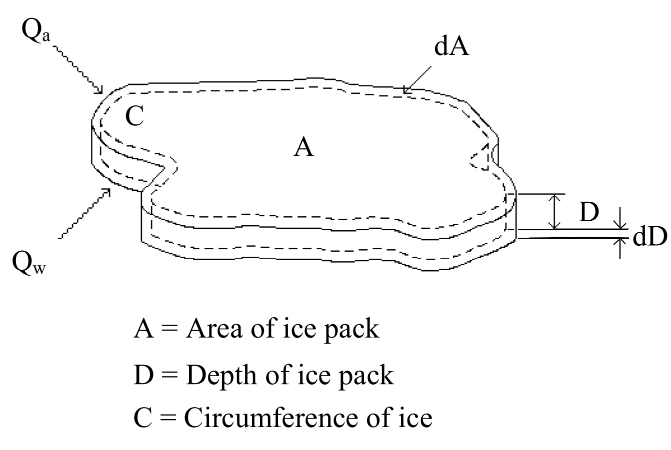

Figure 13. Conceptual Prismatic Ice Pack.

tion model and hysteresis between heat in storage and surface temperature, observed during the heating and cooling cycles on the lakes, is preserved. Water surface temperature becomes (*Croley* 1992a):

$$T_k = 3.98°\mathrm{C} + \sum_{m=1}^{k} f_{k,m} \left(\underset{m \le n \le k}{\mathrm{MIN}} H_n - \underset{m-1 \le n \le k}{\mathrm{MIN}} H_n \right) \tag{38}$$

where T_k = water surface temperature and H_k = heat storage in the lake k days after the last turnover, and $f_{k,m}$ is a "wind-aging" function, defined subsequently, relating surface temperature rise on day k to heat added on day m. Ice surface temperature relates to ice pack heat storage here as:

$$H_k' = \rho C_i V_k T_k'/2 - \rho \gamma_f V_k' \tag{39}$$

where T_k' = ice surface temperature on day k, H_k' = heat storage in the ice pack on day k, ρ = density of ice, C_i = specific heat of ice, V_k = volume of the ice pack on day k, and V_k' = volume of ice formed by freezing or melting on day k. The boundary conditions on water surface temperature and volume of the ice pack for every day (dropping the daily subscript) are:

$$V = 0, \qquad T \ge 0°\mathrm{C} \tag{40}$$

$$T = 0°\mathrm{C}, \qquad V \ge 0 \tag{41}$$

These equations are satisfied by selecting the heat flux between the water and ice, Q_w, appropriately. Q_w, if negative, is yielded as ice forms (to keep water surface temperature from going below freezing) and, if positive, is used in melting ice (to keep water surface temperature at freezing as long as there is ice present). The boundary conditions on ice surface temperature and volume of the ice pack for every day (dropping the daily subscript) are:

$$T' = T_a, \qquad V > 0 \text{ and } T_a \le 0°\mathrm{C} \tag{42}$$

$$T' = 0°\mathrm{C}, \qquad V = 0 \text{ or } T_a > 0°\mathrm{C} \tag{43}$$

where T_a = over-ice air temperature. The volume of the ice pack, V, and the volume of ice formed by freezing or melting, V', are related:

$$\frac{\partial V}{\partial t} = \frac{\partial V'}{\partial t} + S - E \tag{44}$$

where S = volumetric rate of snow falling on the ice and E = volumetric rate of evaporation from the ice. The "wind-aging" function, $f_{k,m}$, is:

$$\begin{aligned} f_{k,m} &= \frac{2 - M_{k,m}/F}{\rho_w C_w M_{k,m}}, && M_{k,m} < \mathrm{MIN}\left(F, \ \frac{2V_c}{1+V_c/F}\right) \\ &= \frac{1}{\rho_w C_w M_{k,m}}, && \mathrm{MIN}\left(F, \ \frac{2V_c}{1+V_c/F}\right) \le M_{k,m} < \mathrm{MAX}\left(V_c, \ \frac{2V_c}{1+V_c/F}\right) \\ &= \frac{1}{\rho_w C_w V_c}, && \mathrm{MAX}\left(V_c, \ \frac{2V_c}{1+V_c/F}\right) \le M_{k,m} \end{aligned} \tag{45}$$

where V_c = volume (capacity) of the lake and $M_{k,m}$ = mixing volume size in the lake, on day k, of the heat added on day m (a function of accumulated wind movement, W_j, from day m through day k),

$$M_{k,m} = V_e \left[1 + a \exp\left(-b \sum_{j=m}^{k} W_j \right) \right]^{-1} \tag{46}$$

Also, a, b, F, and V_e = empirical parameters to be determined in a calibration to observed data. V_e is interpreted as the "equilibrium" volume approached as a limit (in a sufficiently deep lake) since the effects of wind mixing at the surface diminish with distance from the surface. F is interpreted as the mixing volume at which a heat addition is fully mixed throughout. Parameters a, b, and F are defined for water temperatures above 3.98°C ("turnover" temperature of water at maximum density) and are replaced by a', b', and F', respectively, for water temperatures below 3.98°C. Details for the flux terms in (36) and (37) are presented by *Croley* (1989a,b). Derivation details of (38), (45), and (46) are available elsewhere (*Croley* 1992a).

Ice Pack Growth. In (39), linear vertical temperatures are used through the ice pack from T' on the surface to 0°C on the bottom, similar to *Green and Outcalt* (1985). Differentiating (4) and ignoring small terms,

$$\frac{\partial H'}{\partial t} \cong \tfrac{1}{2} \rho C_i V \frac{\partial T'}{\partial t} - \rho \gamma_f \frac{\partial V'}{\partial t} \tag{47}$$

Thus, the heat change is split between a temperature change in the ice pack and a volume change due to melting or freezing. Comparing (37) and (47), note the temperature change in (47) is taken here as resulting from a portion of the heat added from (or lost to) the atmosphere [A (q_i - q_r' - q_e' + q_h' + q_p')]. The remainder of that heat is identified as Q_a:

$$Q_a = A\left(q_i - q_r' - q_e' + q_h' + q_p'\right) - \tfrac{1}{2} \rho C_i V \frac{\partial T'}{\partial t} \tag{48}$$

This heat (Q_a) and all of the heat added from the water body, Q_w, then result in changes to the ice pack volume (freezing or melting); from (37), (44), (47), (48):

$$Q_a + Q_w = -\rho \gamma_f \frac{\partial V'}{\partial t} = -\rho \gamma_f \left(\frac{\partial V}{\partial t} - S + E \right) \tag{49}$$

Consider a prismatic ice pack with surface area A and depth (or thickness) D. The heat exchange between the atmosphere and the ice pack available for freezing or melting, Q_a, is taken as resulting in either melt (along the entire atmosphere-ice surface) or freezing (along the entire water-ice surface). The heat exchange between the water body and the ice pack, Q_w, is taken as resulting in changes along only the water/ice surface (either melt or freezing). After simplification (*Croley and Assel* 1994),

$$\frac{\partial D}{\partial t} = \left\{ -\frac{Q_a}{A + x_w D} I_{(-\infty,0]}(Q_a) - \frac{Q_a}{A + x_a D} I_{(0,\infty)}(Q_a) - \frac{Q_w}{A + x_w D} \right\} \frac{1}{\rho \gamma_f} + \frac{S}{A} - \frac{E}{A + x_a D} \tag{50}$$

$$\frac{\partial A}{\partial t} = \left\{ -\frac{x_w Q_a}{A + x_w D} I_{(-\infty,0]}(Q_a) - \frac{x_a Q_a}{A + x_a D} I_{(0,\infty)}(Q_a) - \frac{x_w Q_w}{A + x_w D} \right\} \frac{1}{\rho \gamma_f} - \frac{x_a E}{A + x_a D} \tag{51}$$

$$x_a = \tau_a A^{1/2} \tag{52}$$

$$x_w = \tau_w A^{1/2} \tag{53}$$

where $I_{(.,.)}(x)$ = indicator function (equal to unity if the quantity in parentheses, x, is within the indicated interval and equal to zero if not), τ_a and τ_w = empirical coefficients depending upon ice pack shape, the ratios of vertical to lateral changes along the atmosphere-ice interface and along the water-ice interface, and the buoyancy of ice. The change in total ice volume is, from (50) and (51):

$$\begin{aligned} \frac{\partial V}{\partial t} &= \frac{\partial (A\,D)}{\partial t} = A\frac{\partial D}{\partial t} + D\frac{\partial A}{\partial t} \\ &= (-Q_a - Q_w)\frac{1}{\rho \gamma_f} + S - E \end{aligned} \tag{54}$$

Note, (49) and (54) agree.

Equations (36)-(48), (50)-(54), and those for the component fluxes, (21)-(35), may be solved simultaneously to determine the heat storage, the water and ice surface temperatures, and the ice pack extents. The Lake Evaporation and Thermodynamics Model is pictured schematically in Figure 14.

Calibration Procedure. Two calibrations are involved in applying the model in a particular setting. The first determines the first eight parameters (a, b, F, a', b', F', V_e, and h). The first seven parameters relate to superposition heat storage (*Croley* 1992a) and the eighth parameter, h, reflects the effect of cloudiness on the atmospheric net long-wave radiation exchange (*Croley* 1989a,b). This calibration minimizes daily water surface temperature root mean square error (RMSE) by using methods described elsewhere (*Croley and Hartmann* 1984). Meteorology data for 1948-1985 and water surface temperature data on each of the Great Lakes, except Lake Michigan, were taken from airplane and satellite measurements, extended through August 1988, and prepared as described by *Croley* (1989a,b). Water surface temperature data for Lake Michigan from

1981 through 1985 were gleaned from areal maps prepared at the National Weather Service's Marine Predictions Branch (*B. Newell*, personal communication, 1990) and extended through August 1988 also. The second calibration determines the two parameters (τ_a and τ_w) that minimize daily ice cover RMSE with these same calibration techniques. Lake-averaged ice cover for model calibration was calculated from GLERL's digital ice cover data base (*Assel* 1983). In most cases, less than 100% of a lake was observed on any given date. If less than 70% of the Lake Superior surface was observed, the ice cover for that date was not included in the model calibration. A subjective estimate of lake-averaged ice cover was made for the other Great Lakes if the data were insufficient.

Parameters are determined, in both cases, in automated systematic searches of the parameter spaces to minimize the RMSE between simulated and model outputs. Each parameter, selected in rotation, is searched until all parameter values converge to four digits, instead of searching only until the RMSE stabilizes. This simple search algorithm does not give unique optima for calibrated parameter sets because of synergistic relationships between parameters which allow parameter compensations to occur. However, the model concepts have been carefully chosen so that the parameters have physical significance; this allows them to be interpreted in terms of the thermodynamics they represent. Initialization of the model corresponds to identifying values from field conditions which may be measured; interpretations of a lake's thermodynamics then can aid in setting both initial and boundary conditions.

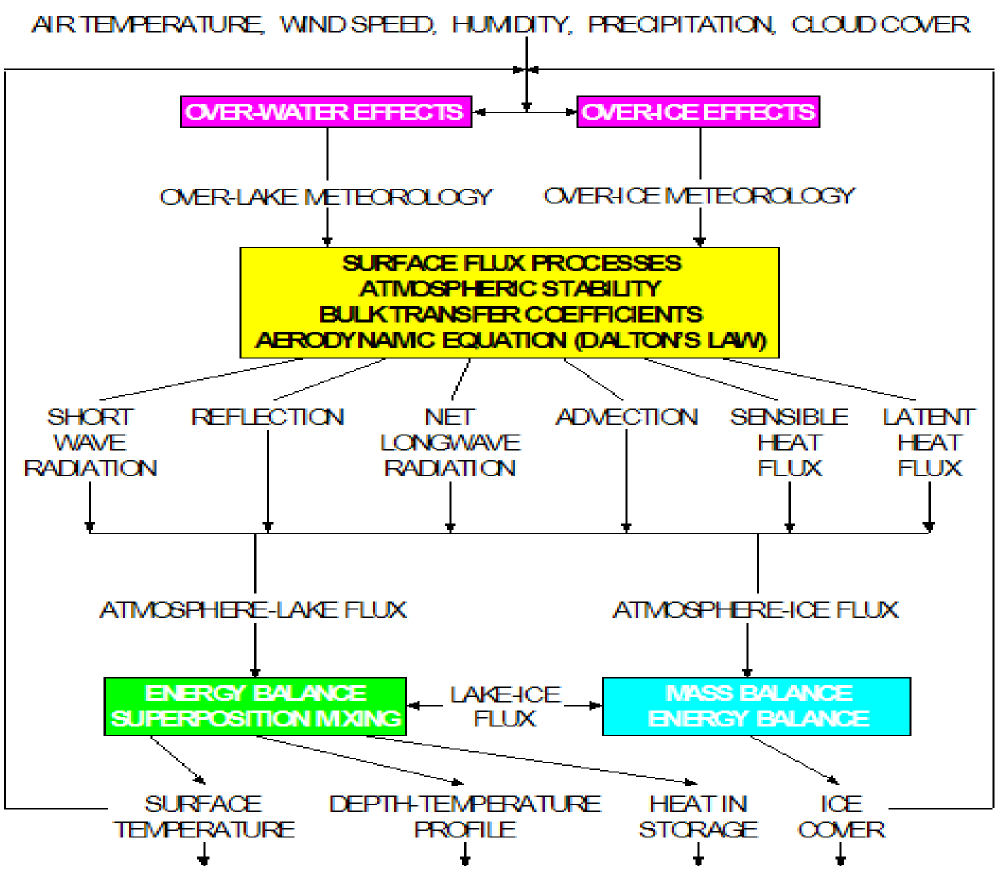

Figure 14. Lake Evaporation and Thermodynamics Model Conceptual Schematic.

Prior to calibration or model use, the (spatial) average temperature-depth profile in the lake and the ice cover must be initialized. While the ice cover is easy to determine as zero during major portions of the year, the average temperature-depth profile in the lake is generally difficult to determine. If the model is to be used in forecasting or for short simulations, then it is important to determine these variables accurately prior to use of the model. If the model is to be used for calibration or for long simulations, then the initial values are generally unimportant. The effect of the initial values diminishes with the length of the simulation, and after 2-3 years of simulation, the effects are nil from a practical point of view.

Empirical coefficients of the evaporation, heat storage, and ice sub-models were calibrated in an iterative process that used the two calibrations sequentially in rotation. GLERL used independent data (lake-averaged daily surface temperature for the lake thermodynamics and heat storage sub-models and lake-averaged daily ice cover for the lake ice cover sub-model). First they minimized the RMSE of daily water surface temperature by calibrating lake thermodynamics model parameters and holding the parameters for the ice cover sub-model constant. they then held lake thermodynamics model parameters constant and calibrated the parameters of the ice cover sub-model to minimize the RMSE of daily ice cover. Then they repeated the process until the RMSEs for both water surface temperatures and ice cover did not significantly reduce.

Application. The results of the parameter calibration, as well as a few statistics on each of the Great Lakes, are summarized in Table 13. Statistics from the calibration and from an independent verification period are presented in Table 14. Turnovers (convective mixing of deep lower-density waters with surface waters as surface temperature passes through that at maximum density) occur as a fundamental behavior of GLERL's thermodynamic and heat storage model. Hysteresis between heat in storage and surface temperature, observed during the heating and cooling cycles on the lakes, is preserved. The model also correctly depicts lake-wide seasonal heating and cooling cycles, vertical temperature distributions, and other mixed-layer developments. There is good agreement between the actual and calibrated-model water surface temperatures; the RMSE is between 1.1-1.6°C on the large lakes [within 1.1-1.9°C for an independent verification period, 1966-79 (*Croley* 1989a,b, 1992a)]. The RMSE for ice concentrations is between 12 and 23% for

Table 13. Lake Evaporation and Thermodynamics Model Constants and Parameters.

	Lake					
	Superior	Michigan	Huron	Georgian	Erie	Ontario
Surface area, km^2	82,100	57,800	40,640	18,960	25,700	18,960
Volume, km^3	12,100	4,920	2,761	779	484	1,640
Average depth, m	147	85.1	67.9	41.1	18.8	86.5
a	$6.298\times10^{+0}$	$7.290\times10^{+0}$	$6.460\times10^{+0}$	$1.585\times10^{+0}$	$2.820\times10^{+0}$	$7.710\times10^{+0}$
b, m^{-1} s	3.298×10^{-3}	2.599×10^{-3}	2.810×10^{-3}	5.473×10^{-3}	5.430×10^{-3}	2.800×10^{-3}
F, km^3	$3.273\times10^{+3}$	$5.100\times10^{+2}$	$4.890\times10^{+3}$	$1.101\times10^{+3}$	$1.000\times10^{+2}$	$2.000\times10^{+2}$
a'	$2.019\times10^{+0}$	$1.158\times10^{+0}$	$3.829\times10^{+0}$	$1.471\times10^{+0}$	$2.610\times10^{+0}$	$4.000\times10^{+0}$
b', m^{-1} s	3.795×10^{-3}	2.301×10^{-3}	3.890×10^{-3}	1.103×10^{-2}	5.600×10^{-3}	5.110×10^{-3}
F', km^3	$5.113\times10^{+3}$	$4.000\times10^{+3}$	$6.789\times10^{+3}$	$8.943\times10^{+2}$	$1.000\times10^{+2}$	$4.600\times10^{+2}$
Ve, km^3	$1.200\times10^{+4}$	$5.006\times10^{+3}$	$8.010\times10^{+3}$	$9.748\times10^{+2}$	$8.490\times10^{+2}$	$2.000\times10^{+3}$
h	$1.299\times10^{+0}$	$1.068\times10^{+0}$	$1.150\times10^{+0}$	$1.223\times10^{+0}$	$1.290\times10^{+0}$	$1.200\times10^{+0}$
τ_a	$9.011\times10^{+8}$	$9.001\times10^{+8}$	$9.119\times10^{+8}$	$9.279\times10^{+8}$	$9.988\times10^{+8}$	$9.010\times10^{+8}$
τ_w	$8.002\times10^{+5}$	$2.003\times10^{+5}$	$1.080\times10^{+6}$	$4.437\times10^{+5}$	$9.202\times10^{+5}$	$8.001\times10^{+4}$

Table 14. Lake Evaporation and Thermodynamics Model Calibration Statistics.

	Lake					
	Superior	Michigan	Huron	Georgian	Erie	Ontario
			CALIBRATION PERIOD STATISTICS			
			Water Surface Temperatures (1980-1988)[a]			
Means Ratio[b]	1.00	1.01	0.98	1.01	1.03	0.99
Variances Ratio[c]	1.01	0.98	0.95	1.02	1.08	0.99
Correlation[d]	0.98	0.97	0.98	0.99	0.99	0.98
R.M.S.E.[e]	1.13	1.56	1.33	1.10	1.58	1.43
			Ice Concentrations (1960-1988)[f]			
Means Ratio[g]	0.92	0.72	0.70	0.98	1.15	0.39
Variances Ratio[h]	1.24	1.02	1.67	1.62	1.09	0.63
Correlation[i]	0.76	0.83	0.73	0.77	0.89	0.54
R.M.S.E.[j]	23.4	12.4	26.0	21.5	19.0	15.4
			VERIFICATION PERIOD STATISTICS			
			Water Surface Temperatures (1966-1979)[k]			
Means Ratio[b]	0.96		1.03	0.98	1.05	0.94
Variances Ratio[c]	1.10		0.95	1.00	1.10	0.97
Correlation[d]	0.97		0.99	0.98	0.98	0.96
R.M.S.E.[e]	1.09		1.10	1.34	1.91	1.92

[a]Data between 1 January 1980 and 31 August 1988 for all lakes except Michigan and between 1 January 1981 and 31 August 1988 for Lake Michigan, with an initialization period for all lakes except Georgian Bay starting 1 January 1948 and 1 January 1953 for Georgian Bay.
[b]Ratio of mean model surface temperature to data mean (ºC/ºC).
[c]Ratio of variance of model surface temperature to data variance.
[d]Correlation between model and data surface temperature.
[e]Root-mean-square-error between model and data surface temperatures in ºC.
[f]Data between 1 January 1960 and 31 August 1988 for all Great Lakes except Superior and between 1 March 1963 and 31 August for Lake Superior, with an initialization period for all lakes starting 1 January 1958.
[g]Ratio of mean model ice concentration to data mean.
[h]Ratio of variance of model ice concentration to data variance.
[i]Correlation between model and data ice concentration.
[j]Root-mean-square-error between model and data ice concentrations in %.
[k]Data between 1 January 1966 and 31 December 1979 for all lakes except Michigan with an initialization period for all lakes except Georgian Bay starting 1 January 1948 and 1 January 1953 for Georgian Bay.

the joint calibration-verification period. There is also good agreement with 8 years of bathythermograph observations of depth-temperature profiles on Lake Superior and 1 year of independently-derived weekly or monthly surface flux estimates on Lakes Superior, Erie, and Ontario (2 estimates).

Calibration Issues. There were several problems in calibrating the model. First, it appears that the models are close to being over-specified in terms of the number of parameters used; i.e., there appear to be almost too many degrees of freedom allowed for the data sets used in the calibrations. The result is that the optimums are not unique and it is not possible to determine meaningful values of any additional parameters. Parameter compensation exists so that changes in one parameter can be offset by changes in other parameters with little change in the RMSE of the calibration. This made it difficult to determine an ice break-up model, not presented here, which had an additional three parameters. GLERL had considered ice breakage and rejoining by developing a differential equation for the rate of change with time of the number of ice pieces as a function of wind stress, melting, and refreezing. GLERL could not meaningfully calibrate this addition to the ice model with the ice cover data sets GLERL had, and so GLERL eliminated ice break-up from the model presented here. Perhaps when other parameters are reduced through model reformulations in calibrations at a later date, it will be possible to model and calibrate for ice break-up in a meaningful manner.

Second, optimizing parameters with regard to two objectives (minimizing RMSEs associated with water surface temperatures and ice cover) does not produce the same parameter sets. There seems to be a trade-off between the two objectives at times and RMSE of water temperatures decreases at the expense of ice cover RMSE and vice-versa.

The model has ten parameters calibrated to match water surface temperatures and ice cover. Seven of them are defined in the superposition heat storage submodel. The number of empirical model parameters could perhaps be reduced by use of other one-dimensional mixed-layer heat-storage models (*McCormick and Meadows* 1988; *Hostetler and Bartlein* 1990). The critical limitation of such models for long-term hydrological forecasting and simulation is the lack of representative or accurate hourly hydrometeorological data over long periods. Secondarily, computer time can be excessive for such models in forecast or multi-year simulation environments.

Models Validity and Applicability

Although GLERL uses a daily resolution of data with their models, basin-wide processes of runoff, over-lake precipitation, and lake evaporation (described with models here) respond discernibly to weekly changes at best, and monthly is usually adequate for net supply and lake level simulation (this ignores short-term fluctuations associated with storm movement which are not addressed in this study). Likewise, spatial resolution finer than about 1000-5000 km^2 (the present average resolution of GLERL's models and their applications) is unnecessary, for use with general circulation models (GCMs) of the atmosphere, and much can be done in assessing hydrology changes at resolutions of 100,000 - 1,000,000 km^2 with lumped versions of the models.

The models were assessed partially by computing net basin supplies to the lakes (basin runoff plus overlake precipitation minus overlake evaporation) with historical meteorological data for 1951-80 and comparing to historical net basin supplies. The absolute average annual difference ranged from 1.6% to 2.7% on the deep lakes, while the Lake St. Clair and Lake Erie applications were 12.0% and 7.0% respectively; month-to-month differences showed more variation. These differences generally reflect poorer evaporation modeling on the shallow lakes and snowmelt and evapotranspiration model discrepancies for the other lake basins. While monthly differences were generally small, a few were significant. The low annual residuals were felt to be acceptable for use of these models in assessing changes from the current climate as they would be consistently applied to both a "present" and a "changed" climate. Further assessment of model deficiencies with comparisons to historical net basin supplies is difficult since the latter are derived from water budgets, which incorporate all budget term errors in the derived net basin supplies.

There is some indication of model applicability outside of the time periods over which the models were calibrated as indicated above and in Tables 12 and 14. To assess the applicability of the process models to a climate warmer than the one under which they were calibrated and verified requires access to meteorological data and process outputs for the warmer climate, which unfortunately do not exist. Warm periods early in this century are not sufficiently documented for the Great Lakes. In particular, data are lacking on watershed runoff to the lakes, water surface temperatures, wind speed, humidity, cloud cover, and solar insolation.

It is entirely possible that the models are tied somewhat to the present climate; empiricism is employed in the evapotranspiration component of the LBRM and in some of the heat flux terms in the heat balance and lake evaporation model. Coefficients were determined or selected in accordance with the present climate. The models are all based on physical concepts that should be good under any climate; however, the assumption is made that they represent processes under a changed climate that are the same as the present ones. These include linear reservoir moisture storages, partial-area infiltration, lake heat-storage relations with surface temperature, and gray-body radiation. However, the calibration and verification periods for the component process models include a range of air temperatures, precipitation, and other meteorological variables that encompass much of the changes in these variables predicted for a changed climate. Even though the changes are transitory in the calibration and verification period data sets, the models appear to work well under these conditions.

This page intentionally left blank.

Great Lakes Climate Change Hydrological Responses

GLERL integrated their hydrological process models into a system to estimate lake levels, whole-lake heat storage, and water and energy balances for forecasts and for assessment of impacts associated with climate change (*Croley* 1990, 1992b; *Croley and Hartmann* 1987; *Croley and Lee* 1993). As mentioned earlier, they used this system to simulate the Great Lakes hydrology for historical meteorology and four climate change scenarios generated through GCM experiments (CGCM2A, CGCM2B, HADCM3A, and HADCM3B). Behavior is characterized by looking at mean annual and seasonal values of each hydrological variable under each of the four climates tested, as well as the base case. Selected measures of the variability of each hydrological variable, for each of the four climates, also were calculated for the annual periods. These means and measures of variability are compared to those determined with the historical meteorology (which serves as a baseline for assessing shifts produced by other regimes). Seasonal steady-state behavior is exemplified here in figures for the Lake Ontario basin and summarized for all lakes and all climate-change scenarios for the entire period in annual tables and figures.

Basin Meteorology

The annual cycles of all meteorological variables were averaged over the 1950—1999 period and inspected; see Table 15 and Figures 15 and 16. The annual air temperatures for the base case increase with decreasing latitude; see Table 15. The overland air temperatures for all four climate change scenarios are higher throughout the annual cycle than the base case. The differences are greatest for the HADCM3A scenario, followed by the CGCM2A, HADCM3B, and CGCM2B scenarios and for the Lakes Michigan and Huron and Georgian Bay; see Table 15. The difference is generally smallest during the late spring and early winter and largest during the late winter and early fall for all lakes and for all transposed scenarios; as an example, see Figure 16 for the Lake Ontario basin. Changes in annual variability of air temperature were remarkably small. Table 16 shows the average annual steady state standard deviation of air temperature, depicting the variability from year to year in the 50-year period. The annual air temperature variability in Table 16 appears artificial and is the result of truncation of annual air temperatures to the nearest 0.1ºC before the standard deviation was calculated.

Overland precipitation shows much more variability than air temperature both among scenarios and among lake basins. Table 15 and Figure 17 show that generally precipitation is greater on all lakes and scenarios, except Michigan and Erie for the CGCM2B scenario and Erie for the CGCM2A scenario. The Canadian GCM scenarios generally increase precipitation much less than

Table 15. Average Annual Basin Meteorology Differences (1950—1999).

Basin	Overland Air Temperature (ºC) & Climate Scenario Absolute Differences[a]					Overland Precipitation (mm) & Climate Scenario Relative Changes[a]				
	BASE	#1	#2	#3	#4	BASE	#1	#2	#3	#4
Superior	2.3	3.0	2.2	3.7	2.7	820	1%	6%	8%	9%
Michigan	7.1	3.6	2.8	3.9	2.9	828	0%	-1%	7%	12%
Huron	7.1	3.6	2.8	4.1	3.1	817	2%	1%	7%	14%
Georgian	4.3	3.4	2.4	4.0	3.0	908	3%	3%	11%	13%
St. Clair	8.4	3.5	2.6	4.2	3.1	857	1%	0%	7%	15%
Erie	9.1	3.1	2.4	4.2	3.0	917	-1%	-4%	6%	16%
Ontario	7.2	3.2	2.2	4.0	3.0	941	5%	1%	9%	13%

[a]Scenario #1 is CGCM2A; #2 is CGCM2B; #3 is HADCM3A; #4 is HADCM3B.

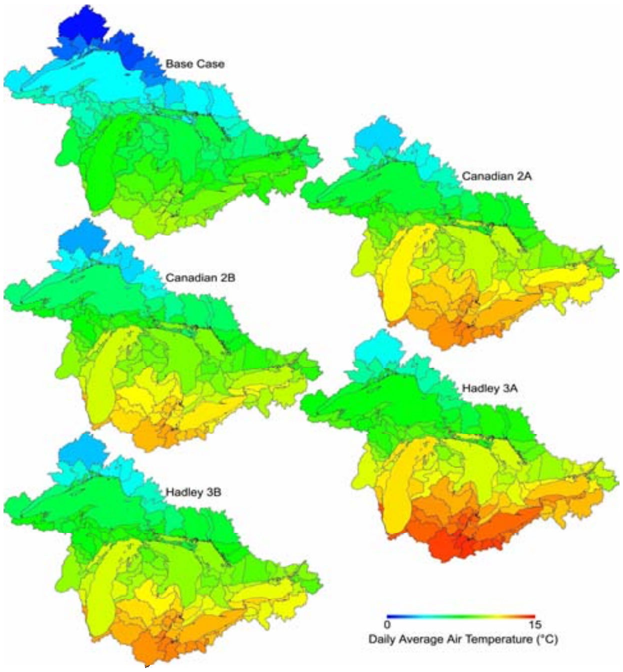

Figure 15. Daily Average Air Temperature Averaged Over The Year.

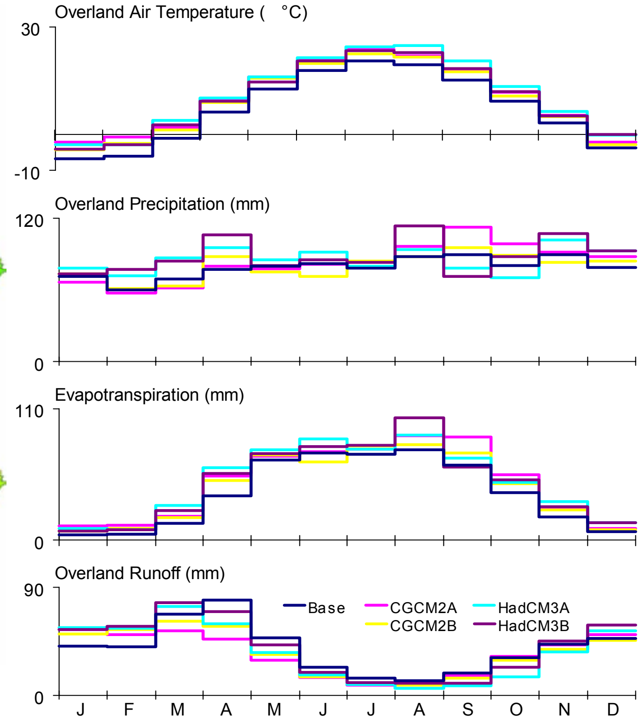

Figure 16. Seasonal Lake Ontario Basin Average Meteorology and Hydrology.

do the Hadley GCM scenarios. The largest increase occurs on Georgian Bay for the HADCM3A scenario and on Erie for the HADCM3B scenario.

The CGCM2B scenario seasonal precipitation variability is similar to the base case for Lake Ontario, see Figure 16 for the Ontario basin. The CGCM2A scenario shows more variability seasonally but the HADCM3B scenario shows the most variability with both spring and late summer peaks for Ontario. On the Lake Superior basin, all scenarios are very similar to the base case with only slightly higher spring precipitation for the HADCM3A and HADCM3B scenarios and slightly higher early summer precipitation for the HADCM3A, HADCM3B, and CGCM2A scenarios. There is also slightly higher fall precipitation for the CGCM2B scenario on Superior. On Michigan, we see a little more variability among the different scenarios throughout the season than with Superior, with the HADCM3B showing higher spring precipitation. Huron is similar to Michigan

Table 16. Average Annual Basin Meteorology Standard Deviation Differences (1950—1999).

Basin	Overland Air Temperature Std. Dev. (ºC) & Climate Scenario Relative Change[a]					Overland Precipitation Std. Dev. (mm) & Climate Scenario Relative Change[a]				
	BASE	#1	#2	#3	#4	BASE	#1	#2	#3	#4
Superior	0.9	0%	0%	0%	0%	81.6	3%	6%	7%	9%
Michigan	0.7	0%	0%	0%	0%	84.7	3%	-1%	7%	11%
Huron	0.7	0%	0%	0%	0%	84.8	4%	2%	6%	15%
Georgian	0.8	0%	-1%	0%	0%	87.9	5%	4%	11%	13%
St. Clair	0.7	-1%	0%	0%	0%	119.8	3%	0%	5%	14%
Erie	0.7	0%	0%	1%	0%	109.8	2%	-3%	6%	16%
Ontario	0.7	0%	0%	0%	0%	88.5	9%	2%	7%	10%

[a]Scenario #1 is CGCM2A; #2 is CGCM2B; #3 is HADCM3A; #4 is HADCM3B.

with the HADCM3B scenario showing higher spring precipitation but also slightly higher summer precipitation also. All scenarios except CGCM2A show higher winter precipitation on Georgian Bay with only slightly higher values through the rest of the year. St. Clair and Erie show higher precipitation for all scenarios except CGCM2A, with the HADCM3B peaking highest in spring and fall.

Changes in annual variability of precipitation are also more pronounced than for air temperature; see Table 16. Generally, the Hadley scenarios, which are the wettest in Table 15, also are the more variable as seen in Table 16. This is expected since if precipitation is generally closer to its lower bound of zero, its variation must therefore be diminished too.

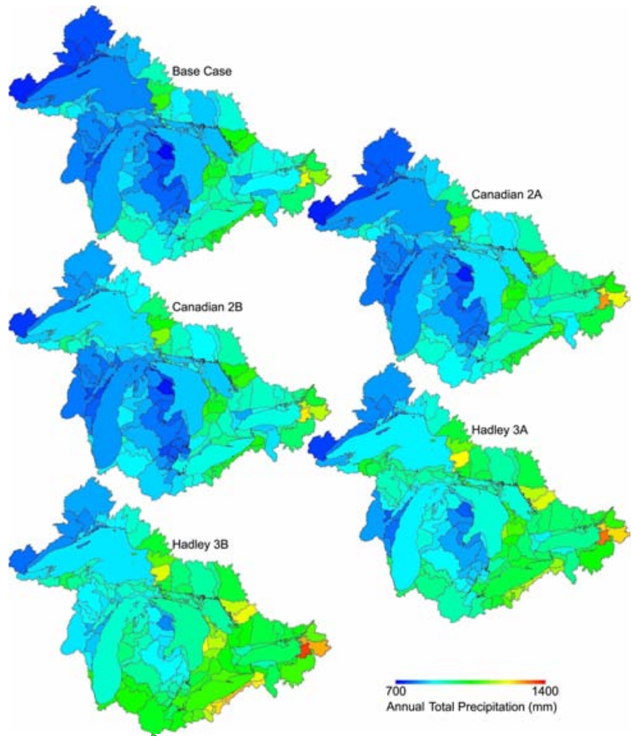

Figure 17. Average Annual Total Precipitation.

Basin Hydrology

The increased air temperatures, consequent in all of the changed climates, significantly alter the heat balance of the surface. As seen in Table 17, the snow pack is drastically reduced as the relative change varies among scenarios and lake basins from a 26% to an 84% drop in accumulated snow moisture. Furthermore, evapotranspiration increases significantly by 8% to 27%. Neither snow moisture reductions nor evapotranspiration increases mirror temperature changes perfectly for the four scenarios; see Figures 18 and 19. The snow pack is reduced the most under scenario CGCM2A and next most under scenario HADCM3A in Table 17 and Figure 18 while Table 15 reveals that scenario HADCM3A is warmer overall than CGCM2A and both are warmer than the remaining scenarios. The remaining scenarios in order of warmest are HADCM3B and CGCM2B; this order appears also for snow pack reductions in Table 17 only for Lakes Superior, St. Clair, Erie, and Ontario, but is reversed for Lakes Michigan and Huron and Georgian Bay. This lack of perfect correspondence between snow pack reductions and air temperature increases is due to the pattern of precipitation changes. Thus, while the HADCM3A scenario is warmer than the CGCM2A scenario, it is also much wetter; this allows higher snow pack reduction under the CGCM2A scenario. Likewise, evapotranspiration is highest for the two Hadley GCM scenarios in Table 17 and Figure 19 since they are the wettest, even though the CGCM2A scenario is warmer than the HADCM3B scenario. After all, evapotranspiration is limited by water supply, which is higher under the two Hadley GCM scenarios. The increased evapotranspiration and decreased snow pack give rise to less moisture available in the soil and groundwater zones. Table 17 and Figures 20 and 21 show a general lowering of soil moisture that is most acute for the CGCM2A scenario and a corresponding loss of groundwater storage in the same pattern. By adding snow water equivalent, soil moisture, groundwater, and surface storage (not shown in Table 17), the total moisture storage is computed as in Table 17 and shown in Figure 22. The pattern is the same there; the CGCM2A scenario shows the most acute loss of moisture storage in the basin, but all scenarios show a general loss as compared to the base case. The next highest loss of moisture storage occurs for the HADCM3A scenario. Note that the anomalously high groundwater (and consequently total moisture storage) for Georgian Bay in Table 17 results from unrealistic initial groundwater conditions in the models consistent with earlier calibrations and are arbitrary. They are omitted in Figures 21 and 22. On other basins, estimated groundwater is much faster, compared to the Georgian Bay calibrations, and initial conditions are unimportant. The net effect of the increased air temperatures, through increased evapotranspiration and decreased moisture storage in the basins, is decreased runoff; see Table 17 and Figure 23. While Table 17 and Figure 23 do indeed show decreased runoff in many cases, there are other cases where runoff increases since moisture reductions are offset by precipitation increases. Table 17 and Figure 23 generally show the greatest runoff decreases for the scenarios in the following order: CGCM2A, CGCM2B, HADCM3A, and HADCM3B.

Table 17. Average Annual Basin Hydrology Differences (1950—1999).

Basin	Snow Water Equivalent (mm) & Climate Scenario Relative Changes[a]					Soil Moisture (mm) & Climate Scenario Relative Changes[a]				
	BASE	#1	#2	#3	#4	BASE	#1	#2	#3	#4
Superior	50.9	-40%	-26%	-39%	-28%	41.9	-15%	-8%	-16%	-7%
Michigan	11.8	-79%	-65%	-66%	-57%	34.9	-21%	-15%	-17%	-5%
Huron	13.6	-84%	-70%	-73%	-67%	29.0	-18%	-13%	-12%	0%
Georgian	37.6	-73%	-53%	-57%	-48%	70.7	-10%	-7%	-8%	-1%
St. Clair	7.9	-83%	-67%	-75%	-70%	6.0	-34%	-26%	-26%	-12%
Erie	5.5	-76%	-58%	-75%	-67%	6.8	-30%	-25%	-29%	-15%
Ontario	15.1	-75%	-58%	-73%	-67%	21.0	-13%	-9%	-10%	-1%

Basin	Groundwater (mm) & Climate Scenario Relative Changes[a]					Total Basin Moisture (mm) & Climate Scenario Relative Changes[a]				
	BASE	#1	#2	#3	#4	BASE	#1	#2	#3	#4
Superior	149	-15%	-9%	-13%	-7%	300	-19%	-11%	-18%	-10%
Michigan	62	-19%	-14%	-14%	-3%	116	-26%	-20%	-20%	-9%
Huron	104	-16%	-12%	-14%	-2%	151	-23%	-18%	-19%	-8%
Georgian	26894	-1%	0%	0%	0%	27014	-1%	-1%	0%	0%
St. Clair	10	-23%	-19%	-14%	2%	27	-43%	-34%	-34%	-22%
Erie	8	-24%	-19%	-14%	2%	24	-38%	-31%	-32%	-18%
Ontario	11	-15%	-10%	-8%	3%	61	-28%	-21%	-25%	-16%

Basin	Overland Evapotranspiration (mm) & Climate Scenario Relative Changes[a]					Runoff as an Overland Depth (mm) & Climate Scenario Relative Changes[a]				
	BASE	#1	#2	#3	#4	BASE	#1	#2	#3	#4
Superior	425	17%	17%	27%	21%	397	-15%	-6%	-11%	-4%
Michigan	506	13%	9%	20%	20%	324	-20%	-16%	-13%	-1%
Huron	502	18%	13%	21%	22%	464	-22%	-16%	-14%	1%
Georgian	482	17%	13%	26%	22%	420	-12%	-7%	-5%	2%
St. Clair	544	17%	11%	20%	22%	315	-26%	-20%	-14%	3%
Erie	572	12%	8%	18%	22%	347	-22%	-22%	-13%	7%
Ontario	476	23%	12%	26%	23%	466	-13%	-10%	-8%	2%

[a]Scenario #1 is CGCM2A; #2 is CGCM2B; #3 is HADCM3A; #4 is HADCM3B.

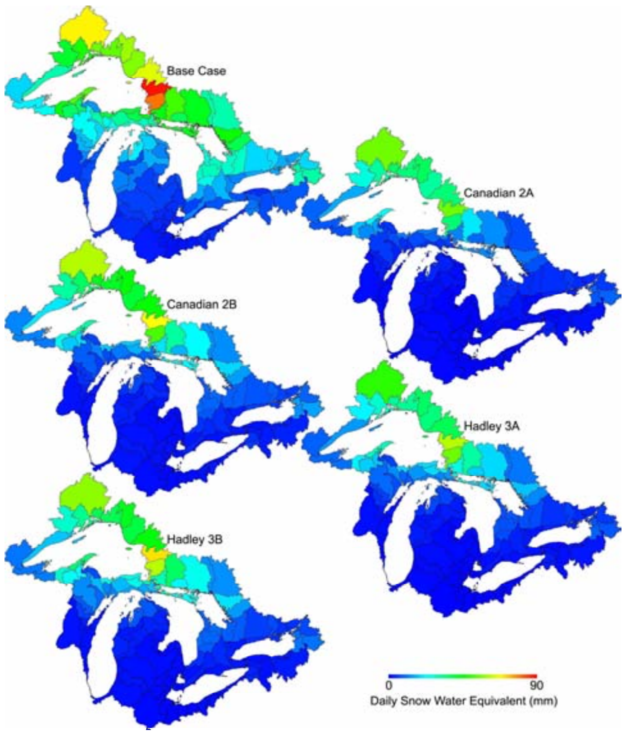

Figure 18. Daily Snow Water Equivalent Averaged Over The Year.

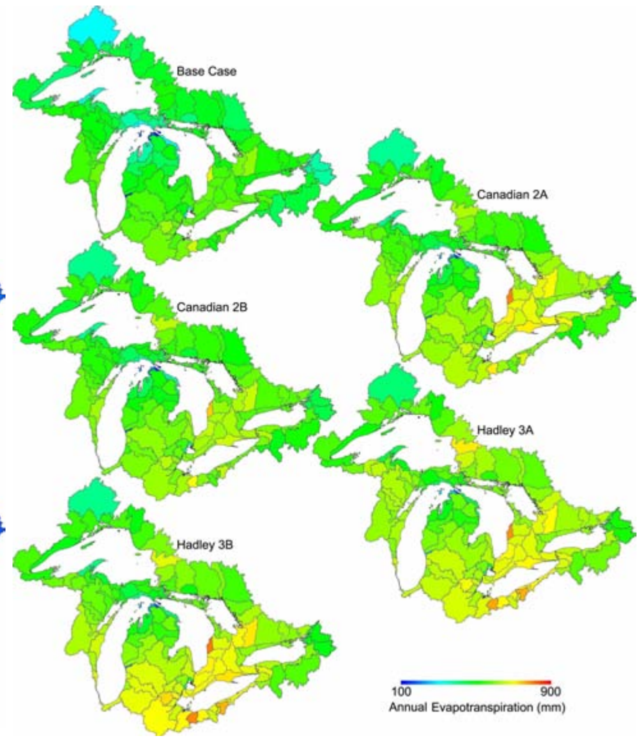

Figure 19. Average Annual Evapotranspiration.

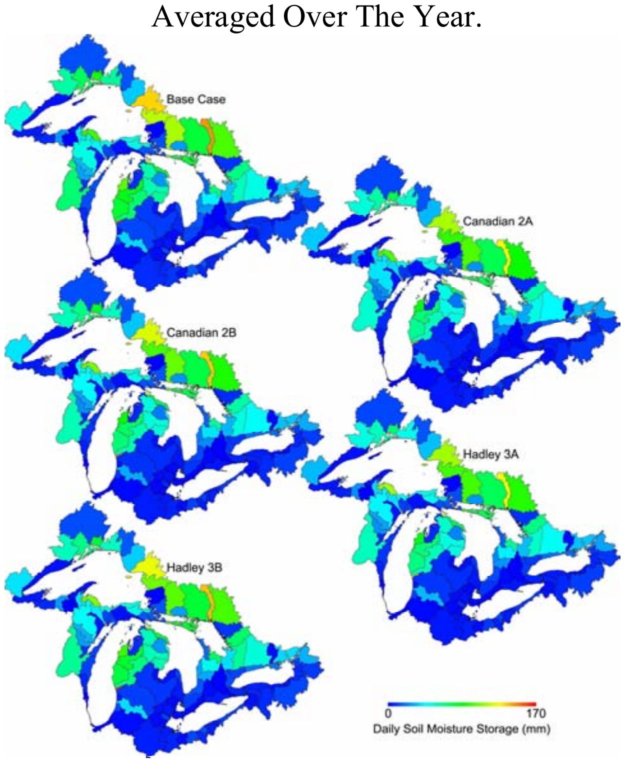

Figure 20. Daily Soil Moisture Storage Averaged Over The Year.

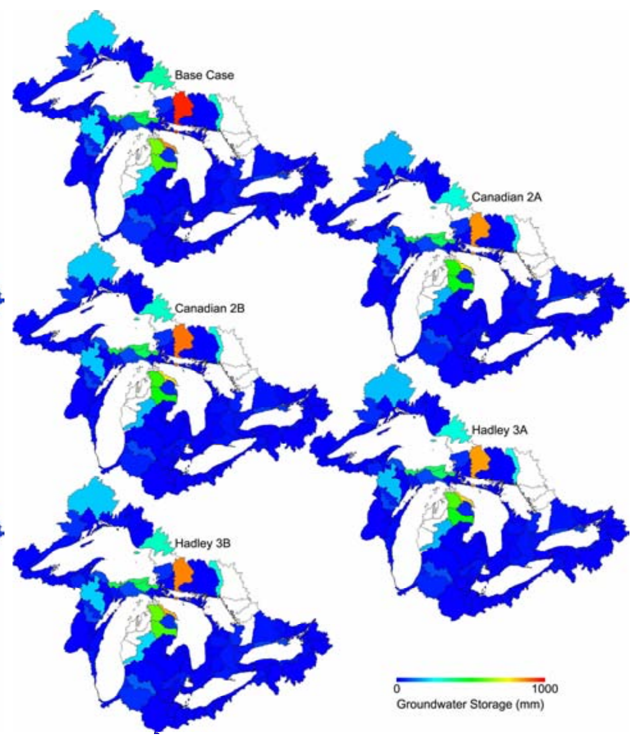

Figure 21. Groundwater Storage Averaged Over The Year.

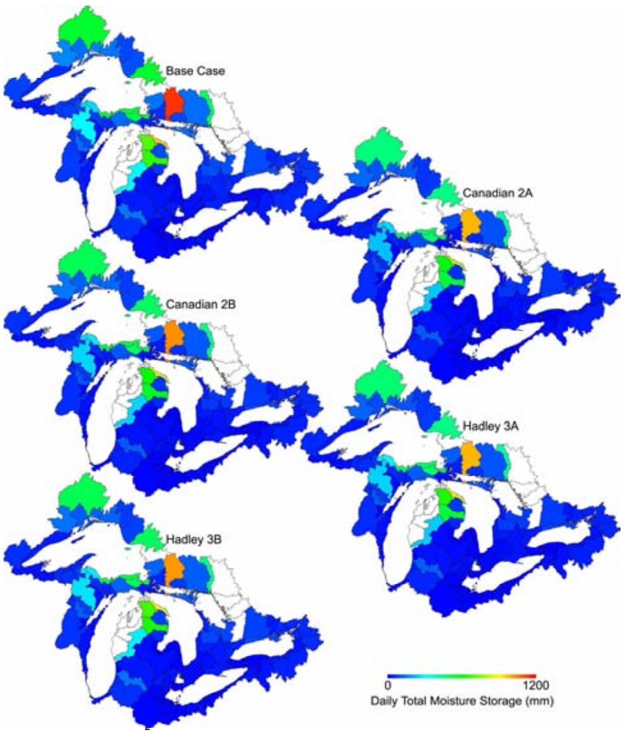

Figure 22. Daily Total Moisture Storage Averaged Over The Year.

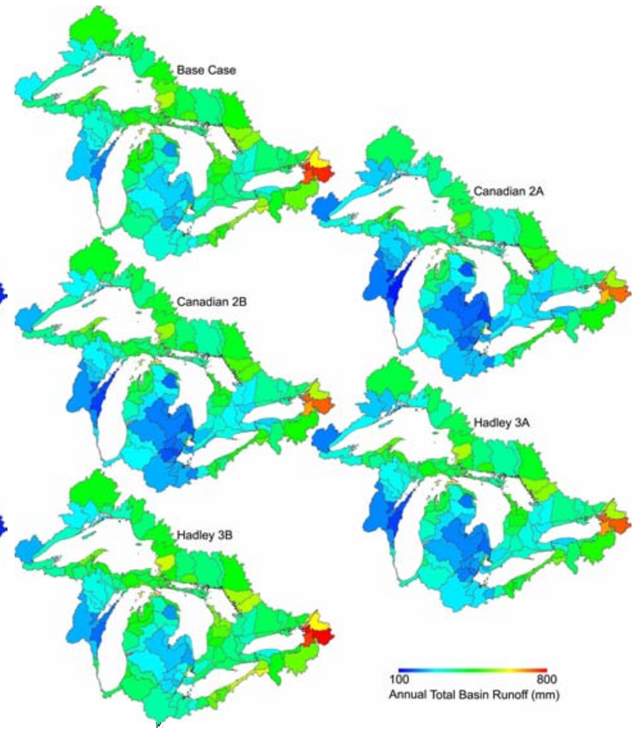

Figure 23. Average Annual Total Basin Runoff.

Figure 16 depicts typical seasonal behavior for evapotranspiration and runoff on the Ontario basin. On the Superior and Michigan basins, there are early summer evapotranspiration peaks, compared to the base case. Huron and Georgian Bay have evapotranspiration peaks extending over the summer and fall and evapotranspiration is still larger than the base case throughout the rest of the year. St. Clair and Erie have evapotranspiration generally with the same seasonal cycle as the base case but with higher values throughout the year. Ontario evapotranspiration (Figure 16) is also generally higher throughout the year with a similar seasonal cycle as the base case, except for the HADCM3B scenario, which has peaks in the late summer. All basins show slightly earlier spring snow melt and earlier but lower runoff peaks, except for the HADCM3B scenario, as shown for Ontario in Figure 16. Georgian Bay includes the HADCM3B scenario; spring runoff is lower for all changed climates than the base case.

Figure 24 shows typical seasonal behavior for basin moisture storage quantities depicted in Figures 20—23. As expected from inspection of seasonal runoff in Figure 16 and discussed

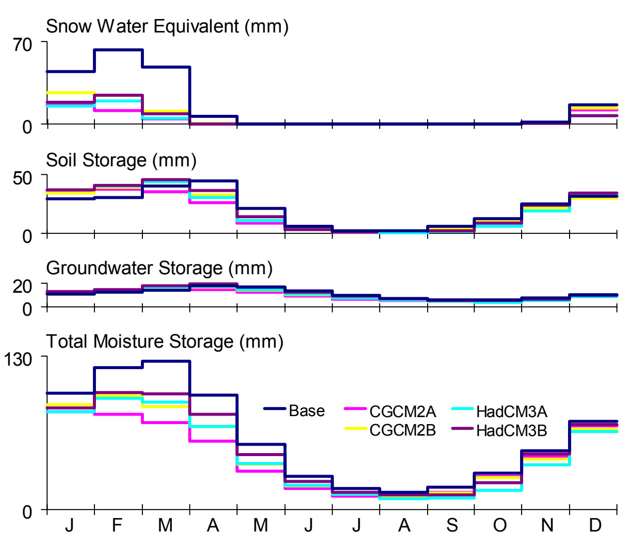

Figure 24. Seasonal Lake Ontario Basin Average Moisture Storage.

previously, the snow pack in Figure 24 is much reduced from the base case under all climate change scenarios. The CGCM2A scenario gives the most snow pack reduction for all lake basins, as seen in Figure 24 for the Lake Ontario basin. Soil moisture storages for all climate change scenarios are correspondingly higher than the base case during the winter months and lower during the rest of the year on all basins, as depicted in Figure 24 for the Lake Ontario basin, except for the Lake St. Clair and Erie basins. There, soil moisture storage for all climate change scenarios are lower than the base case throughout the entire season. Groundwater moisture storages for all climate change scenarios are lower than the base case throughout the entire season on all basins but with the same seasonal pattern as the base case, as depicted in Figure 24 for the Lake Ontario basin, except for the Lake St. Clair and Erie basins. There, the Hadley climate change scenarios show slightly higher groundwater moisture storage than the base case during the winter months only. Total moisture storages in all but one Great Lake basin are similar to that shown in Figure 24 for the Lake Ontario basin. On the Superior, Michigan, Huron, St. Clair, Erie, and Ontario basins, total moisture storage for all changed climate scenarios lies generally below the base case. The CGCM2A scenario has the lowest total moisture storage (most reduction from the base case) during the spring and summer and the HADCM3A has the lowest during the fall and winter. The HADCM3B scenario has the highest total moisture storage (least reduction from the base case) all year round. The Lake Ontario basin has the most winter/spring reductions of total moisture storage of all the lakes, for all climate change scenarios. On the Georgian Bay basin, total moisture storage lies beneath the base case for the CGCM2A, CGCM2B, and HADCM3A scenarios. The CGCM2A scenario has the lowest total moisture storage all year long and the HADCM3B has the highest, almost identical to the base case.

Table 18 shows expected changes in variability for basin moisture storage variables. Snow water variability is greatly decreased simply because snow water is greatly decreased toward its lower bound of zero. Relative annual changes in variability of soil moisture, groundwater, surface storage (not shown), and total basin moisture are small (less than half when ignoring anomalous Georgian Bay groundwater and total moisture storage due to antecedent groundwater conditions on a few subbasins already discussed). Table 18 also shows evapotranspiration with more variability, generally, for the Hadley GCM scenarios. This corresponds the greatest and most variable precipitation; see Tables 15 and 16, respectively. This results from the fact that evapotranspiration is a moisture-limited process; only the amount in storage can evaporate or transpire and where there is more variability in the moisture supply will there be more variability in the evapotranspiration amounts. There generally is not much change in basin runoff variability in Table 18, although the Canadian GCM scenarios do show reduction while the extreme HADCM3B scenario shows a slight increase in variability due to the increased variability of its annual precipitation.

Over Water Meteorology

The over water air temperature, humidity, and wind speed differ from over land since the lower atmospheric layer is affected by the water surface over which it lies. The model corrections to over-land meteorological observations for over-water conditions depend heavily on the water surface temperature, which in turn is a function of the over-water meteorology and heat balance at the surface of the lake. Table 19 and Figures 25—28 summarize annual average steady-state over-water meteorology differences. In general, the synergistic relationship that exists between air and water temperature in a changed climate yields a general increase in both that follows the

Table 18. Average Annual Basin Hydrology Standard Deviation Differences (1950—1999).

Basin	Snow Water Equivalent Std. Dev. (mm) & Climate Scenario Relative Change[a]					Soil Moisture Std. Dev. (mm) & Climate Scenario Relative Change[a]				
	BASE	#1	#2	#3	#4	BASE	#1	#2	#3	#4
Superior	13.2	-9%	1%	-12%	-1%	5.2	-15%	-9%	-15%	-9%
Michigan	5.4	-70%	-50%	-54%	-45%	5.4	-16%	-13%	-14%	-4%
Huron	6.9	-78%	-58%	-65%	-58%	4.3	-16%	-12%	-9%	2%
Georgian	12.0	-52%	-22%	-33%	-24%	8.9	-6%	-4%	1%	4%
St. Clair	5.5	-77%	-56%	-64%	-58%	1.2	-17%	-14%	-13%	-4%
Erie	3.5	-62%	-43%	-61%	-48%	1.1	-20%	-21%	-21%	-11%
Ontario	9.6	-65%	-44%	-68%	-63%	2.4	-11%	-9%	-5%	0%

Basin	Groundwater Std. Dev. (mm) & Climate Scenario Relative Change[a]					Total Moisture Storage Std. Dev. (mm) & Climate Scenario Relative Change[a]				
	BASE	#1	#2	#3	#4	BASE	#1	#2	#3	#4
Superior	11.8	-13%	-12%	-15%	-15%	25.0	-11%	-5%	-12%	-10%
Michigan	6.1	-18%	-16%	-15%	-5%	13.6	-26%	-20%	-19%	-9%
Huron	5.9	-12%	-6%	-3%	5%	11.0	-26%	-20%	-15%	-7%
Georgian	110.6	-68%	-55%	-41%	4%	113.6	-67%	-54%	-39%	5%
St. Clair	1.9	-15%	-13%	-5%	7%	7.1	-49%	-35%	-38%	-30%
Erie	1.3	-17%	-12%	-2%	10%	4.9	-40%	-31%	-36%	-24%
Ontario	1.4	-11%	-9%	1%	8%	10.6	-41%	-29%	-42%	-37%

Basin	Overland Evapotranspira. Std. Dev. (mm) & Climate Scenario Relative Change[a]					Runoff as Overland Depth Std. Dev. (mm) & Climate Scenario Relative Change[a]				
	BASE	#1	#2	#3	#4	BASE	#1	#2	#3	#4
Superior	39.2	23%	21%	34%	25%	38.2	-3%	3%	1%	6%
Michigan	46.6	19%	11%	25%	21%	41.0	-15%	-13%	-6%	5%
Huron	47.0	23%	15%	26%	26%	69.8	-16%	-12%	-8%	6%
Georgian	44.8	21%	15%	26%	22%	44.2	-10%	-6%	0%	7%
St. Clair	66.7	18%	13%	20%	20%	69.0	-14%	-11%	-5%	10%
Erie	59.4	15%	10%	18%	20%	65.2	-11%	-14%	-3%	15%
Ontario	42.0	29%	15%	31%	24%	55.9	-5%	-6%	0%	8%

[a]Scenario #1 is CGCM2A; #2 is CGCM2B; #3 is HADCM3A; #4 is HADCM3B.

base climate patterns, similar to over-land behavior. Table 19 and Figure 25 show that over water air temperatures for all climate scenarios are higher than the base case. The differences are greatest for the HADCM3A scenario, followed by the CGCM2A, HADCM3B, and CGCM2B scenarios and for Lakes Michigan and Huron and Georgian Bay.

While the smallest overland air temperature annual changes occurred for Lake Superior in all climate change scenarios (see Table 15), the smallest over water air temperatures occur on Lakes St. Clair and Erie because of their very low heat storage capacity. Likewise, by comparing Tables 15 and 19, we see that the over-water air temperature increase is larger than the overland air temperature increase for deeper Lakes Superior, Michigan, and Ontario, and is smaller for shallower Lakes St. Clair and Erie. Over-water absolute humidity is increased for all scenarios; see Table 19 and Figure 26 and is greatest for the CGCM2A scenario although it is very similar for all scenarios. Both over water air temperature and overlake humidity show an increase and a slight shift earlier in the seasonal cycle, for all lakes and all scenarios; this is typified in Figure 29 for Lake

Table 19. Average Annual Overlake Meteorology Differences (1950—1999).

Basin	Air Temperature (ºC) & Climate Scenario Absolute Differences[a]					Humidity (mb) & Climate Scenario Absolute Differences[a]				
	BASE	#1	#2	#3	#4	BASE	#1	#2	#3	#4
Superior	3.4	3.7	2.6	4.0	3.3	7.0	2.5	1.8	2.2	2.1
Michigan	7.4	4.2	3.1	4.2	3.4	9.3	3.1	2.2	2.4	2.3
Huron	6.8	3.9	2.8	4.0	3.3	8.8	2.8	2.0	2.2	2.0
Georgian	5.9	4.0	2.7	4.1	3.3	8.4	2.8	1.9	2.1	1.9
St. Clair	10.0	3.2	2.3	3.9	3.1	10.7	2.9	2.1	2.1	2.1
Erie	9.8	3.2	2.3	3.9	3.1	10.7	2.9	2.1	2.3	2.1
Ontario	8.1	3.7	2.6	4.0	3.2	9.5	3.0	2.1	2.2	2.0

Basin	Cloud Cover (%) & Climate Scenario Relative Changes[a]					Wind Speed (m s^{-1}) & Climate Scenario Relative Changes[a]				
	BASE	#1	#2	#3	#4	BASE	#1	#2	#3	#4
Superior	56.7	4%	3%	-5%	-3%	5.3	5%	5%	1%	1%
Michigan	60.7	5%	2%	-5%	-1%	5.9	6%	5%	-1%	1%
Huron	57.3	7%	5%	-4%	-1%	5.6	6%	5%	0%	1%
Georgian	58.8	7%	5%	-4%	-2%	5.6	7%	6%	1%	2%
St. Clair	57.6	1%	0%	-4%	1%	5.3	4%	4%	-1%	1%
Erie	61.4	2%	1%	-3%	1%	6.0	5%	4%	-2%	0%
Ontario	58.1	5%	4%	-4%	-1%	5.8	4%	4%	-2%	0%

[a]Scenario #1 is CGCM2A; #2 is CGCM2B; #3 is HADCM3A; #4 is HADCM3B.

Ontario. The shift reflects interaction of the atmosphere with the lake's heat storage, which is discussed subsequently. This pattern is reflected in water surface temperatures as well, also discussed subsequently.

Cloud cover, shown in Table 19 and Figure 27, is reduced for the Hadley climate change scenarios; this might not be expected since those scenarios were wetter (more precipitation) than the Canadian climate change scenarios. Also absolute humidity was a little higher than base case for all scenarios and all lakes. Seasonally, the behavior is consistent across most of the Great Lakes. Figure 29, while for Lake Ontario, shows the variation in cloud cover that is typical of all lakes except Erie and St. Clair. Generally, all climate change scenarios are slightly higher than the base case during the winter and beginning of spring, as shown in Figure 29. During the late spring, all scenarios are lower than the base case. The CGCM2A and CGCM2B scenarios are then higher and the HADCM3A and HADCM3B scenarios are lower than the base case in the summer and fall. On Lakes Erie and St. Clair, the seasonal cycle is very similar except that during the late summer, cloud cover for all scenarios is less than the base case.

Overlake wind speed, shown in Table 19 and Figure 28, increases over the base case on all Great Lakes for both of the Canadian climate change scenarios and for the HADCM3B scenario. The HADCM3A scenario is slightly above or slightly below the base case, depending on the lake. The Canadian climate change scenarios show more difference with the base case than do the Hadley scenarios. This might be due to additional atmospheric instability associated with slightly drier conditions in the Canadian climate change scenarios. Figure 29 typifies the other Great Lakes; average wind speeds for all climate change scenarios slightly exceed those for the base case in the winter and are very close to the base case throughout the rest of the year.

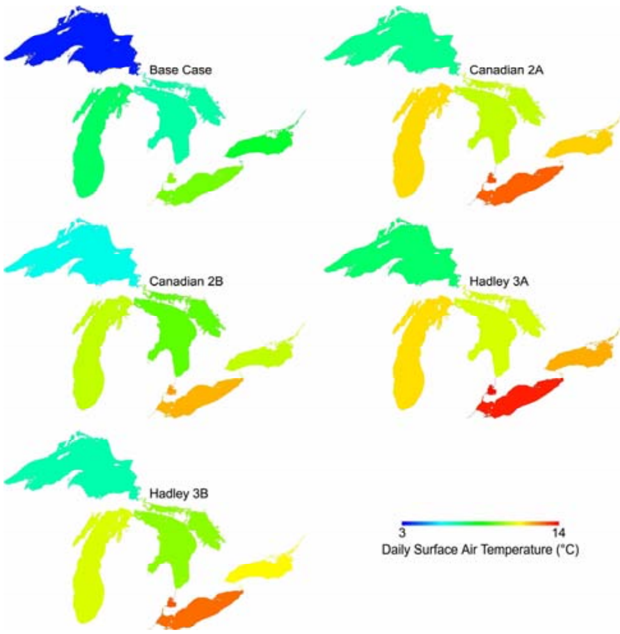

Figure 25. Daily Surface Air Temperature Averaged Over The Year.

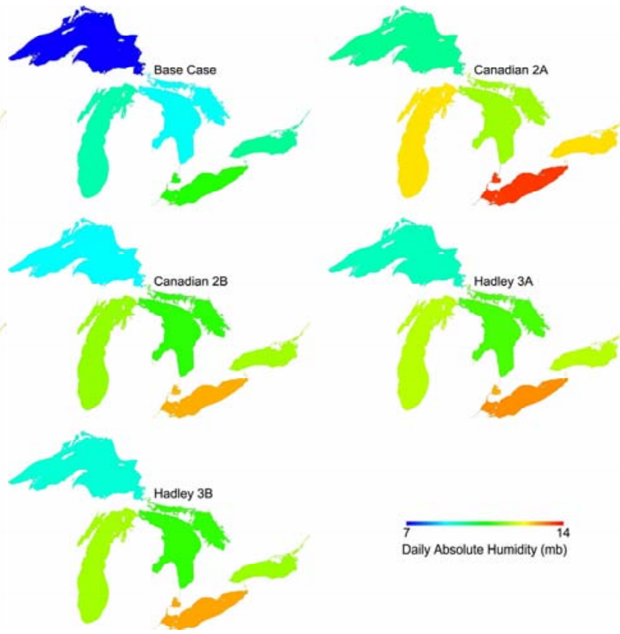

Figure 26. Daily Absolute Humidity Averaged Over The Year.

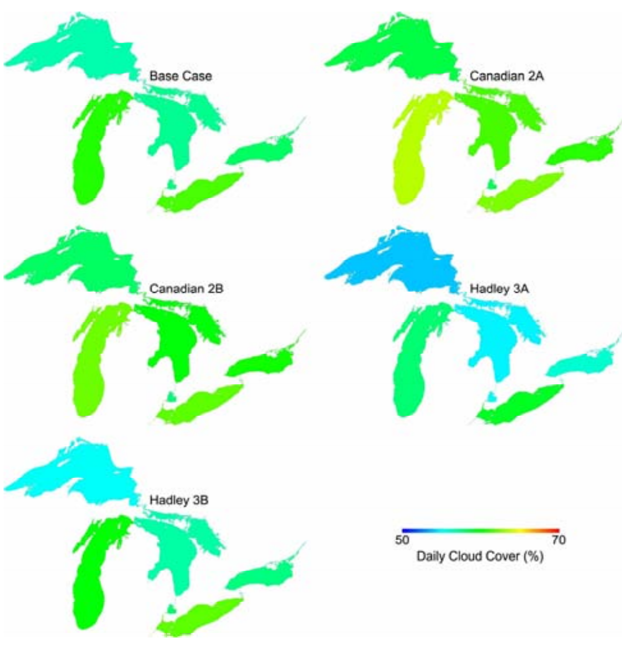

Figure 27. Daily Cloud Cover Averaged Over The Year.

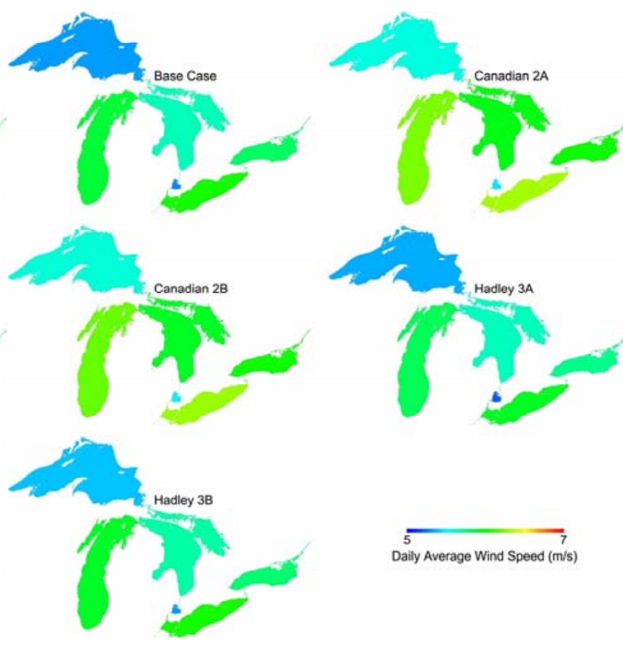

Figure 28. Daily Average Wind Speed Averaged Over The Year.

Variability in overlake meteorology is shown for annual values in Table 20. Overlake air temperature variability is generally reduced on all lakes for all scenarios. The deeper lakes (Michigan, Huron, Georgian Bay, and Ontario), with more heat storage capacity than shallow Lake St. Clair or Lake Erie, have the greatest reduction in variability. Monomictic lakes (where surface temperature never drops below that of maximum water density, failing to induce buoyancy-driven turnover of the water column) have a rather difficult-to-penetrate lower bound on their temperature, which would reduce their variability, while dimictic lakes (where buoyancy-driven turnovers occur), which often have ice, are less constrained. Lakes St. Clair and Erie remain dimictic under the changed climates while the other lakes become largely monomictic. Lake Superior variance drops only a little relative to the other deep lakes even though it is deepest. Superior becomes monomictic less often than the other deep lakes; it is northern most with lower temperatures (see Table 19). Therefore, variability reduction is limited over Lake Superior. Humidity variability increases generally for all climate change scenarios; the largest is associated with the HADCM3A scenario; see Table 20. Cloud cover variability is slightly reduced with the most reduction under the Hadley scenarios. Wind speed variability changes little in the Hadley but increases for all lakes in the Canadian scenarios; see Table 20.

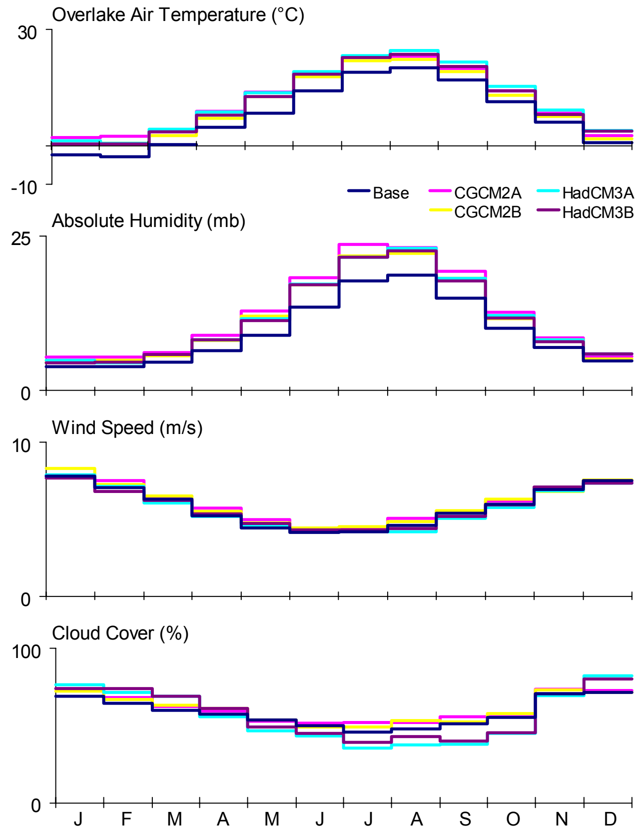

Figure 29. Seasonal Lake Ontario Average Overlake Meteorology.

Table 20. Average Annual Overlake Meteorology Standard Deviation Differences (1950—1999).

Basin	Air Temperature Std. Dev. (ºC) & Climate Scenario Relative Change[a]					Humidity Std. Dev. (mb) & Climate Scenario Relative Change[a]				
	BASE	#1	#2	#3	#4	BASE	#1	#2	#3	#4
Superior	1.0	-5%	0%	-2%	-5%	0.6	8%	13%	24%	5%
Michigan	0.9	-18%	-9%	-11%	-12%	0.6	-7%	-2%	6%	-5%
Huron	0.8	-11%	-6%	-8%	-10%	0.5	1%	2%	14%	-1%
Georgian	1.0	-8%	-5%	-5%	-7%	0.6	5%	6%	17%	2%
St. Clair	0.8	-4%	-3%	-2%	-3%	0.5	4%	3%	16%	3%
Erie	0.9	-7%	-5%	-4%	-6%	0.5	3%	3%	16%	3%
Ontario	0.9	-21%	-12%	-16%	-17%	0.6	-7%	-4%	4%	-7%

Basin	Cloud Cover Std. Dev. (%) & Climate Scenario Relative Change[a]					Wind Speed Std. Dev. (m s^{-1}) & Climate Scenario Relative Change[a]				
	BASE	#1	#2	#3	#4	BASE	#1	#2	#3	#4
Superior	2.5	0%	0%	-2%	-1%	0.4	10%	8%	3%	3%
Michigan	3.1	-1%	-1%	-3%	-2%	0.2	16%	12%	1%	5%
Huron	4.8	-2%	-1%	-4%	-3%	0.2	11%	10%	-1%	1%
Georgian	3.9	-3%	-2%	-5%	-4%	0.3	15%	11%	3%	4%
St. Clair	2.8	-1%	0%	-5%	-4%	0.3	4%	4%	-4%	-2%
Erie	2.9	0%	0%	-3%	-2%	0.2	5%	6%	-4%	-1%
Ontario	3.2	-1%	-1%	-4%	-3%	0.3	8%	8%	1%	2%

[a]Scenario #1 is CGCM2A; #2 is CGCM2B; #3 is HADCM3A; #4 is HADCM3B.

Lake Heat Balance

Annual lake heat balance changes are depicted in Table 21 and a seasonal example for Lake Ontario is given in Figure 30. Insolation changes in Table 21 reflect largely the cloud cover changes given earlier in Table 19; the Hadley GCM changed-climate scenarios transfer more heat into the lakes than do the Canadian GCM scenarios. The increase for the Hadley GCM climate-change scenarios occurs on all Great Lakes beginning in the late spring, extending throughout the summer, and into the early fall; Figure 30 is typical. Insolation for the Hadley GCM climate-change scenarios then is slightly below the base case beginning in the late fall, extending throughout the winter and into the early spring. The insolation for the Canadian GCM climate-change scenarios is slightly less than the base case throughout the year for all lakes; the decrease is spread throughout the annual cycle fairly uniformly and the seasonal insolation variation is similar to the base case. Again, Figure 30 is typical of the other lakes. Reflection generally decreases but changes are very small, relative to the insolation changes, with most of the difference coming in the winter-spring due to the absence of ice cover. Table 21 shows that the Canadian GCM climate-change

Table 21. Average Annual Lake Heat Flux Differences (1950—1999).

Basin	Insolation ($W\ m^{-2}$) & Climate Scenario Absolute Differences[a]					Reflection ($W\ m^{-2}$) & Climate Scenario Absolute Differences[a]				
	BASE	#1	#2	#3	#4	BASE	#1	#2	#3	#4
Superior	158	-4	-2	7	5	-18	2	2	1	2
Michigan	148	-4	-2	7	3	-15	1	1	0	0
Huron	160	-6	-4	8	4	-17	2	1	0	1
Georgian	159	-6	-5	8	5	-23	7	6	6	6
St. Clair	155	-1	-1	7	2	-28	5	4	5	5
Erie	150	-2	-1	7	2	-20	4	3	3	4
Ontario	149	-4	-3	7	3	-15	1	1	0	0

Basin	Net Long Wave Exchange ($W\ m^{-2}$) & Climate Scenario Absolute Differences[a]					Latent Heat Flux ($W\ m^{-2}$) & Climate Scenario Absolute Differences[a]				
	BASE	#1	#2	#3	#4	BASE	#1	#2	#3	#4
Superior	-61	10	7	4	4	-45	-8	-6	-13	-9
Michigan	-58	11	8	5	5	-51	-10	-9	-15	-11
Huron	-65	11	8	4	5	-51	-9	-6	-15	-11
Georgian	-64	12	9	5	5	-49	-11	-8	-18	-14
St. Clair	-55	10	7	7	8	-65	-13	-10	-19	-14
Erie	-42	12	8	7	8	-70	-12	-9	-18	-13
Ontario	-58	10	8	5	5	-53	-8	-5	-14	-10

Basin	Sensible Heat Flux ($W\ m^{-2}$) & Climate Scenario Absolute Differences[a]					Net Heat Flux ($W\ m^{-2}$) & Climate Scenario Absolute Differences[a]				
	BASE	#1	#2	#3	#4	BASE	#1	#2	#3	#4
Superior	-34	0	-1	1	-1	0	0	0	0	0
Michigan	-23	3	3	4	2	-1	-1	0	-1	-1
Huron	-27	2	1	2	1	-1	0	0	-1	0
Georgian	-22	-2	-2	-1	-2	-1	0	0	-1	0
St. Clair	-5	-1	0	2	0	-2	-1	-1	-1	-1
Erie	-16	-2	-1	2	0	-2	-1	-1	-1	-1
Ontario	-23	2	1	4	3	-1	0	0	-1	0

[a]Scenario #1 is CGCM2A; #2 is CGCM2B; #3 is HADCM3A; #4 is HADCM3B.

scenarios reduce reflection more than the Hadley scenarios (reflection is negative coming out of the lake surface). Figure 30, for Lake Ontario, does not show this behavior partly because reflection is plotted at the same scale used in the other plots in Figure 30, which hides its relative seasonal variation, and partly because Lake Ontario ice cover, which was already small compared to the other lakes in the base case, is reduced less by the changed-climate scenarios. Thus, Lake Ontario has less reflection changes during the winter-spring due to absence of ice cover than other Great Lakes under all climate-change scenarios.

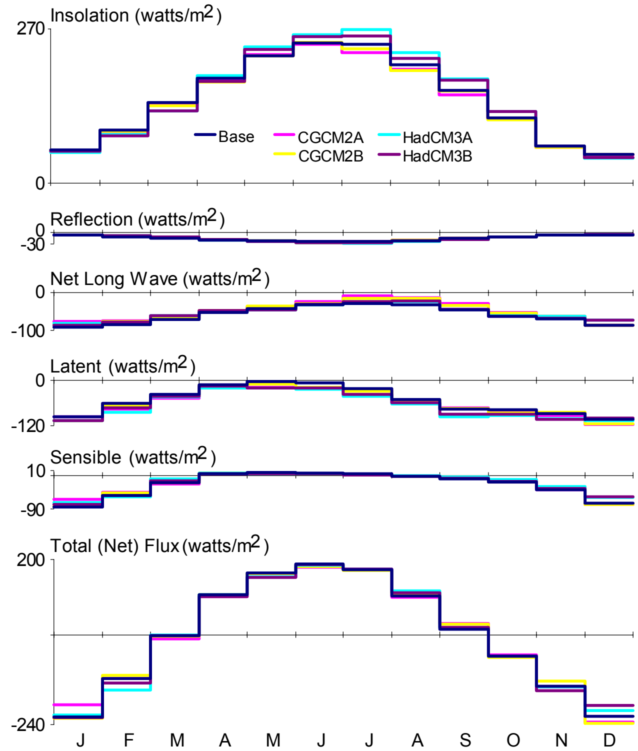

Figure 30. Seasonal Lake Ontario Average Lake Heat Fluxes.

Net long wave exchange increases slightly, implying more heat stays in the lakes. Table 21 shows that the largest increase on all lakes occurs under the CGCM2A scenario followed by the CGCM2B, HADCM3B, and HADCM3A scenarios respectively. Increases are spread fairly uniformly throughout the seasonal cycle as typified in Figure 30 for Lake Ontario, although this is difficult to see because of the scale used. Sensible heat exchange changes are small and vary in direction from lake to lake; see Table 21. The overall increases in heat storage in the lakes thus far discussed are balanced by increases in evaporation, shown in Table 21 as a significant decrease in latent heat transferred into the lake. These evaporation increases are rather large compared to the base case. The seasonal patterns of net long wave exchange, sensible heat transfer, and latent heat transfer are very similar to the base case; see Figure 30. The changes shown in these variables, summarized in Table 21, are distributed fairly uniformly throughout the seasonal cycle; again Figure 30 is fairly typical of the pattern of changes observed on all lakes although it is difficult to see in some cases (for relatively small components like reflection) because of the scale used. The annual total heat flux should remain close to zero for all scenarios, as in the base case, indicating that there is no long-term heat storage in the lakes and energy conservation is satisfied. Table 21 shows this and Figure 30 indicates that the change in the seasonal variation of total heat flux is very similar to the base case; increased heat fluxes are balanced largely by evaporation.

Changes in variability in lake heat balance variables are summarized in Table 22. As seen there, insolation is less variable than in the base case, reflecting the decreased cloud cover variability shown in Table 20. In particular, trends in cloud cover are reflected directly in solar insolation; on any lake, the reduced variability under all scenarios of insolation in Table 22 matches the reduced variability of cloud cover in Table 20. The reduced variability of Lake Ontario insolation in Table 22 matches the reduced variability of cloud cover in Table 20.

Table 22. Average Annual Lake Heat Flux Standard Deviation Differences (1950-1999).

Basin	Insolation Std. Dev. ($W\ m^{-2}$) & Climate Scenario Relative Change[a]					Reflection Std. Dev. ($W\ m^{-2}$) & Climate Scenario Relative Change[a]				
	BASE	#1	#2	#3	#4	BASE	#1	#2	#3	#4
Superior	4.5	0%	0%	-1%	-1%	2.5	-82%	-82%	-82%	-82%
Michigan	5.1	-1%	-1%	-3%	-2%	1.3	-60%	-60%	-61%	-61%
Huron	7.5	-1%	-1%	-3%	-2%	2.2	-66%	-66%	-67%	-67%
Georgian	6.8	-2%	-2%	-3%	-2%	3.5	-79%	-58%	-73%	-69%
St. Clair	4.6	-1%	-1%	-4%	-3%	1.7	11%	-7%	20%	13%
Erie	4.7	0%	0%	-2%	-2%	3.0	-56%	-27%	-49%	-47%
Ontario	5.0	0%	-1%	-3%	-2%	0.8	-38%	-38%	-39%	-39%

Basin	Net Long Wave Exchange Std. Dev. ($W\ m^{-2}$) & Climate Scenario Relative Change[a]					Latent Heat Flux Std. Dev. ($W\ m^{-2}$) & Climate Scenario Relative Change[a]				
	BASE	#1	#2	#3	#4	BASE	#1	#2	#3	#4
Superior	3.0	3%	2%	10%	2%	4.9	-4%	-7%	2%	-6%
Michigan	2.8	7%	4%	11%	5%	5.2	1%	1%	4%	0%
Huron	3.2	1%	1%	4%	2%	5.5	-1%	-3%	2%	-3%
Georgian	2.6	-2%	-1%	2%	0%	6.1	-9%	-8%	-6%	-9%
St. Clair	2.6	-3%	-1%	1%	-5%	4.4	-1%	-1%	-1%	-2%
Erie	2.8	0%	0%	4%	-1%	5.6	-11%	-5%	-6%	-9%
Ontario	2.3	0%	0%	6%	1%	4.7	-3%	-2%	3%	1%

Basin	Sensible Heat Flux Std. Dev. ($W\ m^{-2}$) & Climate Scenario Relative Change[a]					Net Heat Flux Std. Dev. ($W\ m^{-2}$) & Climate Scenario Relative Change[a]				
	BASE	#1	#2	#3	#4	BASE	#1	#2	#3	#4
Superior	5.2	1%	2%	-2%	-2%	0.1	22%	22%	42%	29%
Michigan	3.4	3%	4%	0%	0%	0.1	2%	7%	16%	7%
Huron	4.1	-11%	-10%	-14%	-13%	0.1	29%	18%	39%	26%
Georgian	4.0	-18%	-17%	-20%	-19%	0.2	25%	15%	34%	24%
St. Clair	0.9	19%	10%	19%	17%	0.2	-1%	0%	4%	0%
Erie	2.6	-4%	-1%	-11%	-8%	0.2	8%	5%	15%	6%
Ontario	3.2	-1%	0%	-4%	-3%	0.1	11%	5%	21%	10%

[a]Scenario #1 is CGCM2A; #2 is CGCM2B; #3 is HADCM3A; #4 is HADCM3B.

The variability of reflection in Table 22 is generally greatly reduced, except on Lake St. Clair, reflecting the greatly reduced ice cover under the transposed climates. Without ice cover, reflection is from the water surface only and the fraction of incoming radiation reflected remains more nearly constant throughout the seasonal cycle. Lake St. Clair has the smallest relative change in ice cover under all scenarios of all the Great Lakes, which have ice cover practically eliminated.

Sensible heat transfer is seen in Table 22 to be more variable only on Superior and Michigan for the Canadian GCM climate-change scenarios and on Lake St. Clair for all scenarios; sensible heat transfer variability is greatly increased on Lake St. Clair. Again, the absence of any real heat storage on Lake St. Clair precludes the filtering effect possible with such storages on meteorology and heat transfers. Also, given little heat capacity, the anomaly in reflection results in an anomaly in sensible heat flux on Lake St. Clair. Latent heat transfer is seen in Table 22 to be only slightly less variable than the base case for the Canadian GCM climate-change scenarios on all lakes except Michigan and for the Hadley scenarios on only Georgian Bay, and Lakes St. Clair and Erie.

The net effect of variability changes in all of the heat balance components for a lake is an increase in variability in the total flux as shown in Table 22.

The heat budget gives rise to increased water surface temperatures as seen in Table 23 and Figure 31. Stored heat increases 19% to 42% over the Great Lakes, depending on the changed-climate scenario considered; see Table 23. The largest relative heat increases are seen to occur for the northeastern-most lakes and for the CGCM2A, HADCM3A, HADCM3B, and CGCM2B changed-climates scenarios, in decreasing order of impact on all lakes. The stored heat appears as a constant amount higher throughout the seasonal cycle, since we are looking at steady-state conditions; see Figure 32 for the average Lake Ontario seasonal cycle. The increased heat in storage also means that ice formation will be greatly reduced over winter on the deep Great Lakes. Ice cover is practically eliminated under all transposed climate scenarios on all lakes but Lake St. Clair, and to a lesser extent on Lake Erie; since those lakes have very little heat storage capacity, ice formation is not affected as much as elsewhere; see Table 23.

Table 23 also shows that the average steady-state increase in water surface temperatures for all changed-climate scenarios on all lakes range from 2.1ºC on Lake St. Clair (CGCM2B scenario) to 4.2ºC on Lake Michigan (CGCM2A scenario). The heat storage capacity of a lake influences the increase in water surface temperatures that can almost be seen in Figure 32. Water surface temperatures are seen to peak slightly earlier on deep lakes under the transposed climates than under the base case. The increased heat in storage is sufficient to cause increased lake evaporation on all lakes under all scenarios, even though wind speeds and humidity, by themselves, would not increase evaporation. (Wind speed and humidity changes, in some cases, would decrease lake evaporation, all other things being equal.) Table 23 shows increases in annual lake evaporation of

Table 23. Average Annual Lake Heat Balance Differences (1950—1999).

Basin	Stored Heat (10^{17} cal) & Climate Scenario Relative Changes[a]					Ice Cover (%) & Climate Scenario Relative Changes[a]				
	BASE	#1	#2	#3	#4	BASE	#1	#2	#3	#4
Superior	48.3	36%	24%	36%	32%	4.1	-100%	-100%	-100%	-100%
Michigan	23.2	41%	28%	35%	31%	1.4	-100%	-100%	-100%	-100%
Huron	16.5	42%	28%	40%	34%	2.3	-100%	-100%	-100%	-100%
Georgian	4.8	42%	26%	41%	34%	14.3	-99%	-87%	-96%	-94%
St. Clair	0.0	33%	25%	36%	33%	35.8	-31%	-21%	-33%	-31%
Erie	4.9	26%	19%	28%	23%	13.9	-86%	-53%	-80%	-77%
Ontario	8.8	40%	24%	35%	29%	0.7	-100%	-98%	-100%	-100%

Basin	Water Surface Temperature (ºC) & Climate Scenario Absolute Differences[a]					Lake Evaporation Depth (mm) & Climate Scenario Relative Changes[a]				
	BASE	#1	#2	#3	#4	BASE	#1	#2	#3	#4
Superior	5.8	3.7	2.5	3.9	3.4	575	18%	14%	29%	21%
Michigan	8.3	4.2	3.0	4.1	3.5	651	21%	17%	30%	22%
Huron	8.4	3.7	2.5	3.8	3.2	654	17%	12%	29%	21%
Georgian	7.8	3.4	2.2	3.6	2.9	628	23%	17%	36%	29%
St. Clair	10.6	2.9	2.1	3.2	2.6	835	20%	16%	30%	23%
Erie	11.0	3.0	2.1	3.3	2.7	898	18%	13%	27%	19%
Ontario	9.1	3.8	2.6	3.9	3.3	674	16%	10%	27%	20%

[a]Scenario #1 is CGCM2A; #2 is CGCM2B; #3 is HADCM3A; #4 is HADCM3B.

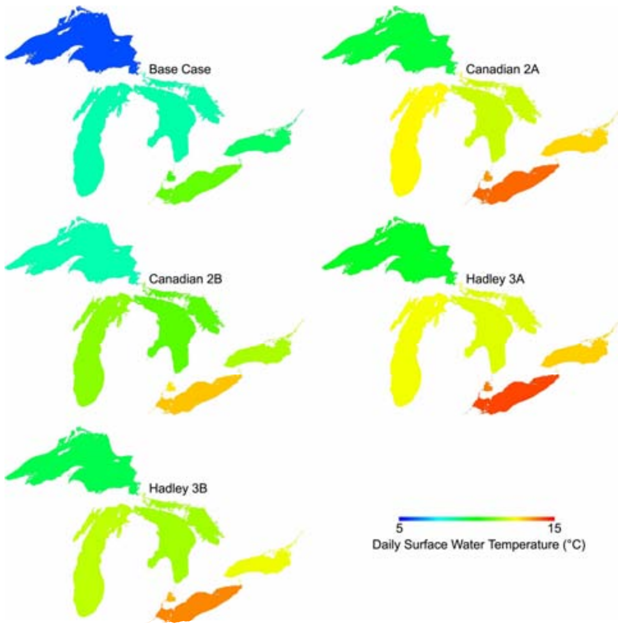

Figure 31. Daily Surface Water Temperature Averaged Over The Year.

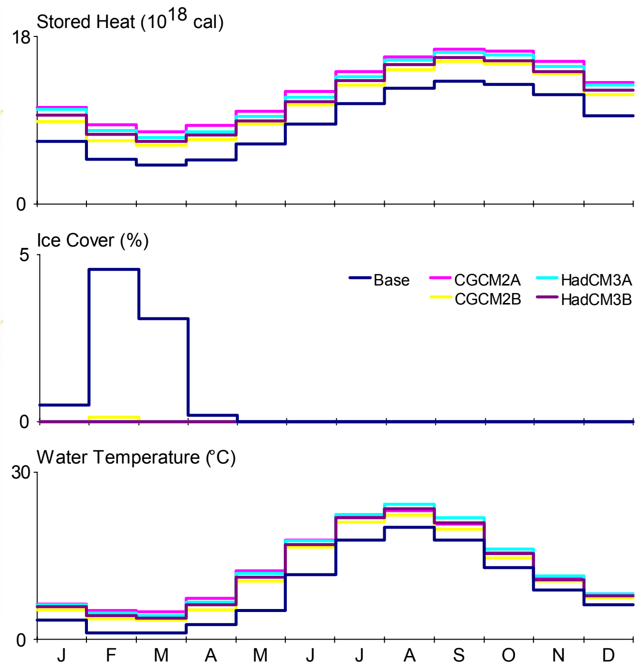

Figure 32. Seasonal Lake Ontario Average Lake Heat Storage Characteristics.

evaporation of 10% to 36%, depending on the lake and the scenario. The most evaporation occurs on all lakes for the HADCM3A scenario, followed in order by the HADCM3B, CGCM2A, and CGCM2B scenarios. See also Figure 33.

The variabilities associated with the lake heat balance variables are summarized in Table 24. The stored heat exhibits some increase in variability, in Table 24, for all scenarios and all lakes except Lake St. Clair for the Hadley GCM climate-change scenarios. Also, since the ice pack is not present anymore, the variability associated with the ice pack is zero (ice pack stays at a constant zero value). This means a relative change of 100% in the standard deviation of ice cover in Table 24. The increased heat storage in the Lakes Michigan, Huron, and Ontario (see Table 23) results in a greater thermal inertia for these lakes and the water surface temperature is less variable; see Table 24. Finally, the variability of lake evaporation ranges from little change to reductions across the Great Lakes and across the various changed-climate scenarios.

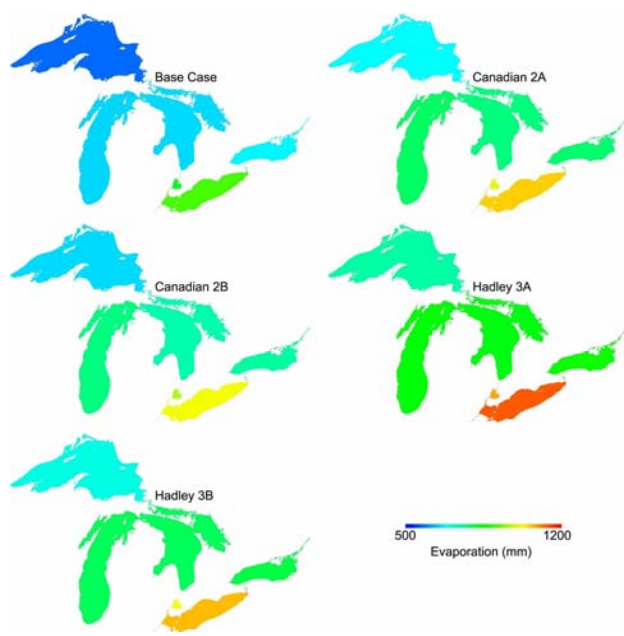

Figure 33. Average Annual Evaporation.

Lake Thermal Structure

The deep lakes (Superior, Michigan, Huron, Georgian Bay, and Ontario) have water surface temperatures that stay above 3.98ºC throughout the annual cycle in some years for

Table 24. Average Annual Lake Heat Balance Standard Deviation Differences (1950—1999).

Basin	Stored Heat Std. Dev. (10^{17} cal) & Climate Scenario Relative Change[a]					Ice Cover Std. Dev. (%) & Climate Scenario Relative Change[a]				
	BASE	#1	#2	#3	#4	BASE	#1	#2	#3	#4
Superior	4.0	35%	33%	38%	25%	5.3	-100%	-100%	-100%	-100%
Michigan	2.1	21%	7%	12%	2%	2.6	-100%	-100%	-100%	-100%
Huron	1.5	26%	15%	25%	14%	4.8	-100%	-100%	-100%	-100%
Georgian	0.5	15%	13%	17%	10%	7.8	-92%	-56%	-79%	-71%
St. Clair	0.0	3%	12%	-25%	-5%	3.7	38%	1%	50%	48%
Erie	0.3	10%	2%	17%	10%	8.1	-54%	-17%	-44%	-38%
Ontario	0.8	50%	20%	47%	29%	1.6	-100%	-95%	-100%	-100%

Basin	Water Surface Temperature Std. Dev. (ºC) & Climate Scenario Relative Change[a]					Lake Evaporation Depth Std. Dev. (mm) & Climate Scenario Relative Change[a]				
	BASE	#1	#2	#3	#4	BASE	#1	#2	#3	#4
Superior	0.9	5%	16%	13%	7%	61.9	-4%	-7%	2%	-6%
Michigan	1.0	-25%	-9%	-12%	-15%	66.9	0%	1%	3%	-1%
Huron	0.9	-13%	-3%	-7%	-10%	69.7	-1%	-3%	3%	-2%
Georgian	1.0	4%	6%	9%	4%	78.9	-9%	-9%	-7%	-9%
St. Clair	0.7	1%	-2%	9%	5%	58.3	-2%	-2%	-2%	-2%
Erie	0.8	5%	1%	12%	6%	72.9	-12%	-5%	-7%	-10%
Ontario	1.0	-29%	-15%	-20%	-22%	60.3	-4%	-2%	3%	0%

[a]Scenario #1 is CGCM2A; #2 is CGCM2B; #3 is HADCM3A; #4 is HADCM3B.

some of the changed-climate scenarios (less often on Superior since it is so far north). Figure 32 partly illustrates this for Lake Ontario for all of the changed-climate scenarios. This means that buoyancy-driven turnovers of the water column do not occur in the same way as they do at present. In some years, the large lakes are changed from dimictic lakes (turnovers occur twice a year as water temperatures pass through the point of maximum density, 3.98ºC) to monomictic lakes (maximum turnover occurs at the temperature "reversal" where temperatures stop declining and start rising again and the minimum temperature is greater than 3.98ºC).

Lake Water Balance

Overlake precipitation, runoff, and lake evaporation, all expressed as depths over each lake surface, sum algebraically as the net basin supply to the lake and are presented in Table 25. Annual summaries on all lakes for evaporation, precipitation, runoff, and net basin supply are shown in Figures 33, 34, 35, and 36, respectively. Overlake precipitation in Table 25 is not identical with over land precipitation in Table 15; they were both estimated via Thiessen weighting over different areas. The observations, presented previously, on overland precipitation equally apply for overlake precipitation; recall lake effects are ignored for precipitation. Table 25 and Figure 34 show that generally precipitation is greater on all lakes and scenarios, except Michigan, St. Clair, and Erie for the Canadian GCM climate-change scenarios. The Canadian GCM scenarios generally increase precipitation much less than do the Hadley GCM scenarios. The largest increases again occur on Georgian Bay for the HADCM3A scenario and on Erie for the HADCM3B scenario (see Tables 25 and 15).

Basin runoff in Table 25 is expressed as an over water depth and will appear different than values in Table 18 where it is expressed as an over land depth. While Table 25 and Figure 35 do indeed

Table 25. Average Annual Lake Water Balance Differences (1950—1999).

Basin	Overlake Precipitation (mm) & Climate Scenario Absolute Differences[a]					Runoff as Overwater Depth (mm) & Climate Scenario Absolute Differences[a]				
	BASE	#1	#2	#3	#4	BASE	#1	#2	#3	#4
Superior	796	16	59	73	67	620	-94	-35	-70	-27
Michigan	821	-5	-12	49	89	648	-133	-106	-85	-8
Huron	833	25	10	73	112	393	-86	-65	-53	3
Georgian	913	33	7	103	120	1811	-209	-135	-89	28
St. Clair	813	-13	-39	46	127	4445	-1142	-901	-641	142
Erie	923	-12	-29	82	162	818	-179	-181	-108	57
Ontario	878	52	15	75	111	1722	-219	-169	-144	42

Basin	Lake Evaporation Depth (mm) & Climate Scenario Absolute Differences[a]					Net Basin Supply (mm) & Climate Scenario Absolute Differences[a]				
	BASE	#1	#2	#3	#4	BASE	#1	#2	#3	#4
Superior	575	103	78	165	119	841	-180	-54	-161	-80
Michigan	651	135	113	196	141	818	-273	-232	-232	-59
Huron	654	112	80	187	136	572	-173	-135	-168	-21
Georgian	628	147	105	229	180	2096	-323	-232	-215	-33
St. Clair	835	170	133	251	188	4423	-1325	-1073	-847	81
Erie	898	159	119	239	173	843	-350	-330	-266	45
Ontario	674	105	69	185	132	1926	-272	-223	-254	21

[a]Scenario #1 is CGCM2A; #2 is CGCM2B; #3 is HADCM3A; #4 is HADCM3B.

show decreased runoff in many cases, there are other cases where runoff increases since moisture reductions are offset by precipitation increases. Table 25 and Figure 35 generally show the greatest runoff decreases for the scenarios in the following order: CGCM2A, CGCM2B, HADCM3A, and HADCM3B, as was true for runoff expressed as an overland depth in Table 18 and Figure 23.

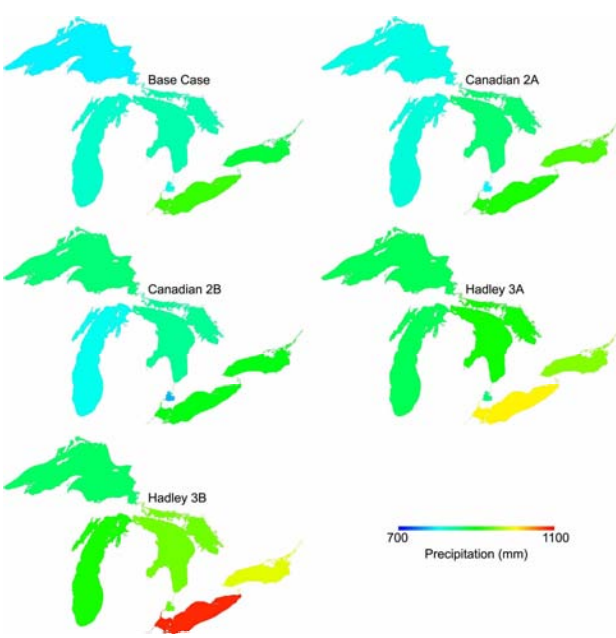

Figure 34. Average Annual Precipitation.

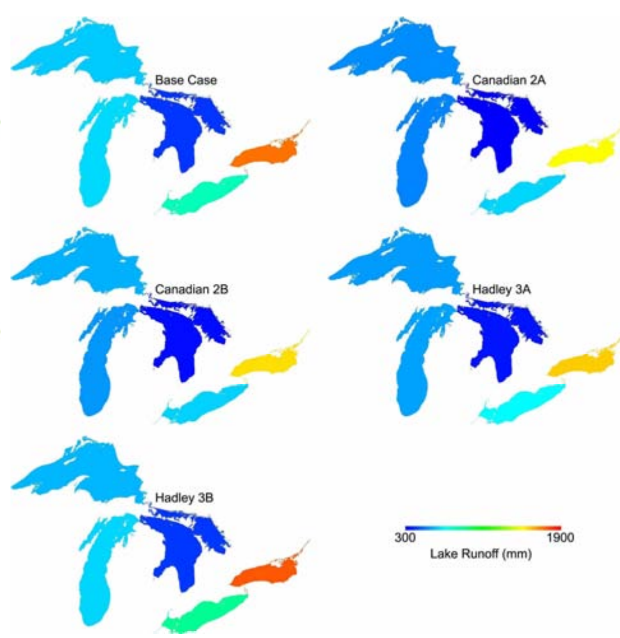

Figure 35. Average Annual Lake Runoff.

Evaporation in Table 25, however, does agree with Table 23 since it is expressed as an over water depth in both places. Lake evaporation is simply repeated from Table 23 for convenience. Also, precipitation, runoff, and evaporation are presented as absolute differences from the base case, rather than relative changes. Net basin supply in Table 25 and Figure 36 is generally less than the base case for all changed-climate scenarios on all lakes except for HADCM3B scenario on St. Clair, Erie, and Ontario. The greatest reductions in net basin supply occur on all lakes under the CGCM2A scenario, followed by either the CGCM2B or HADCM3A scenarios depending on the lake; the smallest reductions occur on all lakes under the HADCM3B scenario.

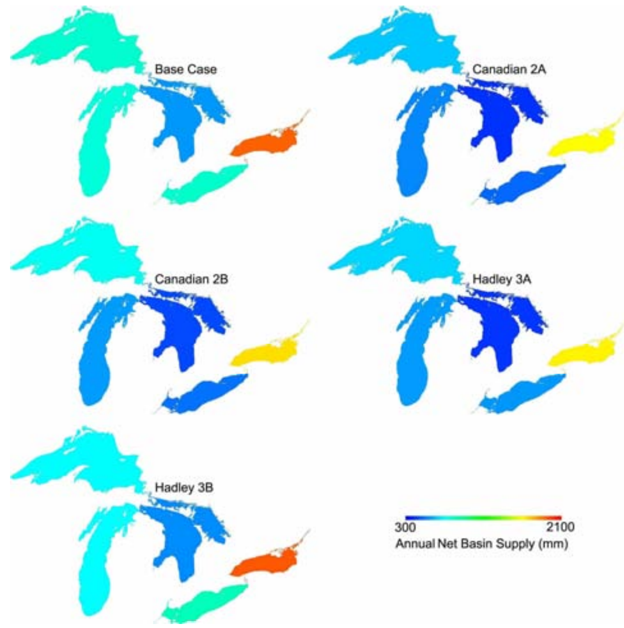

Figure 36. Average Annual Net Basin Supply.

A seasonal summary for Lake Ontario is given in Figure 37. Observations on seasonal variability in over water precipitation mirror those made for over land precipitation in Figure 16. The CGCM2B scenario seasonal precipitation variability is similar to the base case for Lake Ontario. The CGCM2A scenario shows more variability seasonally but the HADCM3B scenario shows the most variability with both spring and late summer peaks for Ontario. On the Lake Superior basin, all scenarios are very similar to the base case with only slightly higher spring precipitation for the HADCM3A and HADCM3B scenarios and slightly higher early summer precipitation for the HADCM3A, HADCM3B, and CGCM2A scenarios. There is also slightly higher fall precipitation for the CGCM2B scenario on Superior. On Michigan, we see a little more variability among the different scenarios throughout the season than with Superior, with the HADCM3B showing higher spring precipitation. Huron is similar to Michigan with the HADCM3B scenario showing higher spring precipitation and slightly higher summer precipitation. All scenarios except CGCM2A show higher winter precipitation on Georgian Bay with only slightly higher values through the rest of the year. St. Clair and Erie show higher precipitation for all scenarios except CGCM2A, with the HADCM3B peaking in spring and fall. Likewise, observations on seasonal variability in runoff are similar to those made earlier in Figure 16. All basins show earlier but lower runoff peaks, except for the

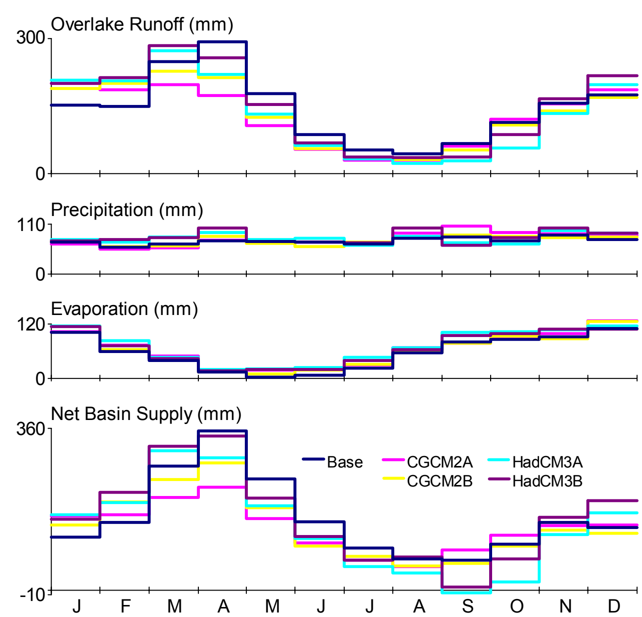

Figure 37. Seasonal Lake Ontario Average Net Basin Supply Components.

HADCM3B scenario, as shown for Ontario in Figure 37. The exception is Georgian Bay; there, spring runoff is lower for all changed climates than the base case, including the HADCM3B scenario. Observations on lake evaporation were already made (for latent heat flux) in Figure 30. Figure 37 illustrates that most of the seasonal variability in net basin supply comes from the runoff and to a lesser extent from the evaporation while the variability among the climate-change scenarios in net basin supply comes from the runoff. The seasonal variability for net basin supply is similar to the base case for all changed-climate scenarios and lakes, as exemplified in Figure 37 for Lake Ontario. Lake Superior has all changed-climate scenario net basin supplies below the base case for the late spring through the fall; for the winter to the late spring, each changed-climate scenario is greater than the base for just one month, but otherwise lower. Lakes Michigan and Huron are similar to Superior except that the HADCM3B scenario exceeds the base case net basin supply for December and February-April. Michigan net basin supply under the CGCM2B scenario also exceeds the base case for February-March. Georgian Bay net basin supply, under all changed-climate scenarios, is below the base for mid-spring through mid-fall and above for the springtime. St. Clair and Erie net basin supply, under all changed-climate scenarios, are below the base for mid-spring through the summer; the HADCM3B scenario rises above the base during mid-fall through early spring. As seen in Figure 37, Lake Ontario net basin supply for both Hadley GCM changed-climate scenarios is above the base case during the late fall through the winter and below during the spring to late fall. The Canadian GCM changed-climate scenarios have net basin supply generally below the base case except for the late summer and early winter.

The variabilities associated with the net basin supplies and its components are summarized in Table 26 for all lakes and scenarios. Changes in annual variability of over lake precipitation in Table 26 are similar to those for over land precipitation in Table 16. Generally, the Hadley scenarios,

Table 26. Average Annual Lake Water Balance Standard Deviation Differences (1950—1999).

Basin	Overlake Precipitation Std. Dev. (mm) & Climate Scenario Relative Change[a]					Runoff as Overwater Depth Std. Dev. (mm) & Climate Scenario Relative Change[a]				
	BASE	#1	#2	#3	#4	BASE	#1	#2	#3	#4
Superior	95	2%	8%	8%	9%	60	-3%	3%	1%	6%
Michigan	90	1%	-1%	6%	9%	82	-15%	-13%	-6%	5%
Huron	82	4%	2%	9%	15%	59	-16%	-12%	-8%	6%
Georgian	94	5%	2%	12%	15%	191	-10%	-6%	0%	7%
St. Clair	135	0%	-5%	3%	13%	975	-14%	-11%	-5%	10%
Erie	119	-1%	-2%	8%	16%	154	-11%	-14%	-3%	15%
Ontario	91	11%	3%	6%	10%	206	-5%	-6%	0%	8%

Basin	Lake Evaporation Depth Std. Dev. (mm) & Climate Scenario Relative Change[a]					Net Basin Supply Std. Dev. (mm) & Climate Scenario Relative Change[a]				
	BASE	#1	#2	#3	#4	BASE	#1	#2	#3	#4
Superior	61.9	-4%	-7%	2%	-6%	162	-5%	-1%	1%	2%
Michigan	66.9	0%	1%	3%	-1%	192	-5%	-5%	0%	4%
Huron	69.7	-1%	-3%	3%	-2%	158	-3%	-3%	0%	7%
Georgian	78.9	-9%	-9%	-7%	-9%	289	-5%	-5%	2%	8%
St. Clair	58.3	-2%	-2%	-2%	-2%	1102	-12%	-11%	-4%	10%
Erie	72.9	-12%	-5%	-7%	-10%	285	-9%	-10%	-1%	11%
Ontario	60.3	-4%	-2%	3%	0%	305	-3%	-4%	-1%	6%

[a]Scenario #1 is CGCM2A; #2 is CGCM2B; #3 is HADCM3A; #4 is HADCM3B.

which are the wettest in Table 25, also are the more variable as seen in Table 26. This is expected since if precipitation is generally closer to its lower bound of zero, its variation must therefore be diminished too. There generally is not much change in basin runoff variability in Table 26, although the Canadian GCM scenarios do show reduction while the extreme HADCM3B scenario shows a slight increase in variability due to the increased variability of its annual precipitation. This is as observed, of course, in Table 18 and the results (relative changes in standard deviation) are identical. Finally, the variability of lake evaporation ranges from little change to reductions across the Great Lakes and across the various changed-climate scenarios, as shown in Tables 24 and 26.

Table 27 summarizes the changes in the hydrological and net basin supply components for the entire Great Lakes basin; they were computed by converting the equivalent depths of Table 26 to annual flow rates on each lake and adding them over all the lakes. The changes from the base case are also expressed relatively in Table 27. Also expressed relatively are changes from other studies that used other GCMs (*Croley* 1990, 1993a; *Lofgren et al.* 2002; *Croley and Luukkonen* 2003), or transposed climates (*Croley et al.* 1998; *Kunkel et al.* 1998); they are provided for comparison. Net basin supplies to the Great Lakes taken as a whole are seen to drop to about one sixth to one quarter under both Canadian GCM changed-climate scenarios and the first Hadley scenario (CGCM2A, CGCM2B, and HADCM3A). This drop in net basin supply seems to result from the increases in overlake evaporation and overland evapotranspiration (reducing subsequent runoff to the lakes). While evaporation and evapotranspiration have increased just as significantly under the second Hadley GCM changed-climate scenario (HADCM3B) as well, the precipitation increases (both overland and overlake) compensate and the net basin supplies are very close to the base case. The results from the Canadian GCM changed-climate scenarios then, are similar to the earlier studies with the previous Canadian GCMs, also reported in Table 27; the net supplies drop in the same range due to increased basin evapotranspiration and lake evaporation. The results from the Hadley GCM changed-climate scenarios however, are not similar to the earlier studies with the previous Hadley GCMS, also reported in Table 27; the newer runs show a drop in net basin supply while the older ones showed an increase. Table 27 also shows that the present results are contained within (bounded by) results of the earlier climate transposition study and are not as severe as the early IJC or 1989 EPA studies.

Table 27. Average Annual Great Lakes Basin Hydrology Summary.

Scenario	Overland Precipitation ($m^3\ s^{-1}$)		Evapo-transpiration ($m^3\ s^{-1}$)		Basin Runoff ($m^3\ s^{-1}$)		Overlake Precipitation ($m^3\ s^{-1}$)		Overlake Evaporation ($m^3\ s^{-1}$)		Net Basin Supply ($m^3\ s^{-1}$)	
Base[a]	14,300		8,060		6,240		6,480		5,050		7,660	
CGCM2A[b]	14,520	2%	9,370	16%	5,200	-17%	6,590	2%	6,000	19%	5,790	-24%
CGCM2B[c]	14,500	1%	9,030	12%	5,510	-12%	6,610	2%	5,770	14%	6,350	-17%
HADCM3A[d]	15,450	8%	9,920	23%	5,580	-11%	7,030	8%	6,530	29%	6,080	-21%
HADCM3B[e]	16,070	12%	9,790	21%	6,250	0%	7,230	12%	6,130	21%	7,350	-4%
CGCM1 2030[f]						-10%		2%		15%		-16%
CGCM1 2050[g]						-14%		3%		22%		-23%
CGCM1 2090[h]						-20%		12%		34%		-29%
HADCM2 2030[i]						1%		7%		6%		2%
HADCM2 2050[j]						3%		7%		11%		1%
HADCM2 2090[k]						7%		19%		17%		10%
6ºS × 10ºW[l]		6%		31%		-25%		3%		49%		-48%
6ºS × 0ºW[m]		24%		43%		-1%		25%		33%		-1%
10ºS × 11ºW[n]		17%		48%		-21%		13%		75%		-54%
10ºS × 5ºW[o]		45%		78%		2%		45%		69%		-5%
CCC[p]		-2%		22%		-32%		0%		32%		-46%
GISS[q]		2%		21%		-24%		4%		27%		-37%
GFDL[r]		1%		19%		-23%		0%		44%		-51%
OSU[s]		6%		19%		-11%		6%		26%		-23%

[a]Historical (1950-1999) period simulation.
[b]Canadian Centre for Climate Modeling and Analysis, GCM 2, run A21 (warm and dry).
[c]Canadian Centre for Climate Modeling and Analysis, GCM 2, run B23 (not as warm but dry).
[d] Hadley Centre for Climate Prediction and Research, GCM 3, run A1FI (warm and wet).
[e] Hadley Centre for Climate Prediction and Research, GCM 3, run B22 (not as warm but wet).
[f]Canadian Centre for Climate Modeling and Analysis, GCM 1, run 2021—2040 (*Lofgren et al.* 2002).
[g]Canadian Centre for Climate Modeling and Analysis, GCM 1, run 2041—2060 (*Lofgren et al.* 2002).
[h]Canadian Centre for Climate Modeling and Analysis, GCM 1, run 2081—2100 (*Lofgren et al.* 2002).
[i]Hadley Centre for Climate Prediction and Research, GCM 2, run 2021—2040 (*Lofgren et al.* 2002).
[j]Hadley Centre for Climate Prediction and Research, GCM 2, run 2040—2060 (*Lofgren et al.* 2002).
[k]Hadley Centre for Climate Prediction and Research, GCM 2, run 2081—2100 (*Lofgren et al.* 2002).
[l]Climate transferred from 6ºS and 10ºW of Great Lakes (*Croley et al.* 1998).
[m]Climate transferred from 6ºS of Great Lakes (*Croley et al.* 1998).
[n]Climate transferred from 10ºS and 11ºW of Great Lakes (*Croley et al.* 1998).
[o]Climate transferred from 10ºS and 5ºW of Great Lakes (*Croley et al.* 1998).
[p]Canadian Climate Centre (*Croley* 1993a); IJC study.
[q]Goddard Institute for Space Studies GCM (*Croley* 1990); 1989 EPA study.
[r]Geophysical Fluid Dynamics Laboratory GCM (*Croley* 1990); 1989 EPA study.
[s]Oregon State University GCM (*Croley* 1990); 1989 EPA study.

Hydrological Sensitivities

Main Findings

Without temperatures below freezing, the snow pack is insensitive to precipitation. Although the changed-climate scenarios on different lakes show different estimates of precipitation change, each shows increases in air temperatures that significantly reduce the snow pack. Thus, even if precipitation increases more than suggested by these scenarios, the snow pack will be much reduced under warmer climates. The increased air temperatures significantly increase evapotranspiration. Neither snow moisture reductions nor evapotranspiration increases mirror temperature changes perfectly for the four scenarios; this lack of perfect correspondence is due to the pattern of precipitation changes. The increased evapotranspiration and decreased snow pack give rise to less moisture available in the soil and groundwater zones, and consequently decreased runoff. While there is decreased runoff in many cases, there are other cases where runoff increases since moisture reductions are offset by precipitation increases. Runoff decreases, from largest to smallest, for scenarios in order: CGCM2A, CGCM2B, HADCM3A, and HADCM3B.

Insolation changes reflect largely the cloud cover changes; the Hadley GCM changed-climate scenarios transfer more heat into the lakes than do the Canadian GCM scenarios. The increase for the Hadley GCM changed-climate scenarios occurs on all Great Lakes beginning in the late spring, extending throughout the summer, and into the early fall. Insolation for the Hadley GCM changed-climate scenarios then is slightly below the base case beginning in the late fall, extending throughout the winter and into the early spring. The insolation for the Canadian GCM climate-change scenarios is slightly less than the base case throughout the year for all lakes; the decrease is spread throughout the annual cycle fairly uniformly and the seasonal insolation variation is similar to the base case. Reflection generally decreases but changes are very small, relative to the insolation changes, with most of the difference coming in the winter-spring due to the absence of ice cover. The Canadian GCM climate-change scenarios reduce reflection more than the Hadley scenarios. Net long wave exchange increases slightly, implying more heat stays in the lakes. The largest increase on all lakes occurs under the CGCM2A scenario followed by the CGCM2B, HADCM3B, and HADCM3A scenarios respectively. Increases are spread fairly uniformly throughout the seasonal cycle. Sensible heat exchange changes are small and vary in direction from lake to lake.

The heat budget gives rise to increased water surface temperatures and stored heat increases over the Great Lakes, depending on the changed-climate scenario considered. The largest relative heat increases are seen to occur for the northeastern-most lakes and for the CGCM2A, HADCM3A, HADCM3B, and CGCM2B changed-climates scenarios, in decreasing order of impact on all lakes. The increased heat in storage also means that ice formation will be greatly reduced over winter on the deep Great Lakes. Ice cover is practically eliminated under all changed climate scenarios on all lakes but Lake St. Clair, and to a lesser extent on Lake Erie; since those lakes have very little heat storage capacity, ice formation is not affected as much as elsewhere.

Water surface temperatures are seen to peak slightly earlier on deep lakes under the changed climates than under the base case. The increased heat in storage is sufficient to cause increased lake evaporation on all lakes under all scenarios, even though wind speeds and humidity, by themselves, would not increase evaporation. (Wind speed and humidity changes, in some cases, would decrease lake evaporation, all other things being equal.) The most evaporation occurs on all lakes for the HADCM3A scenario, followed in order by HADCM3B, CGCM2A, and CGCM2B.

The deep lakes have water surface temperatures that stay above 3.98ºC throughout the annual cycle in some years for some of the changed-climate scenarios. This means that buoyancy-driven turnovers of the water column do not occur in the same way as they do at present. In some years, the large lakes are changed from dimictic lakes to monomictic lakes. Without biannual turnovers, hypolimnion chemistry may be altered; oxygen may be depleted, releasing nutrients and metals from lake sediments. The lakes may experience more than a single winter turnover if temperature gradients are small and winds are strong enough to induce mixing (*Hutchinson* 1957).

The Hadley scenarios generally increase precipitation more than do the Canadian GCM scenarios. Precipitation is greater than the base case on all lakes for the Hadley scenarios. For the Canadian scenarios, precipitation is greater on all lakes except Michigan, St. Clair, and Erie. The largest occur on Georgian Bay for the HADCM3A scenario and on Erie for HADCM3B.

Net basin supply is generally less than the base case for all changed-climate scenarios for all lakes except for the HADCM3B scenario on Lakes St. Clair, Erie, and Ontario. The greatest reductions in net basin supply occur on all lakes under the CGCM2A (warm, dry) scenario, followed by either the CGCM2B (less warm, dry) or HADCM3A (warm, wet) scenarios depending on the lake; the smallest reductions occur on all lakes under the HADCM3B (less warm, wet) scenario.

Summary

The higher air temperatures under the changed-climate scenarios lead to higher over-land evapotranspiration and lower runoff to the lakes with earlier runoff peaks since snow pack is reduced and the snow season is greatly reduced. This also results in a reduction in available soil moisture. Water temperatures increase and peak earlier; heat resident in the deep lakes increases throughout the year. Mixing of the water column diminishes, as most of the lakes become mostly monomictic, and lake evaporation increases. Ice formation is greatly reduced over winter on the deep Great Lakes, and lake evaporation increases; average net supplies drop most where precipitation increases are modest.

References

Allsopp, T. R., and S. J. Cohen, 1986. CO_2-Induced climate change and its potential impact on the Province of Ontario. In: *Preprint Volume, Conference on Climate and Water Management - A Critical Era*, American Meteorological Society, Boston, Massachusetts, 285-290.

Assel, R. A., 1983. A computerized data base of ice concentration for the Great Lakes. *NOAA Data Report ERL GLERL-24*, Great Lakes Environmental Research Laboratory, Ann Arbor, Michigan.

Assel, R. A., F. H. Quinn, G. A. Leshkevich, and S. J. Bolsenga, 1983. NOAA Great Lakes Ice Atlas. Great Lakes Environmental Research Laboratory, Ann Arbor, Michigan.

Barrow, E., 2002. Climate change in the Great Lakes—St. Lawrence region, a comparison of climate change scenarios. Report prepared for the International Joint Commission's Lake Ontario—St. Lawrence River Study.

Bates, G. T., S. W. Hostetler, and F. Giorgi, 1995. Two-year simulation of the Great Lakes Region with a coupled modeling system. *Monthly Weather Review*, **123**:1505-1522.

Blumberg A. F., and D. M. DiToro, 1989. The effects of climate warming on Lake Erie water quality. In *The Potential Effects of Global Climate Change on the United States*, J. B. Smith and D. A. Tirpak (Eds.), U. S. Environmental Protection Agency report no. EPA-230-05-89-051, 7-1 - 7-28.

Bolsenga S. J., 1977. Lake-land precipitation relationships using Northern Lake Michigan data. *Journal of Applied Meteorology*, **16**(11):1158-1164.

Bolsenga S. J., 1979. Determining overwater precipitation from overland data: the methodological controversy analyzed. *Journal of Great Lakes Research*, **5**(3-4):301-311.

Bolsenga, S. J., and J. C. Hagman, 1975. On the selection of representative stations for Thiessen polygon networks to estimate Lake Ontario overwater precipitation. *International Field Year for the Great Lakes Bulletin 16*, National Oceanic and Atmospheric Administration, Rockville, 57-62.

Campbell J. E., A. H. Clites, and G. M. Green, 1987. Measurements of ice motion in Lake Erie using satellite-tracked drifter buoys. *NOAA Data Report ERL GLERL-30*, Great Lakes Environmental Research Laboratory, Ann Arbor, Michigan.

Charlson, R. J., S. E. Schwartz, J. M. Hales, R. D. Cess, J. A. Coakley, Jr., J. E. Hansen, and D. J. Hofmann, 1992: Climate forcing by anthropogenic aerosols. Science, 255, 423-430.

Cohen, S. J., 1986. Impacts of CO_2-induced climatic change on water resources in the Great Lakes basin. *Climatic Change*, **8**:135-153.

Cohen, S. J., 1990a. Methodological issues in regional impacts research. In: *Proceedings of an International Symposium/Workshop on Climate Change, Implications for Water and Ecological Resources*, G. Wall and M. Sanderson (Eds.), Department of Geography Publication Series, Occasional Paper No. 11, University of Waterloo, Waterloo, Ontario, 31-43.

Cohen, S. J., 1991. Caveats in applying GCM output to regional impact assessments. *Proceedings of A Symposium on Climate Scenarios*, The Water Network, University of Waterloo, Waterloo, 16-32.

Coordinating Committee on Great Lakes Basic Hydraulic and Hydrologic Data, 1977. Coordinated Great Lakes Physical Data. U. S. Army District Engineer, Detroit.

Croley, T. E., II, 1982. Great Lakes basins runoff modeling. *NOAA Technical Memorandum ERL GLERL-39*, National Technical Information Servicer, Springfield.

Croley, T. E., II, 1983a. Great Lakes basins (U.S.A.-Canada) runoff modeling. *Journal of Hydrology*, **64**:135-158.

Croley, T. E., II, 1983b. Lake Ontario basin (U.S.A.-Canada) runoff modeling. *Journal of Hydrology*, **66**:101-121.

Croley, T. E., II, 1989a. Lumped modeling of Laurentian Great Lakes evaporation, heat storage, and energy fluxes for forecasting and simulation. *NOAA Technical Memorandum ERL GLERL-70*, Great Lakes Environmental Research Laboratory, Ann Arbor.

Croley, T. E., II, 1989b. Verifiable evaporation modeling on the Laurentian Great Lakes. *Water Resource Research*, **25**(5):781-792.

Croley, T. E., II, 1990. Laurentian Great Lakes double-CO_2 climate change hydrological impacts. *Climatic Change*, **17**:27-47.

Croley, T. E., II, 1992a. Long-term heat storage in the Great Lakes. *Water Resources Research*, **28**(1):69-81.

Croley, T. E., II, 1992b. Climate change impacts on Great Lakes water supplies. *Proceedings of the Symposium on Managing Water Resources During Global Change*, Twenty-Eighth American Water Resources Association Conference, 241-250.

Croley, T. E., II, 1993a. CCC GCM 2xCO_2 hydrological impacts on the Great Lakes. In: Climate, Climate Change, Water Level Forecasting and Frequency Analysis, Supporting Documents, Volume 1 - Water Supply Scenarios, International Joint Commission, Washington, D. C.

Croley, T. E., II, 1993b. Probabilistic Great Lakes hydrology outlooks. *Water Resources Bulletin*, **29**(5):741-753.

Croley, T. E., II, and R. A. Assel, 1994. A one-dimensional ice thermodynamics model for the Laurentian Great Lakes. *Water Resources Research*, **30**(3):625-639.

Croley, T. E., II, and H. C. Hartmann, 1984. Lake Superior basin runoff modeling. *NOAA Technical Memorandum ERL GLERL-50*, National Technical Information Service, Springfield.

Croley, T. E., II, and H. C. Hartmann, 1985. Resolving Thiessen polygons. *Journal of Hydrology*, **76**:363-379.

Croley, T. E., II, and H. C. Hartmann, 1986. Near-real-time gorecasting of large-lake water supplies; a user's manual. *NOAA Technical Memorandum ERL GLERL-61*, Environmental Research Laboratories, Boulder, Colorado.

Croley, T. E., II, and H. C. Hartmann, 1987. Near-real-time forecasting of large lake supplies. *Journal of the Water Resources Planning and Management Division*, **113**(6):810-823.

Croley, T. E., II, and H. C. Hartmann, 1989. Effects of climate changes on the Laurentian Great Lakes levels. In *The Potential Effects of Global Climate Change on the United States: Appendix A-Water Resources* J. B. Smith and D. A. Tirpak (Eds.), U.S. Environmental Protection Agency, Washington, D.C., 4-1 - 4-34.

Croley, T. E., II, and D. H. Lee, 1993. Evaluation of Great Lakes net basin supply forecasts. *Water Resources Bulletin*, **29**(2):267-282.

Croley, T. E., II, and C. L. Luukkonen, 2003. Potential climate change impacts on Lansing, Michigan ground water. *Journal of the American Water Resources Association*, **39**(1): 149-163.

Croley, T. E., II, F. H. Quinn, K. E., Kunkel, and S. J. Changnon, 1998. Great Lakes hydrology under transposed climates, *Climatic Change*, **38**:405-433.

DeCooke, B. G., and D. F. Witherspoon, 1981. Terrestrial water balance. In *IFYGL - The International Field Year for the Great Lakes*, E. J. Aubert and T. L. Richards (Eds.), Great Lakes Environmental Research Laboratory, Ann Arbor, 210-219.

Freeman, N. G., and W. S. Haras, 1978. What you always wanted to know about Great Lakes levels and didn't know whom to ask. Environment Canada, Ottawa.

Gauthier, R. L., R. A. Melloh, T. E. Croley II, and H. C. Hartmann, 1984. *In Proceedings 18th International Symposium on Remote Sensing of the Environment*, Paris, 1-12.

Gray, D. M., G. A. McKay, and J. M. Wigham, 1973. Energy, evaporation, and evapotranspiration. In *Handbook on the Principles of Hydrology*, DM Gray (Ed.), Water Information Center, New York, 3.1-3.66.

Green, G. M., and S. I. Outcalt, 1985. A simulation model of river ice cover thermodynamics. *Cold Reg. Sci. & Technol.*, **10**:251-262.

Hartmann, H. C., 1987. An evaluation of Great Lakes hydraulic routing models. *NOAA Technical Memorandum ERL GLERL-66*, Great Lakes Environmental Research Laboratory, Ann Arbor.

Hartmann, H. C., 1988. Historical basis for limit on Lake Superior water level regulations. *Journal of Great Lakes Research*, **14**(3):316-324.

Hartmann, H. C., 1990. Climate change impacts on Laurentian Great Lakes levels. *Climatic Change*, **17**:49-67.

Hostetler, S. W., and P. J. Bartlein, 1990. Simulation of lake evaporation with application to modeling lake level variations of Harney-Malheur Lake, Oregon. *Wat. Resour. Res.*, **26**(10):2603-2612.

Hutchinson, G. E., 1957. A Treatise on Limnology, Volume 1, Part 1 - Geography and Physics of Lakes, John Wiley and Sons, New York.

Intergovernmental Panel on Climate Change, 2000. *Special Report on Emissions Scenarios*. N. Nakicenovic and R. Swart (Eds.), Cambridge University Press, Cambridge, United Kingdom and New York.

International Great Lakes Diversions and Consumptives Uses Study Board, 1981. *Great Lakes Diversions and Consumptive Uses*. International Joint Commission, Washington, D. C.

International Great Lakes Diversions and Consumptives Uses Study Board, 1985. *Great Lakes Diversions and Consumptive Uses*. International Joint Commission, Washington, D. C.

International Lake Superior Board of Control, 1981. *Regulation of Lake Superior: Plan 1977 Development, Description, and Testing*. International Joint Commission, Washington, D. C.

International Lake Superior Board of Control, 1982. *Regulation of Lake Superior: Operational Guides for Plan 1977*. International Joint Commission, Washington, D. C.

International St. Lawrence River Board of Control, 1963. *Regulation of Lake Ontario: Plan 1958-D*. International Joint Commission, Washington, D. C.

Keijman, J. Q., 1974. The estimation of the energy balance of a lake from simple weather data. *Boundary-Layer Meteorology*, **7**:399-407.

Kraus, E. B., and J. S. Turner, 1967. A one-dimensional model of the seasonal thermocline II; the general theory and its consequences. *Tellus*, **19**:98-105.

Kunkel, K. E., S. J. Changnon, T. E. Croley II, and F. H. Quinn, 1998. Transposed climates for study of water supply variability on the Laurentian Great Lakes, *Climatic Change*, **38**:387-404.

Larsen, C. E., 1985. A stratigraphic study of beach features on the southwestern shore of Lake Michigan: new evidence of holocene lake level fluctuations. Environmental Geology Notes 112, Illinois State Geological Survey, Champaign.

Lofgren, B. M, F. H. Quinn, A. H. Clites, R. A. Assel, A. J. Eberhardt, and C. L. Luukkonen, 2002. Evaluation of potential impacts on Great Lakes water resources based on climate scenarios of two GCMs. *J. Great Lakes Res.*, **28**(4):537-554.

Louie, P. Y. T., 1991. Proposed GCM scenarios for the phase 2 study. *Proceedings of A Symposium on Climate Scenarios*, The Water Network, University of Waterloo, Waterloo, 67-78.

Manabe, S., and R. T. Wetherald, 1975. The effects of doubling the CO_2 concentration on the climate of a general circulation model. *J. Atmos. Sci.*, **32**:3-15.

McCormick, M. J., 1989. Potential climate changes to the Lake Michigan thermal structure. In *The Potential Effects of Global Climate Change on the United States*, J. B. Smith and D. A. Tirpak (Eds.), U. S. Environmental Protection Agency report no. EPA-230-05-89-051, 6-1 - 6-26.

McCormick, M. J. and G. A. Meadows, 1988. An intercomparison of four mixed layer models in a shallow inland sea. *J. Geophys. Res*., **93**(C6):6774-6788.

McFarlane, N. A., 1991. The Canadian Climate Centre second-generation global circulation model. *Proceedings of A Symposium on Climate Scenarios*, The Water Network, University of Waterloo, Waterloo, 3-15.

Phillips, W. D., and J. G. Irbe, 1978. Land-to-lake comparison of wind, temperature, and humidity on Lake Ontario during the International Field Year for the Great Lakes (IFYGL). *Report CLI-2-77*, Environment Canada, Atmospheric Environment Service, Downsview.

Quinn, F. H., 1978. Hydrologic response model of the North American Great Lakes. *Journal of Hydrology*, **37**:295-307.

Quinn, F. H., 1979. An improved aerodynamic evaporation technique for large lakes with application to the International Field Year for the Great Lakes. *Water Resources Research*, **15**(4):935-940.

Quinn, F. H., 1981. Secular changes in annual and seasonal Great Lakes precipitation, 1854-1979, and their implications for Great Lakes water resource studies. *Water Resources Research*, **17**:1619-1624.

Quinn, F. H., 1982. Trends and extremes of Lake Erie water supplies. *Proceedings International Symposium on Hydrometeorology*, American Water Resources Association, Minneapolis, 267-270.

Quinn, F. H., 1985. Great Lakes water levels. In *Great Lakes Water Levels*, Briefing of Senators and Representatives from the Great Lakes Basin July 19, International Joint Commission, Washington, 1-24.

Quinn, F. H., 1988. Likely effects of climate changes on water levels in the Great Lakes. In: *Proceedings, First North American Conference on Preparing for Climate Change*, Climate Change Institute, Washington, D. C., 481-487.

Quinn, F. H., and T. E. Croley II, 1981. The role of precipitation climatology in hydrologic design and planning on the Laurentian Great Lakes. *Proceedings Fourth Conference on Hydrometeorology*, American Meteorological Society, Boston, 218-223.

Quinn, F. H., and T. E. Croley II, 1983. Climatic water balance models for Great Lakes forecasting and simulation. In: *Preprint Volume: Fifth Conference on Hydrometeorology*, American Meteorological Society, Boston, Massachusetts, 218-223.

Quinn, F. H., and R. N. Kelley, 1983. Great Lakes monthly hydrologic data. *NOAA Technical Memorandum ERL GLERL-39*, National Technical Information Service, Springfield.

Quinn, F. H., and D. C. Norton, 1982. Great Lakes precipitation by months, 1900-80. *NOAA Technical Memorandum ERL GLERL-20*, National Technical Information Service, Springfield.

Quinn, F. H., T. E. Croley II, K. Kunkel, and S. J. Changnon, 1997. Laurentian Great Lakes hydrology and lake levels under the transposed 1993 Mississippi River flood climate. *Journal of Great Lakes Research,* **23**(3):317-327.

Robinson, P. J. and P. Finkelstein, 1989. *Strategies for the Development of Climate Scenarios for Impact Assessment*. U. S. Environmental Protection Agency, Research Triangle Park, North Carolina.

Rondy, D. R., 1976. Great Lakes ice cover, Appendix 4, *Great Lakes Basin Framework Study*, Great Lakes Basin Commission, Ann Arbor.

U. S. Army Corps of Engineers, 1985. *Great Lakes water level facts*. U. S. Government Printing Office, Washington, D. C.

U. S. Environmental Protection Agency, 1984. Potential Climatic Impacts of Increasing Atmospheric CO_2 with Emphasis on Water Availability and Hydrology in the United States, EPA Office of Policy, Planning, and Evaluation, Washington, D. C.

U. S. Environmental Protection Agency, 1989. *The Potential Effects of Global Climate Change on the United States. Report to Congress*. J. B. Smith and D. A. Tirpak (Eds.), Report EPA-230-05-89-050, EPA Office of Policy, Planning, and Evaluation, Washington, D. C.

Wilson, J. W., 1977. Effect of Lake Ontario on precipitation. *Monthly Weather Review*, **105**:207-214.

Appendix - Notation

a	=	wind parameter, T > 3.98°C ***[evaporation model empirical parameter]***
a'	=	wind parameter, T < 3.98°C ***[evaporation model empirical parameter]***
a_s	=	proportionality constant for snowmelt per degree-day ***[runoff model empirical parameter]***
A	=	area of the ice surface
A_b	=	area of the watershed
A_w	=	area of the open-water (ice-free) lake surface
α_{dp}	=	deep percolation coefficient ***[runoff model empirical parameter]***
α_{gw}	=	groundwater coefficient ***[runoff model empirical parameter]***
α_{int}	=	interflow coefficient ***[runoff model empirical parameter]***
α_{per}	=	percolation coefficient ***[runoff model empirical parameter]***
α_{sf}	=	surface outflow coefficient ***[runoff model empirical parameter]***
b	=	wind parameter, T > 3.98°C ***[evaporation model empirical parameter]***
b'	=	wind parameter, T < 3.98°C ***[evaporation model empirical parameter]***
b_1	=	empirical constant
b_2	=	empirical constant
β	=	partial linear reservoir coefficient
β_{eg}	=	groundwater zone evapotranspiration coefficient ***[runoff model empirical parameter]*** (= 0)
β_{el}	=	lower zone evapotranspiration coefficient ***[runoff model empirical parameter]*** (= 0)
β_{es}	=	surface zone evapotranspiration coefficient ***[runoff model empirical parameter]***
β_{eu}	=	upper zone evapotranspiration coefficient ***[runoff model empirical parameter]***
C_i	=	specific heat of ice
C_p	=	specific heat of air at constant temperature
C_w	=	specific heat of water
C_E	=	bulk evaporation coefficient over water
C_E'	=	bulk evaporation coefficient over ice
C_H	=	sensible heat coefficient over water
C_H'	=	sensible heat coefficient over ice
D	=	ice pack depth (thickness)
DD	=	degree-days per day
Δ	=	time increment of mass balance computation period
e	=	evaporation or evapotranspiration rate
e_p	=	rate of evaporation or evapotranspiration still possible
e_w	=	over-water evaporation rate
e_w'	=	over-ice evaporation rate
E	=	volumetric rate of evaporation from ice
E_g	=	evapotranspiration from the groundwater zone storage
E_l	=	evapotranspiration from the lower soil zone storage
E_s	=	evapotranspiration from the surface storage
E_u	=	evapotranspiration from the upper soil zone storage
ε_w	=	emissivity of water
ε_a	=	emissivity of the atmosphere
f	=	infiltration rate
$f_{k,m}$	=	ratio of surface temperature rise on day k from heat added on day m to that heat addition
F	=	representing lake volume at which a heat addition is uniformly fully mixed, T > 3.98°C ***[evaporation model empirical parameter]***
F'	=	representing lake volume at which a heat addition is uniformly fully mixed, T < 3.98°C ***[evaporation model empirical parameter]***

GZM	=	content of groundwater zone
γ_f	=	latent heat of fusion
γ_v	=	latent heat of vaporization
H	=	heat stored in the lake
H'	=	heat stored in the ice pack
H_s	=	nonlatent heat released to the atmosphere
η	=	parameter relating cloudiness to atmospheric long-wave radiation ***[evaporation model empirical parameter]***
K	=	units and proportionality constant
LSZM	=	moisture content of lower soil zone
m	=	daily snowmelt rate
m_p	=	daily potential snowmelt rate
M	=	number of days in long-term heat balance
$M_{k,m}$	=	mixing volume size on day k of heat added on day m
n	=	number of days in the mass balance computation period
ns	=	daily net supply rate to the watershed surface
N	=	fraction of sky covered in clouds
p	=	precipitation rate
q	=	specific humidity of the air over the water
q'	=	specific humidity of the air over the ice
q_0	=	unit (per unit area) cloudless sky short-wave radiation rate
q_e	=	unit evaporative (latent and advected) heat transfer rate
q_e'	=	unit evaporative (latent and advected) heat transfer rate from ice pack
q_h	=	unit sensible heat transfer rate
q_h'	=	unit sensible heat transfer rate to ice pack
q_i	=	unit incident short-wave radiation rate
q_p	=	unit precipitation heat advection rate to water surface
q_p'	=	unit precipitation heat advection rate to ice pack
q_r	=	unit reflected short-wave radiation rate
q_r'	=	unit reflected short-wave radiation rate to ice pack
q_w	=	specific humidity of saturated air at temperature of water
q_w'	=	specific humidity of saturated air at temperature of ice
$q\uparrow$	=	long-wave radiation emitted by the water body
$q\downarrow$	=	long-wave radiation from the atmosphere absorbed by the water surface
Q	=	basin outflow volume for n days
Q_a	=	heat flux between atmosphere and ice pack used for freezing or melting
Q_l	=	net long-wave radiation exchange rate
Q_w	=	total heat flux between the water body and the ice pack
Q_I	=	net heat advection to the lake from surface flows
Θ_i	=	sum of all surface inflows to lake
Θ_o	=	sum of all outflows from lake
r_a	=	reflectivity of the water surface
rr	=	daily solar insolation at the watershed surface
ρ	=	density of ice
ρ_a	=	density of air
ρ_w	=	density of water
S	=	volumetric rate of snow falling on ice
SNW	=	water content of the snowpack

SS	=	content of surface storage zone
σ	=	Stephan-Bolzmann constant
t	=	time
T	=	water surface temperature
T'	=	ice surface temperature
T_a	=	air temperature
T_a'	=	over-ice air temperature
T_b	=	a base scaling temperature ***[runoff model empirical parameter]***
T_{max}	=	maximum daily air temperature
T_{min}	=	minimum daily air temperature
τ	=	daily extra-terrestrial solar radiation
τ_a	=	parameter reflecting ice pack shape, vertical-lateral change ratios along atmosphere-ice boundary, and ice buoyancy ***[evaporation model empirical parameter]***
τ_w	=	parameter reflecting ice pack shape, vertical-lateral change ratios along water-ice boundary, and ice buoyancy ***[evaporation model empirical parameter]***
U	=	wind speed over water
$USZC$	=	capacity of the upper soil zone (= 2 cm)
$USZM$	=	moisture content of upper soil zone
V	=	volume of the ice pack
V'	=	volume of ice formed by only by freezing or melting
V_c	=	lake volume (capacity)
V_e	=	equilibrium lake volume approached as a limit by mixing ***[evaporation model empirical parameter]***
W	=	daily wind movement
X	=	ratio of hours of bright sunshine to maximum possible
Ψ	=	total heat available for evapotranspiration during the day
Z	=	volume of water in storage